

# Titan's Atmosphere and Climate

S. M. Hörst<sup>1</sup>

<sup>1</sup>Department of Earth and Planetary Sciences, Johns Hopkins University, Baltimore, MD, USA.

**Key Points.**

- Titan has the most complex atmospheric chemistry in the solar system.
- Titan's atmosphere and surface share a unique connection.
- Titan provides the opportunity to test our understanding of many planetary processes

**Abstract.**

Titan is the only moon with a substantial atmosphere, the only other thick N<sub>2</sub> atmosphere besides Earth's, the site of extraordinarily complex atmospheric chemistry that far surpasses any other solar system atmosphere, and the only other solar system body with stable liquid currently on its surface. The connection between Titan's surface and atmosphere is also unique in our Solar system; atmospheric chemistry produces materials that are deposited on the surface and subsequently altered by surface-atmosphere interactions such as aeolian and fluvial processes resulting in the formation of extensive dune fields and expansive lakes and seas. Titan's atmosphere is favorable for organic haze formation, which combined with the presence of some oxygen bearing molecules indicates that Titan's atmosphere may produce molecules of prebiotic interest. The combination of organics and liquid, in the form of water in a subsurface ocean and methane/ethane in the surface lakes and seas, means that Titan may be the ideal place in the solar system to test ideas about habitability, prebiotic chemistry, and the ubiquity and diversity of life in the Universe. The Cassini-Huygens mission to the Saturn system has provided a wealth of new information allowing for study of Titan as a complex system. Here I review our current understanding of Titan's atmosphere and climate forged

from the powerful combination of Earth-based observations, remote sensing and *in situ* spacecraft measurements, laboratory experiments, and models.

I conclude with some of our remaining unanswered questions as the incredible era of exploration with Cassini-Huygens comes to an end.

## 1. Introduction

Titan is unique in our solar system: it is the only moon with a substantial atmosphere, the only other thick N<sub>2</sub> atmosphere besides that of Earth, the site of extraordinarily complex atmospheric chemistry that far surpasses any other solar system atmosphere, and the only other solar system body that currently possesses stable liquid on its surface. Titan's mildly reducing atmosphere is favorable for organic haze formation and the presence of some oxygen bearing molecules suggests that molecules of prebiotic interest may form in its atmosphere [Hörst *et al.*, 2012]. The combination of liquid and organics means that Titan may be the ideal place in the solar system to test ideas about habitability, prebiotic chemistry, and the ubiquity and diversity of life in the Universe [Lunine, 2009].

The possible existence of an atmosphere around Titan was first suggested in 1908 in a paper titled “Observations des satellites principaux de Jupiter et de Titan” by José Comas Solà. He believed he observed limb darkening, which is indicative of an atmosphere [Comas Solà, 1908]. Gerard Kuiper’s discovery of methane (CH<sub>4</sub>) around Titan provided conclusive evidence that Titan possesses an atmosphere [Kuiper, 1944].

During the 1970s, analyses of ground-based infrared spectra began to provide constraints on the temperature structure [Morrison *et al.*, 1972; Danielson *et al.*, 1973] and composition [Trafton, 1972a, b; Gillett *et al.*, 1973; Gillett, 1975] of Titan’s atmosphere. The detection of a greenhouse effect [Morrison *et al.*, 1972] coupled with detailed investigations of the spectral features of CH<sub>4</sub> [Trafton, 1972b; Lutz *et al.*, 1976] led to the conclusion that CH<sub>4</sub> might be only a minor constituent in Titan’s atmosphere and that other absorbers, such as C<sub>2</sub>H<sub>6</sub> or some type of dust particle, might be present [Daniel-

*son et al.*, 1973]. The presence of N<sub>2</sub> in Titan's atmosphere was first suggested by *Lewis* [1971] based on the idea that Titan accreted NH<sub>3</sub> during formation, which later photolyzed to form N<sub>2</sub>. Photochemical models predicted significant abundances of C<sub>2</sub>H<sub>2</sub> and C<sub>2</sub>H<sub>6</sub> [Strobel, 1974; *Allen et al.*, 1980], although only a few models included N<sub>2</sub> and nitrogen chemistry [*Atreya et al.*, 1978]. The encounter of Pioneer 11 with Titan in 1979 confirmed the presence of an aerosol absorber in the atmosphere [Tomasko, 1980] and provided a lower limit of 1.37 g/cm<sup>2</sup> on Titan's density [Smith, 1980]. The encounters of Voyager 1 and 2 with Titan in the early 1980s confirmed that Titan possesses a substantial N<sub>2</sub> atmosphere, with a surface pressure 1.5 times that of Earth and a surface temperature of 94 K [Broadfoot *et al.*, 1981; Lindal *et al.*, 1983; Hunten *et al.*, 1984]. Infrared spectra taken by the Voyager spacecraft revealed the presence of a variety of organic molecules (C<sub>2</sub>H<sub>2</sub>, C<sub>2</sub>H<sub>4</sub>, C<sub>2</sub>H<sub>6</sub>, C<sub>3</sub>H<sub>8</sub>, CH<sub>3</sub>C<sub>2</sub>H, C<sub>4</sub>H<sub>2</sub>, etc.) [Hanel *et al.*, 1981; Kunde *et al.*, 1981] and provided the first glimpse of the complexity of the chemical and physical processes occurring in Titan's atmosphere.

Despite providing an enormous amount of new information about Titan's atmosphere, Titan's thick photochemical haze and abundant methane prevented the instruments carried by Pioneer 11 and the Voyager spacecraft from seeing Titan's surface. Images beamed back to Earth as the spacecraft sped through the Saturnian system showed only a featureless orange ball, providing no hint of the incredible landscape below. It remained shrouded for another 23 years until the arrival of the Cassini-Huygens mission in 2004.

The arrival of the Cassini-Huygens mission to the Saturn system ushered in a new era in the study of Titan. Carrying a variety of instruments capable of remote sensing and *in situ* investigations of Titan's atmosphere and surface, the Cassini Orbiter and the Huygens

Probe have provided a wealth of new information about Titan and have finally allowed humankind to see the surface. Perhaps more so than anywhere else in the solar system, Titan's atmosphere and surface are intimately linked. As discussed in detail below, the organic material transported to form Titan's extensive sand seas was formed initially by chemical and physical processes in the atmosphere, the liquids that carve out dendritic channels like those seen at the Huygens landing site cycle between the atmosphere and the surface (in the case of methane) or are produced by chemistry in the atmosphere (in the case of ethane, propane, hydrogen cyanide, etc). Long term climate cycles result in the observed asymmetry of lakes and seas on the surface [Aharonson *et al.*, 2009].

Cryovolcanism may resupply methane and other gases to the atmosphere.

Here I review our current understanding of Titan's atmosphere and climate forged from the powerful combination of Earth-based observations, remote sensing and *in situ* space-craft measurements, laboratory experiments, and models. I conclude with a discussion of some of our remaining unanswered questions as the incredible era of exploration with Cassini-Huygens comes to an end.

## 2. Titan's atmospheric structure and composition

The two main constituents of Titan's atmosphere are molecular nitrogen ( $N_2$ ) and methane ( $CH_4$ ). Titan receives about 1% of the solar flux that reaches Earth. Of the flux incident at the top of Titan's atmosphere, only 10% reaches the surface (compared to 57% for Earth) (see e.g., *Griffith et al.* [2012a]; *Read et al.* [2015]). Titan is therefore much colder than Earth, with an effective temperature of  $\sim 82$  K. The combination of the greenhouse effect provided by  $CH_4$  and collision induced absorption ( $N_2-N_2$ ,  $N_2-CH_4$ ,  $N_2-H_2$ ) and the anti-greenhouse from the stratospheric haze layer [*McKay et al.*, 1991] results

in a surface temperature of approximately 94 K [*Lindal et al.*, 1983; *Fulchignoni et al.*, 2005; *Schinder et al.*, 2011]. The pressure at Titan's surface is  $\sim$ 1.5 bar [*Lindal et al.*, 1983; *Fulchignoni et al.*, 2005] resulting in surface conditions that are near the triple point of methane, much like water on Earth, which allows for liquid methane on the surface and gaseous methane in the atmosphere. The fluvial and aeolian features on the surface, discussed in Section 7 indicate that Titan has an active “hydrological” cycle that is, in many ways, both very similar to and very different from that of Earth. In addition to the features observed on the surface, large storms occasionally erupt in Titan's atmosphere and are presumably responsible for many of the fluvial features.

## 2.1. Temperature structure

The vertical temperature structure in Titan's atmosphere (see Figure 1) is most analogous to that of Earth, with well defined tropo-, strato-, meso-, and thermospheres (see e.g., *Smith et al.* [1982b]; *Lindal et al.* [1983]; *Hubbard et al.* [1990]; *Sicardy et al.* [1990]; *Fulchignoni et al.* [2005]). Although Titan's atmosphere is colder than Earth's, Titan's atmosphere is more extended, with scale heights of 15 to 50 km compared to 5 to 8 km on Earth due to Titan's lower gravity [*Flasar et al.*, 2014]. Finer scale structure in temperature measurements attributed to atmospheric waves has also been observed throughout the atmosphere (see e.g., *Sicardy et al.* [1999]; *Fulchignoni et al.* [2005]; *Müller-Wodarg et al.* [2006]; *Sicardy et al.* [2006]; *Strobel* [2006]; *Zalucha et al.* [2007]; *Aboudan et al.* [2008]; *Koskinen et al.* [2011]; *Lorenz et al.* [2014a]). Temperatures in the thermosphere are similar to those in the mesosphere, despite the significant EUV heating rates in the thermosphere, due to efficient cooling by HCN rotational lines [*Yelle*, 1991].

The thermal structure of the upper atmosphere is more variable and complex than expected and there are still a number of outstanding questions regarding its variability. On average the night side is warmer than the day side [Müller-Wodarg *et al.*, 2006; *de La Haye et al.*, 2007; *Cui et al.*, 2009; *Westlake et al.*, 2011; *Snowden et al.*, 2013]. There does not seem to be any correlation between temperature and latitude indicating that solar input does not control the temperature [Yelle *et al.*, 2014]. Additionally, the highest temperatures are seen when Titan is inside Saturn's magnetosphere, while the coldest temperatures are measured when Titan is outside the magnetosphere [*Westlake et al.*, 2011; *Snowden et al.*, 2013].

The temperature profile measured by the Huygens Atmospheric Structure Instrument (HASI) finally constrained the location of Titan's planetary boundary layer (PBL), which is important for understanding surface-atmosphere interactions. Analyses of the HASI data find that the PBL is located at 300 m [Fulchignoni *et al.*, 2005; Tokano *et al.*, 2006a], which was incompatible with analyses of other temperature measurements [Lindal *et al.*, 1983; Schinder *et al.*, 2011] and dune spacing [Lorenz *et al.*, 2010] that find the PBL is located at 2-3 km. The General Circulation Model (GCM) of Charnay and Lebonnois [2012] showed that Titan should have two PBLs, a seasonal one located at 2 km and a diurnal one that reaches up to 800 m over the course of a day and the Huygens' measurement at 300 m is consistent with the mid-morning arrival of the Huygens Probe. The presence of diurnal and seasonal boundary layers indicates that Titan's troposphere is more dynamic than previously thought.

## 2.2. Methane abundance

Deep in the troposphere and at the surface, the CH<sub>4</sub> mixing ratio is obtained only by *in situ* measurements and the Gas Chromatograph Mass Spectrometer (GCMS) carried by Huygens found the methane mixing ratio at the surface to be  $5.65 \pm 0.18\%$  [Niemann *et al.*, 2010]. This value is consistent with estimates made from spectra taken by the Descent Imager/Spectral Radiometer (DISR) in the last 25 m of the descent [Schröder and Keller, 2008; Jacquemart *et al.*, 2008]. The mixing ratio is constant within the error bars until about 7 km where it decreases with altitude until near 45 km where it is constant throughout the rest of the GCMS measurements (up to 140 km). The decrease is a result of condensation and the temperature at the tropopause limits the methane mixing ratio in the stratosphere. Unfortunately, this profile is limited to a single location at a single point in time (10.3°S 167.7°W, 14 January 2005), and there is some evidence of tropospheric methane variations of  $\sim 10\text{--}40\%$  [Tokano, 2014; Ádámkovics *et al.*, 2016]. The average stratospheric value from GCMS is  $1.48 \pm 0.09\%$ , which is consistent with initial determinations of the stratospheric methane mixing ratio from the Composite Infrared Spectrometer (CIRS) ( $1.6 \pm 0.5\%$ , Flasar *et al.* [2005]) and DISR [Bézard, 2014]. However, measurements from the Cassini Visible and Infrared Mapping Spectrometer (VIMS) ( $1.28 \pm 0.06\%$ , Maltagliati *et al.* [2015]) and Herschel SPIRE ( $1.33 \pm 0.07\%$ , Courtin *et al.* [2011]) and PACS ( $1.29 \pm 0.03\%$ , Rengel *et al.* [2014]) find lower stratospheric values. Recent analyses of Cassini CIRS measurements find variation with latitude from 1% at low latitudes to 1.5% at polar latitudes, indicating that the methane mixing ratio in the stratosphere may be more complicated than previously thought [Lellouch *et al.*, 2014]. In the mesosphere composition is measured by stellar/solar UV occultation or UV

dayglow and the CH<sub>4</sub> profile was measured by Voyager UVS (Ultraviolet Spectrometer) [Smith *et al.*, 1982a; Vervack *et al.*, 2004] and the Cassini Ultraviolet Imaging Spectrograph (UVIS) [Shemansky *et al.*, 2005; Koskinen *et al.*, 2011; Stevens *et al.*, 2015]. The mesospheric methane abundance appears to be relatively constant with altitude until it begins diffusively separating around 900 km [Koskinen *et al.*, 2011; Capalbo *et al.*, 2013; Stevens *et al.*, 2015]. From 950 to 1500 km, the CH<sub>4</sub> mixing ratio is measured by the Ion and Neutral Mass Spectrometer (INMS) [Müller-Wodarg *et al.*, 2008; Magee *et al.*, 2009; Cui *et al.*, 2009] and varies from 1.31% at 981 km to 3% at 1150 km. These results are also consistent with UVIS EUV occultation measurements that probe up to 1600 km [Kammer *et al.*, 2013; Capalbo *et al.*, 2015].

### 2.3. Voyager and Earth-based composition measurements

The Infrared Radiometer Interferometer and Spectrometer (IRIS) carried by Voyager first revealed the complexity of Titan's atmospheric chemistry with the measurements of methane (CH<sub>4</sub>), molecular hydrogen (H<sub>2</sub>), ethane (C<sub>2</sub>H<sub>6</sub>), acetylene (C<sub>2</sub>H<sub>2</sub>), ethylene (C<sub>2</sub>H<sub>4</sub>), hydrogen cyanide (HCN), methylacetylene (C<sub>3</sub>H<sub>4</sub>), propane (C<sub>3</sub>H<sub>8</sub>), diacetylene (C<sub>4</sub>H<sub>2</sub>), cyanoacetylene (HC<sub>3</sub>N), cyanogen (C<sub>2</sub>N<sub>2</sub>), and carbon dioxide (CO<sub>2</sub>) [Hanel *et al.*, 1981; Kunde *et al.*, 1981; Samuelson *et al.*, 1981, 1983]. In the decades between the Voyager encounters and Cassini-Huygens' arrival in the Saturn system, carbon monoxide (CO) (Lutz *et al.* [1983], Mayall Telescope Kitt Peak), acetonitrile (CH<sub>3</sub>CN) (Bézard *et al.* [1993]; Marten *et al.* [2002], IRAM 30 m), water (H<sub>2</sub>O) (Coustonis *et al.* [1998], ISO), and benzene (C<sub>6</sub>H<sub>6</sub>) ([Coustonis *et al.*, 2003], ISO) were discovered using Earth-based telescopes. Earth-based telescopes have continued to discover new molecules in Titan's atmosphere during the Cassini-Huygens mission; Herschel measurements revealed the presence

of hydrogen isocyanide (HNC) [Moreno *et al.*, 2011] and ethyl cyanide ( $C_2H_5CN$ ) was discovered in measurements from the Atacama Large Millimeter Array (ALMA) [Cordiner *et al.*, 2015], demonstrating the capabilities and importance of Earth-based observations.

#### 2.4. Composition measurements from Cassini-Huygens

Cassini-Huygens carries a powerful combination of remote sensing and *in situ* instruments allowing for detection and measurement of gas phase species and characterization of aerosol particles from the troposphere to the ionosphere. CIRS has provided the temporal and spatial measurements of Titan's stratosphere necessary to understand the small molecule chemistry and constrain dynamics and seasonal change. CIRS also discovered propene ( $C_3H_6$ ) [Nixon *et al.*, 2013a]. UVIS senses the previously unexplored mesosphere providing composition and temperature information necessary to complete our understanding of Titan's atmospheric structure. As discussed in Section 8, GCMS and INMS are particularly important because they measure noble gases and  $^{14}N/^{15}N$  in nitrogen, which are powerful tools for understanding the origin and evolution of atmospheres but cannot be detected from remote sensing. Additionally, the GCMS carried to the surface and INMS and CAPS carried by the orbiter allow us to measure regions of the atmosphere that cannot be accessed with remote sensing due to density. Numerous previously undetected species have been identified in measurements obtained by the Ion and Neutral Mass spectrometer in Titan's thermosphere [Vuitton *et al.*, 2007, 2008; Cui *et al.*, 2009]. A list of molecules detected in Titan's atmosphere by Voyager, Cassini-Huygens, and ground-based telescopes is found in Table 1. In particular, analyses of INMS data have discovered previously undetected nitrogen bearing molecules including  $HC_5N$ ,  $NH_3$ ,  $C_2H_3CN$ , etc. indicating that nitrogen plays a more prominent role in Titan's atmospheric chemistry than

previously thought [*Vuitton et al.*, 2007]. It is now clear that our pre-Cassini understanding of Titan atmospheric chemistry underestimated the chemical complexity of Titan's upper atmosphere. However, the limited mass range of INMS (1-100 Da/q) does not allow for characterization of the larger molecules that are certainly involved in aerosol formation.

The vertical profiles of molecular abundances have also been investigated in the stratosphere by CIRS and the mixing ratios of most species increase with altitude, which is a characteristic of molecules produced by photochemistry at higher altitudes that then condense in the lower stratosphere or at the tropopause (near 40 km where the temperature reaches a minimum of 70 K [*Fulchignoni et al.*, 2005]) [*Vinatier et al.*, 2007, 2010a]. This trend generally continues into the mesosphere and thermosphere as confirmed by VIMS, UVIS, and INMS measurements (see e.g., *Adriani et al.* [2011]; *Koskinen et al.* [2011]; *Vuitton et al.* [2007]; *Cui et al.* [2009]; *Magee et al.* [2009]). Representative measurements from some of these instruments are shown in Figure 2. Latitudinal and seasonal variations will be discussed in Section 5.

In general, the vertical profiles of the trace species are well understood. One exception is the abundance of H<sub>2</sub>. The tropospheric value ( $1 \times 10^{-3}$ , *Niemann et al.* [2010]) and thermospheric values ( $3.72 \times 10^{-3}$  at 1025 km, *Yelle et al.* [2008]; *Cui et al.* [2009]) are incompatible by a factor of 2 [*Strobel*, 2010], implying a downward flux of H<sub>2</sub> that is comparable to the escape flux. Measurements from CIRS and IRIS [*Samuelson et al.*, 1981; *Courtin et al.*, 1995, 2012] are consistent with the results from GCMS in the regions where they overlap [*Courtin et al.*, 2012]. This result is surprising given the long chemical lifetime and enormous escape flux of H<sub>2</sub> [*Strobel*, 2010, 2012]. *Courtin et al.* [2012] find a

non-uniform distribution of H<sub>2</sub> in the troposphere with an enhancement at high northern latitudes; this variation was not expected and may provide information required to resolve the apparent contradiction between the tropospheric and thermospheric measurements.

Perhaps one of the most surprising and significant discoveries from Cassini has been the discovery of very heavy ions in Titan's upper atmosphere. Although INMS can only measure masses up to 100 Da/q, CAPS is able to detect much heavier masses, albeit at very low resolution. CAPS/ELS (Electron spectrometer) has measured negative ions up to  $\sim$ 10,000 Da/q [Coates *et al.*, 2007, 2009]! The higher mass negative ions are observed preferentially at low thermospheric altitudes ( $\sim$ 950 km) and tend to increase in mass with depth, at high latitudes, and in the region of the terminator [Coates *et al.*, 2009, 2010]. The extremely low mass resolution of the spectra has precluded identification of all but a few of the negative ions, CN<sup>-</sup>, C<sub>3</sub>N<sup>-</sup>, and C<sub>5</sub>N<sup>-</sup> [Vuitton *et al.*, 2009a]. CAPS/IBS (Ion Beam Spectrometer) has detected positive ions with masses up to 350 Da/q, that appear to have regular spacing between 12 and 14 Da, which indicates they are likely organic [Crary *et al.*, 2009]. INMS data below 100 Da/q has been compared to the CAPS/IBS measurements and the composition has been estimated to include mostly aromatic compounds including naphthalene (C<sub>10</sub>H<sub>8</sub><sup>+</sup>) and anthracene (C<sub>14</sub>H<sub>10</sub><sup>+</sup>) in addition to some heteroaromatics [Waite *et al.*, 2007; Crary *et al.*, 2009]. Delitsky and McKay [2010] argue that based on thermodynamics and laboratory experiments, high temperature reactions produce fused ring polycyclic aromatic hydrocarbons (PAHs) while low temperature reactions will result in the formation of polyphenyls and accordingly some of the peaks in the CAPS spectrum could be biphenyl (154 Da), terphenyl (230 Da), and quaterphenyl (306 Da). Fullerenes have also been suggested as candidates for the negative ions [Sittler

*et al.*, 2009]. An unidentified feature at 3.28  $\mu\text{m}$  in mesospheric measurements from VIMS [Dinelli *et al.*, 2013] has been attributed to a collection of PAHs with an average mass of 430 Da [López-Puertas *et al.*, 2013]. However, unambiguous identifications in this mass range will require a higher resolution mass spectrometer on a future mission. These large ions represent the transition from small gas phase molecules to haze particles; an ion with a mass of 10,000 Da could be a particle with a radius of  $\sim$ 1.5 nm [Lavvas *et al.*, 2013], and therefore understanding the haze will require more information about these ions.

### 3. Complex organic chemistry

#### 3.1. Energy sources

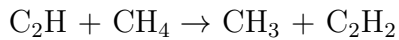
Energetic particles and solar ultraviolet photons dissociate and ionize N<sub>2</sub> and CH<sub>4</sub> initiating chemical reactions that result in the irreversible destruction of CH<sub>4</sub> leading to the formation of H<sub>2</sub> and a wealth of other complex organic molecules including the hydrocarbons and nitriles described above. The subsequent aggregation and heterogeneous chemistry of these molecules produce the aerosols responsible for Titan's characteristic orange color and distinctive haze layers. A schematic of the processes occurring in Titan's atmosphere is shown in Figure 1.

There are a number of sources of ionization and dissociation in Titan's atmosphere: solar EUV and UV photons, energetic photoelectrons (resulting from solar X-ray and EUV photons), electrons from the Saturnian magnetosphere, other energetic ions (protons, oxygen), metallic ions created by micrometeorite ablation, and galactic cosmic rays (GCRs). Constraints on the energy available to drive chemical reactions and dynamics are of paramount importance for understanding Titan's atmosphere; instruments carried by Cassini-Huygens have significantly improved our knowledge of the distribution and rel-

ative importance of different sources of ionization and dissociation. The electron density can be measured by the Permittivity, Waves, and Altimetry analyzer (PWA) (40 to 140 km, *Hamelin et al.* [2007]; *López-Moreno et al.* [2008]), radio occultations (above 120 km, *Kliore et al.* [2008]), Radio and Plasma Wave Science (RPWS) (above 950 km, *Wahlund et al.* [2005]), and the Cassini Plasma Spectrometer (CAPS) (ionosphere, *Coates et al.* [2007, 2010]). Additionally, UVIS measurements of EUV and FUV emissions [*Ajello et al.*, 2007, 2008] place constraints on the N\* and N+\* densities (\* indicates excited states), which are dissociation fragments of N<sub>2</sub>. These instruments find that electron densities peak near 1200 km on the day side ( $2\text{-}4 \times 10^3 \text{ cm}^{-3}$ , compared to  $4\text{-}10 \times 10^2 \text{ cm}^{-3}$  on the night side) [*Ågren et al.*, 2009]. Day side ionization is dominated by solar photons, whereas night side ionization is dominated by Saturnian magnetospheric electrons [*Ågren et al.*, 2009; *Galand et al.*, 2010]. Energetic protons and oxygen ions are also a source of ionization from 500 to 1000 km [*Cravens et al.*, 2008] and micrometeorite ablation results in ion formation from 500 to 700 km [*Molina-Cuberos et al.*, 2001; *Kliore et al.*, 2008]. A secondary peak in the electron distribution is observed at 59 km ( $0.5\text{-}1 \times 10^3 \text{ cm}^{-3}$ ) [*Hamelin et al.*, 2007; *López-Moreno et al.*, 2008] that results from the deposition of GCRs, which is comparable in ionization to solar photons in the upper atmosphere [*Gronoff et al.*, 2009]. Note that based on measurements from Cassini's magnetometer, Titan does not currently have an internal magnetic field [*Backes et al.*, 2005].

The dominant source of energy to drive chemistry on Titan is solar photons, which are responsible for about 90% of N<sub>2</sub> destruction [*Lavvas et al.*, 2011a]. N<sub>2</sub> is the dominant source of absorption for photons with energies greater than 12.4 eV (100 nm), CH<sub>4</sub> for photons between 8.56 (145 nm) and 12.4 eV (100 nm), and the less energetic photons

penetrate deeper in the atmosphere where they are absorbed by species produced from chemistry like C<sub>2</sub>H<sub>2</sub> and C<sub>4</sub>H<sub>2</sub> [Lavvas *et al.*, 2011a]. C<sub>2</sub>H<sub>2</sub> is particularly important because it absorbs above 5.17 eV (240 nm), a region where there is a significant photon flux. C<sub>2</sub>H<sub>2</sub> and C<sub>4</sub>H<sub>2</sub> play a particularly interesting role in photodissociation of methane. They absorb photons at lower energies than CH<sub>4</sub> and dissociate to form C<sub>2</sub>H or C<sub>4</sub>H, respectively, which then react with methane to produce methyl radicals (CH<sub>3</sub>) and C<sub>2</sub>H<sub>2</sub> and C<sub>4</sub>H<sub>2</sub> as shown below:



In this way, C<sub>2</sub>H<sub>2</sub> and C<sub>4</sub>H<sub>2</sub> behave as catalysts for methane destruction using photons that methane does not absorb and destroying methane in the stratosphere, much deeper than direct photolysis of CH<sub>4</sub> (see e.g., Yung *et al.* [1984]).

### 3.2. Atmospheric Chemistry

Photochemical models of Titan's atmosphere prior to Voyager predicted the presence of organic molecules resulting from CH<sub>4</sub> photochemistry [Strobel, 1974; Atreya *et al.*, 1978; Allen *et al.*, 1980]. The post-Voyager model of Yung *et al.* [1984] approximately reproduced many of the observed column densities from Voyager but numerous reaction rates and products had to be estimated due to lack of experimental data and altitude profiles were not yet available from observations for comparison. In the decades between Voyager and Cassini-Huygens, improvements in reaction rate networks and improved observational constraints from analysis of Voyager data and Earth-based observations led to continued improvements in photochemical models (see e.g., Toublanc *et al.* [1995]; Lara *et al.* [1996]; Wong *et al.* [2002]). In preparation for Cassini-Huygens, Wilson and Atreya [2004] de-

veloped a model that included the ionosphere and therefore included some ion chemistry, resulting in improved fits to pre-Cassini measurements.

One significant set of measurements from Cassini-Huygens are the composition measurements from mass spectrometry in the troposphere and thermosphere that have provided our first real constraints on the eddy diffusion profile in those regions of Titan's atmosphere [Yelle *et al.*, 2008; Bell *et al.*, 2010; Cui *et al.*, 2012; Mandt *et al.*, 2012; Li *et al.*, 2014], which is important because it determines the amount of time species spend in a given region of the atmosphere affecting their loss to reaction, photolysis, and condensation. For example, the relatively low eddy diffusion coefficient in the lower atmosphere allows large amounts of photochemically generated products to build up in the stratosphere, because transport to the deeper atmosphere where they are removed by condensation is slow; even so, as shown in Figure 3 condensation is one of the main loss processes for molecules in Titan's atmosphere. The amount of material deposited on the surface varies depending on the model but in general models agree that liquids are more abundant than solids (by factors ranging from 1.5 to 14 depending on the model, Vuitton *et al.* [2014]) and over the age of the solar system would produce a global layer of liquid a few hundred meters deep composed primarily of ethane with a layer of solids tens of meters deep. While these estimates are lower than predicted by post-Voyager models [Lunine *et al.*, 1983], they are still greater than what is observed on the surface as discussed in Section 7.

Another significant improvement in our ability to model the chemistry in Titan's atmosphere comes from the characterization of aerosols discussed in Section 3.3; the distribution, size, and optical properties information obtained from Cassini-Huygens is an

important input to any models of radiative transport in Titan's atmosphere and allows for more accurate treatment of photochemistry in models.

Photochemical models are now able to reproduce the observed abundances of most of the small (less than 100 Da) molecules in Titan's atmosphere (see e.g., *Vuitton et al.* [2007]; *Hörst et al.* [2008]; *Lavvas et al.* [2008a, b]; *Vuitton et al.* [2008]; *Yelle et al.* [2010]; *Krasnopolsky* [2012]; *Vuitton et al.* [2012]; *Westlake et al.* [2012]; *Hébrard et al.* [2013]; *Dobrijevic et al.* [2014]; *Li et al.* [2015]; *Dobrijevic et al.* [2016]) but the formation of heavier molecules is not well understood. Figure 3 shows a summary of the major production and loss pathways for 10 of the most abundant photochemically produced molecules in Titan's atmosphere (see extensive discussion in *Vuitton et al.* [2014]).

Models generally agree that for the most part the hydrocarbon chemistry is driven by neutral reactions. However, to reproduce the INMS data, models need to take into account ion reactions as some species that are partially produced in the ionosphere, such as benzene ( $C_6H_6$ ), may result from ion chemistry ( $C_6H_7^+ + e^- \rightarrow C_6H_6 + H$ ) [*Vuitton et al.*, 2008]. The nitrile chemistry begins with formation of HCN through neutral reactions and proceeds through the formation of CN from photolysis of HCN. CN can then react with acetylene or ethylene to produce cyanoacetylene or acrylonitrile respectively. Like benzene, formation of ammonia ( $NH_3$ ) in the upper atmosphere seems to rely on the coupling of ion and neutral chemistry [*Yelle et al.*, 2010].

The oxygen containing molecules present in Titan's atmosphere (CO,  $CO_2$ , and  $H_2O$ ) were discovered by Voyager and Earth-based telescopes [*Samuelson et al.*, 1983; *Lutz et al.*, 1983; *Coustenis et al.*, 1998], but their origin was uncertain. CO is a remarkably stable molecule, and its discovery in Titan's atmosphere [*Lutz et al.*, 1983] led to inves-

tigations into whether the observed abundance is a primordial remnant, is supplied to the atmosphere from the interior or surface, or is delivered to the atmosphere from an external source. The existence of remnant primordial CO would place useful constraints on models for the origin and evolution of Titan in the Saturnian nebula as discussed in Section 8. Pre-Cassini models were unable to simultaneously reproduce the abundances of all three oxygen bearing species. CAPS measurements revealed a previously unknown source of oxygen in Titan's atmosphere, an external flux of O<sup>+</sup> ions [Hartle *et al.*, 2006] flowing into the top of Titan's atmosphere, most likely from Enceladus. Hörst *et al.* [2008] demonstrated that this previously unknown source explains the presence of oxygen bearing species and the plumes of Enceladus are likely responsible for the fourth most abundant molecule in Titan's atmosphere (CO), revealing a unique connection between two very different moons in the Saturnian system. Subsequent measurements of H<sub>2</sub>O [Cotterini *et al.*, 2012; Moreno *et al.*, 2012; Rengel *et al.*, 2014] have shown some disagreement with their model and further refinement may be necessary [Krasnopolsky, 2012; Moreno *et al.*, 2012; Dobrijevic *et al.*, 2014; Lara *et al.*, 2014]. The oxygen bearing species are unique in Titan's atmosphere because they include photochemically produced molecules that span atmospheric lifetimes of ~10 yrs (H<sub>2</sub>O) to ~1 Gyr (CO) [Hörst *et al.*, 2008]; as such they provide an important opportunity to test photochemical models of Titan's atmosphere.

The O<sup>+</sup> ions observed by CAPS are deposited near 1100 km altitude, in the same region as the very heavy ions observed by CAPS. The addition of an oxygen source to complex organic compounds leads to the exciting possibility that molecules of prebiotic interest may form. Experiments indicate that amino acids and nucleobases may form

under Titan atmospheric conditions [Hörst *et al.*, 2012], but the instruments carried by Cassini-Huygens do not have a large enough mass range or sufficiently high resolution to detect such molecules.

The major positive ions in Titan's atmosphere are produced mostly through ion-molecule reactions that begin with  $\text{CH}_3^+$  that form from direct ionization or charge transfer with  $\text{N}_2^+$ .  $\text{HCNH}^+$  forms from  $\text{N}^+ + \text{CH}_4$  or from proton transfer to HCN. Indeed a number of positive ion species form via proton transfer to abundant neutral species (see e.g., Keller *et al.* [1998]; Vuitton *et al.* [2007]; Carrasco *et al.* [2008]; Vuitton *et al.* [2008]).

The presence of negative ions in Titan's ionosphere was not expected. Models of the troposphere looked at ion formation by electron attachment to radicals, which requires a three body collision and is therefore unlikely at the very low pressures in the ionosphere (see e.g., Capone *et al.* [1976]; Borucki *et al.* [1987]; Molina-Cuberos *et al.* [2000]). However, as discussed above, negative ions with m/z up to 10,000 Da/q have been measured by CAPS. The model of Vuitton *et al.* [2009a] finds that  $\text{CN}^-$  forms from dissociative electron attachment on HCN and  $\text{HC}_3\text{N}$  and  $\text{C}_3\text{N}^-$  forms from proton transfer of  $\text{HC}_3\text{N}$  to  $\text{CN}^-$ . The negative ion chemistry on Titan has numerous sources of uncertainty: identifications from the CAPS measurements are difficult due to the low resolution of the instrument and lack of experimental measurements and/or theoretical calculations for negative ion production and destruction [Vuitton *et al.*, 2014].

Photochemical models of Titan's atmosphere generally only include species containing CHON atoms as those are the only ones thus far detected. Upper limits on  $\text{PH}_3$  and  $\text{H}_2\text{S}$  were obtained from Cassini CIRS [Nixon *et al.*, 2013b] and additional efforts using ALMA to search for sulfur-bearing species are ongoing. Photochemical models indicate that

better constraints on sulfur-bearing species may provide insight regarding external sources of material to Titan's atmosphere such as Enceladus, micrometeorites, and comets [Hickson *et al.*, 2014]. Phosphorous and sulfur, in addition to CHON, are important from an astrobiological perspective and to improve our understanding of Titan's formation and evolution.

Improvements in understanding Titan's atmospheric chemistry require additional experiments and theoretical calculations. Models and experiments show that heterogeneous chemistry on the surfaces of aerosol particles may affect the gas phase composition (through adsorption, reaction with liquid/solid phase, and/or release of new gas phase species) [Bakes *et al.*, 2003; Lebonnois *et al.*, 2003; Lebonnois, 2005; Lavvas *et al.*, 2008b; Krasnopolsky, 2009] but current models tend to include few, if any, of these processes. Modeling ionospheric chemistry is particularly challenging because it is difficult for experiments to access the conditions in Titan's upper atmosphere and therefore models lack numerous necessary measurements. The lack of measurements often leads people to ignore entire classes of reactions, such as dissociative electron attachment [Vuitton *et al.*, 2009a] and radiative association reactions [Vuitton *et al.*, 2012] that turn out to be important when later included. Efforts to understand the largest sources of uncertainty in models will help focus limited resources on reactions that have the greatest impact (see e.g., Hébrard *et al.* [2005, 2013]; Dobrijevic *et al.* [2014]). Given the wealth of composition information from Cassini-Huygens, 3-D models will play an important role in improving our understanding of many of the seasonal changes discussed in Section 5.

### 3.3. Photochemical haze

#### 3.3.1. Observations

A brief note about nomenclature- the word aerosol refers to any particle suspended in a gas and is therefore the most general term to use to describe particles in Titan's atmosphere. Here "cloud" will be used to refer to a collection of particles that form by condensation of species in Titan's atmosphere (and may be solid or liquid phase). Haze will be used to refer to the photochemically generated involatile particles in Titan's atmosphere. It is often the case that "tholin" is used interchangeably with haze in the literature. However, for the sake of clarity, tholin is used here only to refer to laboratory generated analogues to Titan's photochemical haze (see *Cable et al.* [2012]).

The presence of an aerosol absorber in Titan's atmosphere was strongly suspected prior to the arrival of Pioneer 11 and the Voyager spacecraft based on ground-based observations that found a low geometric albedo in the ultraviolet [Caldwell, 1975], a temperature inversion inferred from IR spectra [Gillett, 1975], significant scattering in the atmosphere based on the morphology of the methane bands [Trafton, 1975], and the inability to reproduce the optically thick atmosphere in the visible seen through polarization measurements using only gaseous absorbers [Everka, 1973; Zellner, 1973]. Images and polarization measurements from Pioneer 11 and Voyager 1 and 2 further constrained the properties of the aerosols in Titan's atmosphere and in combination with models suggested that Titan's aerosols are composed of organic material [Rages and Pollack, 1980] and are fractal aggregates because two conflicting size dimensions (radii less than 0.1  $\mu\text{m}$  and greater than 0.2  $\mu\text{m}$ ) were required to fit the data [Rages et al., 1983; Tomasko, 1980; West et al., 1983; Hunten et al., 1984; West, 1991; West and Smith, 1991]. Images taken by Voyager 1 and 2 also revealed a North-South asymmetry in the haze with a  $\sim$ 25% decrease in brightness at blue wavelengths observed in the northern hemisphere [Smith et al., 1981, 1982a]. Ver-

tical structure in the haze profile was also discovered in these images, including a detached haze layer between 340 and 360 km [Rages and Pollack, 1983].

Prior to the arrival of Cassini-Huygens, it was generally assumed that haze formed where it was observed, in the stratosphere [Sagan and Thompson, 1984; McKay *et al.*, 2001; Lebonnois *et al.*, 2002; Wilson and Atreya, 2003]; instead, we now know that particles are present from Titan's surface to the ionosphere. Photochemically generated haze is the dominant source of opacity short of  $5 \mu\text{m}$  but is optically thin in the IR and therefore plays a key role in the radiative balance and dynamics of Titan's atmosphere, acting to cool the surface while heating the stratosphere. The particles also affect and are affected by gas phase chemistry and can serve as condensation nuclei for cloud formation. Particles play a key role in atmospheric processes from the ionosphere to the surface, as discussed below.

As shown in Figure 4, stellar occultation measurements by UVIS revealed particles up to 1000 km [Liang *et al.*, 2007; Koskinen *et al.*, 2011] and allowed retrieval of aerosol extinction coefficients up to 850 km [Koskinen *et al.*, 2011]. Near-IR stellar and solar occultations observed by Cassini VIMS show evidence of fractal aggregates at altitudes above where DISR obtained measurements, a feature at  $3.4 \mu\text{m}$  attributed to hydrocarbons that is not seen in laboratory analogues (discussed below), and a lack of NH and CN features at 3 and  $4.6 \mu\text{m}$ , respectively, indicating that Titan's aerosol particles may have less nitrogen than their laboratory analogues [Bellucci *et al.*, 2009; Kim *et al.*, 2011; Sim *et al.*, 2013; Kim and Courtin, 2013]. They identify  $\text{CH}_4$ ,  $\text{C}_2\text{H}_6$ ,  $\text{CH}_3\text{CN}$ ,  $\text{C}_5\text{H}_{12}$ ,  $\text{C}_6\text{H}_{12}$ , and  $\text{C}_6\text{H}_{14}$  as possible constituents based on the VIMS measurements from  $\sim 60$ -500 km [Kim *et al.*, 2011; Sim *et al.*, 2013; Kim and Courtin, 2013]. Analysis of VIMS

solar occultation measurements from 250-700 km show composition variations that may indicate aerosol aging and/or condensation onto particles as the particles become more aliphatic in character with decreasing altitude [*Courtin et al.*, 2015].

Below 300 km the haze is ubiquitous; though the distribution of particles varies as a function of altitude and latitude it does not vary spectrally in the far- and mid-IR indicating that chemical evolution measurable by CIRS is not occurring at a rate fast enough to compete with dynamics below 300 km (see e.g., *Anderson and Samuelson* [2011]; *Vinatier et al.* [2010b, 2012]). The rate of dynamical mixing is not sufficient to homogenize the particle distribution though so it seems likely that most of the significant aerosol chemistry is occurring above 300 km. This is generally consistent with our understanding of chemical processes in Titan's atmosphere although it is potentially surprising given that gas phase chemistry still occurs at these altitudes. Measurements from CIRS and VIMS find that the signature of C-H and C-C bonds dominate the spectrum [*Rannou et al.*, 2010; *Vinatier et al.*, 2012].

DISR provided the first ground truth on Titan's aerosol properties by measuring the absorption and scattering properties of the aerosols as a function of altitude. Many layers of condensates were predicted to form just above the temperature minimum at  $\sim 44$  km (see e.g., [*Sagan and Thompson*, 1984]), however no distinct layers were observed with DISR in that region [*Tomasko et al.*, 2005]. Their measurements are fit well by aerosol particles that are fractal aggregates composed of 4000 monomers with radii of 0.04 microns [*Tomasko et al.*, 2008, 2009]. DISR did not observe a significant vertical variation in the monomer size over their measurement range (surface to 140 km) [*Tomasko et al.*, 2008]. Below 80 km, the observed change in the wavelength dependence of the optical depth

and the single scattering albedo is attributed to the addition of condensate [Tomasko *et al.*, 2009; Doose *et al.*, 2016a]. There is also evidence of an increase in the volume extinction coefficient below 55 km [Doose *et al.*, 2016b]. DISR measurements below 80 km indicate that the aerosols are a combination of photochemically generated hazes and condensed organics [Tomasko *et al.*, 2008]. In the visible, the particles' optical constants are roughly consistent with Khare *et al.* [1984] but in the infrared Titan's particles are more absorbing than predicted from lab measurements [Tomasko *et al.*, 2008], which is also seen in CIRS measurements [Vinatier *et al.*, 2012]. The haze model used to fit the DISR measurements can be used to predict the spectra seen by VIMS. At the Huygens landing site, the spectrum is a good fit to the VIMS data [Tomasko *et al.*, 2009] and small changes in the ground albedo and haze thickness/absorption above 80 km provide good fits to the VIMS observations between  $-60^{\circ}$  and  $50^{\circ}$  latitude [Penteado *et al.*, 2010].

Unlike on Earth, galactic cosmic rays (GCRs) do not penetrate all the way to Titan's surface. Theoretical models predicted that their deposition in the atmosphere would result in the creation of an ionosphere in the lower stratosphere [Borucki *et al.*, 1987; Molina-Cuberos *et al.*, 1999a, b; Borucki and Whitten, 2008]. Measurements from the mutual impedance (MI) and relaxation probe (RP) (part of the PWA) detected this ionosphere in the range of 50 to 80 km with a peak near 65 km ( $2 \times 10^9 \text{ m}^{-3}$  positive ions and  $4.5 \times 10^8 \text{ m}^{-3}$  electrons) [Fulchignoni *et al.*, 2005; Grard *et al.*, 2006; Hamelin *et al.*, 2007; López-Moreno *et al.*, 2008]. The presence of more positive than negative ions is consistent with the presence of negatively charged aerosols; the models of Lavvas *et al.* [2010] and Larson *et al.* [2014] find that the average particle charge density in the lower atmosphere should be  $15 \text{ e}^-/\mu\text{m}$  or  $7.5 \text{ e}^-/\mu\text{m}$ , respectively.

Huygens carried the Aerosol Collector Pyrolyzer (ACP), which collected a sample in the stratosphere and one in the troposphere, that were pyrolyzed, releasing gases to be analyzed by GCMS. GCMS detected HCN and NH<sub>3</sub>, which may indicate that Titan's aerosol particles contain significant amounts of nitrogen [Israël *et al.*, 2005, 2006], in apparent contradiction to the measurements from VIMS and CIRS discussed above. Note that others have argued for a different interpretation of the ACP measurements [Biemann, 2006].

### 3.3.2. Particle formation

Given the discovery of very heavy ions and particles in the thermosphere, we now know particle production begins there. The haze production rate was constrained prior to the arrival of the Voyager spacecraft; *Podolak and Bar-Nun* [1979] calculated an aerosol production rate of  $3.5 \times 10^{-14}$  g cm<sup>-2</sup> s<sup>-1</sup> based on the observed optical properties of Titan's haze. More recent calculations also find values on the order of  $10^{-14}$  g cm<sup>-2</sup> s<sup>-1</sup> [McKay *et al.*, 1989, 2001; Rannou *et al.*, 2003; Lavvas *et al.*, 2009, 2011b; Larson *et al.*, 2014]. *Wahlund et al.* [2009] found an ionospheric mass flux of  $3.2 \times 10^{-15}$  g cm<sup>-2</sup> s<sup>-1</sup>, demonstrating that a significant fraction of the mass of the haze particles is generated very high in the atmosphere.

Chemistry involving aromatic molecules, benzene in particular, has been suggested as one possible pathway for aerosol formation based on chemical models (see e.g., *Lebonnois et al.* [2002]; *Wilson and Atreya* [2003]; *Lavvas et al.* [2008b]; *Delitsky and McKay* [2010]) and laboratory experiments [*Trainer et al.*, 2013; *Sciamma-O'Brien et al.*, 2014; *Sebree et al.*, 2014; *Yoon et al.*, 2014]. Models find that benzene production peaks in the ionosphere and has a higher relative abundance at higher altitudes [*Vuitton et al.*, 2008].

Indeed most, if not all, of the proposed precursors (HCN, C<sub>2</sub>H<sub>2</sub>, C<sub>2</sub>H<sub>4</sub>, etc.) (see e.g., *Lebonnois et al.* [2002]; *Wilson and Atreya* [2003]; *Lavvas et al.* [2008b]; *Krasnopolsky* [2009]) have larger mixing ratios in the ionosphere, where they are produced, than in the stratosphere. Titan's upper atmosphere is a much more energetic environment than the stratosphere, which may allow for greater degrees of nitrogen incorporation, important for prebiotic molecule formation, in aerosol particles. The specific chemical pathways leading to particle formation are still poorly understood; for example, models that use only neutral chemistry (see e.g., *Lebonnois et al.* [2002]; *Wilson and Atreya* [2003]) produce particles too deep in the atmosphere.

Ionospheric chemistry results in the formation of small spherical particles. Using a starting point of 0.35 nm radius particles, *Lavvas et al.* [2013] modeled their growth through chemistry and coagulation, as shown in Figure 4. They demonstrate that the particles are preferentially negatively charged and grow rapidly by addition of positive ions. They maintain their negative charge through electron photoemission and continue to grow. Their model explains a number of features from the CAPS observations: the striking difference in observed mass ranges for positive and negative ions, the high mass cutoff for negative ions, and the observed altitude dependent behavior. It is also consistent with the smaller than expected electron densities measured by the Langmuir Probe [*Ågren et al.*, 2012]. They conclude that Titan's lower ionosphere behaves as a dusty plasma and the contribution of particles must be included to fully understand Titan's ionosphere.

Deeper in the atmosphere, the aerosols form and grow by nucleation and deposition. As the atmospheric density increases and the sedimentation rate decreases, the aerosols grow by aggregation in the region of 650-500 km. Between 500 km and 400 km surface chemistry,

which affects both composition and morphology, dominates as the aerosols react directly with gas phase radicals such as HCCN [Lavvas *et al.*, 2011b]. Photochemical models do not generally include heterogeneous chemistry on the surfaces of the aerosols due to lack of necessary laboratory measurements, however Sekine *et al.* [2008a, b] showed that the atomic hydrogen abundance in Titan's atmosphere can be significantly affected by addition or recombination processes on the surfaces of the aerosols. Additionally, the inclusion of heterogeneous chemistry can act to reduce the abundances of saturated hydrocarbons, decrease HCN, and increase the abundance of phenyl radicals [Sekine *et al.*, 2008a, b].

Once the particles reach the stratosphere and troposphere, they are subject to dynamical processes and condensation described elsewhere in this work. Indeed, Rannou *et al.* [1997] noted that microphysics alone could not explain the observed properties of Titan's haze and therefore dynamics must also play a role. Given that the particle growth processes are altitude dependent, it follows that the composition of the particles likely varies with altitude at least until they reach the stratosphere. This set of processes is similar to the qualitative description of Sagan and Thompson [1984], although in their scenario haze formation occurred at a much lower altitude and results in a maximum heavy atom number of 9 or 10 ( $\sim$ 130 Da) in the haze.

The resulting particles are fractal aggregates with a fractal dimension of 2, intermediate between linear aggregates (1) and spherical aggregates (3) (see e.g., Cabane *et al.* [1993]; Rannou *et al.* [1997]; Lavvas *et al.* [2009]). The morphology is important since aggregates coagulate faster and fall slower because they have a larger cross sectional area for a given mass [Cabane *et al.*, 1993; Larson *et al.*, 2014] and fractals absorb more in the UV to mid visible than spherical particles of the same mass and have different optical properties

because light interacts with multiple dimensions [Lavvas *et al.*, 2010; Larson *et al.*, 2014]. Microphysical models are able to reproduce the properties of the haze inferred from DISR including number of monomers, particle size, and density. However, below 80 km the aerosol characteristics require the addition of mass with different optical properties. This is probably indicative of condensation [Lavvas *et al.*, 2010, 2011c] as discussed in Section 6. Larson *et al.* [2014] note that with their model it takes particles 395 years to get from the mesosphere to the surface.

### 3.3.3. Particle composition

Based on assumptions regarding the molecular precursors to haze, photochemical models can estimate the composition of the haze particles as a function of altitude. Frequently used precursors include aliphatic copolymers, nitriles, aromatics, and polyyynes. Even if the same precursors are used, models differ on the relative importance of the classes of molecules involved in haze formation. Wilson and Atreya [2003] found that haze formation is dominated by aromatics peaking in production at 220 km, with a smaller production peak for nitriles at  $\sim$ 900 km. Other models have found that the total production of aerosols is dominated by aliphatic copolymers in the upper atmosphere and nitriles in the lower atmosphere (a result of energy deposited by GCRs) [Lavvas *et al.*, 2008a, b]. The C/N ratio of the haze is then estimated and ranges from 1.3-2 [Lara *et al.*, 1999; Lavvas *et al.*, 2008b] to 16.7 [Krasnopolsky, 2009] and the estimated C/H ratio ranges from 0.83 [Krasnopolsky, 2009] to 1.3 [Lavvas *et al.*, 2008b]. The wide range in values can be attributed to assumptions made about the chemical pathways involved in haze formation. Lebonnois *et al.* [2003] calculated the C/N ratio of the aerosols based on 3 previously suggested pathways. Polymers of  $C_2H_2$  and  $HC_3N$  [Clarke and Ferris, 1997]

result in C/N of 10-20 depending on the altitude, PAHs with HCN and HC<sub>3</sub>N resulted in a C/N of 8-20, and polymers of HCN and other nitriles result in a C/N of 1.5. Other laboratory haze simulation experiments, discussed below, tend to produce particles with C/N values ranging from 1 to 3.5 (see e.g., *Sarker et al.* [2003]; *Imanaka et al.* [2004]; *Imanaka and Smith* [2010]; *Sciamma-O'Brien et al.* [2010]; *Trainer et al.* [2012]), although it increases with inclusion of trace aromatics [*Trainer et al.*, 2013; *Yoon et al.*, 2014]. In all cases, these models and experiments show that the haze may be an important sink for both hydrogen and nitrogen in the atmosphere, which is consistent with the results from Huygens ACP [*Israël et al.*, 2005, 2006] but inconsistent with the lack of nitrogen in the Cassini CIRS and VIMS measurements mentioned above (see e.g., *Rannou et al.* [2010]; *Vinatier et al.* [2012]).

Laboratory experiments, with their ability to control conditions and access to state-of-the-art analytical techniques, play an important role in understanding Titan's haze. Titan haze analogues are often called tholins, a term first coined by *Sagan and Khare* [1979]. They wrote, "The product, synthesized by ultraviolet (UV) light or spark discharge, is a brown, sometimes sticky, residue, which has been called, because of its resistance to conventional analytical chemistry, 'intractable polymer.'...It is clearly not a polymer— a repetition of the same monomeric unit— and some other term is needed...We propose, as a model-free descriptive term 'tholins'..., although we were tempted by the phrase 'star-tar'." The word tholin does not refer to a unique material, rather a class of materials that are produced under a range of conditions but share the general characteristics of starting with a cosmically abundant gas or ice and exposing it to an energy source that results

in the formation of a refractory solid material. For a broad overview of tholin work, see *Cable et al.* [2012].

Although the optical properties of a variety of tholins have been measured [*Podolak et al.*, 1979; *Khare et al.*, 1984; *Bar-Nun et al.*, 1988; *Coll et al.*, 2001; *Ramírez et al.*, 2002; *Tran et al.*, 2003; *Bernard et al.*, 2006; *Quirico et al.*, 2008; *Vuitton et al.*, 2009b; *Hasenkopf et al.*, 2010; *Gautier et al.*, 2012; *Imanaka et al.*, 2012; *Sciamma-O'Brien et al.*, 2012; *Mahjoub et al.*, 2012; *Hadamcik et al.*, 2013], no laboratory analogue completely reproduces Titan's haze optical properties over the measured wavelength regions [*Tomasko et al.*, 2008; *Bellucci et al.*, 2009; *Lavvas et al.*, 2010; *Rannou et al.*, 2010; *Anderson and Samuelson*, 2011; *Kim et al.*, 2011; *Vinatier et al.*, 2012; *Hirtzig et al.*, 2013; *Kim and Courtin*, 2013; *Sim et al.*, 2013; *Courtin et al.*, 2016]. *Brassé et al.* [2015] review the current state of optical constants for tholins. It is important to be aware that the optical constants of *Khare et al.* [1984] are used most frequently because they are the only in depth study of optical constants for planetary haze particles that span a wide spectral range. The *Khare et al.* [1984] optical constants are particularly bad fits to Cassini measurements at 3, 3.4, 13-17, and 72  $\mu\text{m}$ . Although some Titan tholins do have features at 3.4  $\mu\text{m}$ , the retrieved value from Cassini VIMS is significantly higher than what is measured in the lab [*Rannou et al.*, 2010]. The observations at 3.4  $\mu\text{m}$  are complicated by a significant contribution from C<sub>2</sub>H<sub>6</sub> gas at that wavelength [*Maltagliati et al.*, 2015]. The regions of spectral agreement indicate that there are conjugated structures (often the result of alternating single and double bonds) in Titan's haze particles [*West et al.*, 2014]. *Sebree et al.* [2014] recently showed that the addition of aromatic molecules during tholin

production results in a better fit to the feature seen at  $140\text{ cm}^{-1}$  in CIRS, indicating aromatic molecules are likely present in the haze.

Experiments have shown that photoionization of  $\text{N}_2$  is important for the nitrogen chemistry and the formation of heavy organics such as benzene and toluene because the yields of those molecules increase at shorter wavelengths [Imanaka and Smith, 2007; Thissen et al., 2009]. It has also been noted based on comparisons of gas and solid products that nitrogen appears to be very efficiently incorporated into the solid phase [Imanaka and Smith, 2010]. Indeed a number of experiments have demonstrated that the presence of  $\text{N}_2$  increases the particle production rate in laboratory simulations [Imanaka and Smith, 2010; Trainer et al., 2012]. Further, work by Hörst and Tolbert [2014] shows that the presence of CO also increases particle production rates. The combination of  $\text{N}_2$ ,  $\text{CH}_4$ , and CO in Titan's atmosphere make it an ideal place for photochemical generation of particles.

The wealth of *in situ* and remote sensing observations obtained by Cassini-Huygens has provided new constraints on Titan's aerosols and indicates that their formation initiates much higher in the atmosphere than previously believed. The aerosols therefore carry the signature of upper atmosphere processes, though they undergo additional chemical and physical processing as they settle to the surface. During this time the initially spherical particles eventually form fractal aggregates, which can serve as condensation nuclei for molecules that condense in the lower atmosphere such as HCN,  $\text{C}_2\text{H}_6$ , and  $\text{CH}_4$ . Since the aerosols are produced globally, they are eventually deposited onto a wide variety of surface environments, possibly allowing for further alteration under different conditions including processing in the lakes and seas or in cryovolcanic flows or impact generated

melt pools. Experiments have shown that tholins produced from mixtures of N<sub>2</sub> and CH<sub>4</sub> can be hydrolyzed to form molecules of prebiotic interest including amino acids (the building blocks of proteins) [Neish *et al.*, 2010a; Poch *et al.*, 2012].

## 4. Dynamics

### 4.1. Winds

The winds in Titan's atmosphere result primarily from solar forcing, which varies seasonally. There are a number of different ways to constrain wind speeds on Titan. Direct measurements of the wind speeds come from a few methods, each with limitations: measurements from the Doppler Wind Experiment (DWE) carried by the Huygens probe [Bird *et al.*, 2005; Folkner *et al.*, 2006], measuring doppler shifts in the emission lines of atmospheric constituents like ethane (see e.g., Kostiuk *et al.* [2001, 2005]; Luz *et al.* [2005]; Moreno *et al.* [2005]; Kostiuk *et al.* [2006]; Luz *et al.* [2006]; Kostiuk *et al.* [2010]), and cloud tracking [Bouchez and Brown, 2005; Porco *et al.*, 2005; Turtle *et al.*, 2011a]. The DWE provided measurements at one place and time from 145 km to the surface. The doppler shift technique has the advantage of being possible from Earth, but provides limited spatial resolution. Cloud tracking is often used to measure wind speeds in planetary atmospheres (see e.g., Vasavada *et al.* [2006]) but the general paucity of clouds on Titan means that cloud tracking provides temporally and spatially limited wind speed measurements. Indirect techniques have also been used to constrain the winds on Titan including use of the thermal wind equation to calculate wind speeds from temperature measurements (see e.g., Flasar *et al.* [2005]; Achterberg *et al.* [2008a]) and stellar occultations [Sicardy *et al.*, 1990; Hubbard *et al.*, 1993; Bouchez, 2004; Sicardy *et al.*, 2006]. Wind speeds can also be constrained through evidence of aeolian processes such as dunes and

wind-driven waves on the lakes and seas as discussed in Section 7. Of all these techniques, only use of the thermal wind equation on CIRS temperature measurements provides us with significant amounts of temporal and spatial information including seasonal changes (see e.g., [Achterberg *et al.*, 2011]).

The wind speed profile obtained by the DWE is shown in Figure 5. In the troposphere, cloud tracking measurements, which are generally consistent with the DWE, find wind speeds primarily eastward ranging from 0.5 to 10 m/s [Bouchez and Brown, 2005; Turtle *et al.*, 2011a], although speeds up to  $34 \pm 13$  m/s have been reported [Porco *et al.*, 2005]. Higher in the atmosphere, Titan exhibits stratospheric superrotating winds (up to  $\sim 200$  m/s) [Flasar *et al.*, 1981, 2005; Achterberg *et al.*, 2008a; Sicardy *et al.*, 1990; Hubbard *et al.*, 1993; Kostiuk *et al.*, 2001; Bouchez, 2004; Kostiuk *et al.*, 2005; Luz *et al.*, 2005; Kostiuk *et al.*, 2006; Sicardy *et al.*, 2006; Luz *et al.*, 2006], which then decrease in the upper stratosphere and lower mesosphere [Moreno *et al.*, 2005; Achterberg *et al.*, 2008a]. Taken together, the zonal wind speeds are very low ( $< 1$  m/s) at the surface increasing to  $\sim 40$  m/s near 60 km where they begin decreasing until they reach a minimum ( $\sim 5$  m/s) around 75 km before increasing again to speeds up to 200 m/s near 200 km then decreasing to 60 m/s at higher altitudes (near 450 km). Li *et al.* [2012] referred to this minimum as the “zonal wind collapse” and although some atmospheric models find a minimum in the wind profile in this region of the atmosphere, they are unable to reproduce the magnitude and/or altitude of the feature [Lebonnois *et al.*, 2012; Li *et al.*, 2012].

Achterberg *et al.* [2008a] averaged CIRS measurements from 2004 to 2006 (Northern winter) and showed that the stratospheric jet was centered between  $30^\circ\text{N}$  and  $50^\circ\text{N}$  at a pressure of  $\sim 0.1$  mbar and argue that although pre-Cassini temporal coverage is sparse, it

is consistent with the presence of a strong jet in the winter hemisphere, which forms sometime in the fall and dissipates after spring equinox. The length of the Cassini-Huygens mission and the spatial coverage of Cassini CIRS enables monitoring of Titan's stratospheric winds as the seasons change. *Achterberg et al.* [2011] showed that from 2005 to 2009, the southern hemisphere zonal winds exhibited very little change in the stratosphere. In the northern hemisphere, the superrotating jet extended to higher altitudes.

The meridional wind speeds have been estimated based on images taken by DISR in the lower troposphere (up to  $\sim$ 20 km) to be an average of  $\sim$ 0.1 m/s northward above 1 km (peaking at 0.4 m/s) and southward below 1 km (peaking at 0.9 m/s) [*Karkoschka*, 2016a]. These results are consistent with estimates of the very near surface wind speeds (north-south, 0.4 m/s) made through analysis of tracking the parachute [*Karkoschka et al.*, 2007], cooling of the probe on the surface [*Lorenz*, 2006], and conclusions about the motion of the Huygens probe as it landed made from a synthesis of the various data it acquired [*Schröder et al.*, 2012]. The meridional winds are difficult to measure; however, meridional circulation transports both trace gas species and particles, which can be used as tracers of the circulation as discussed below.

#### 4.2. General Circulation

Titan's slow rotation allows for global Hadley circulation, with ascending motion in the summer hemisphere and descending motion near the winter pole, to redistribute heat. As with Earth, Titan's large obliquity ( $\sim$ 26.7°) results in seasonal variations in solar forcing. Unlike Earth, where the strength of the Coriolis force limits the latitudinal extent of meridional circulation cells, Titan generally has 1 main cell (pole-to-pole), except near the equinoxes when there are two cells (equator-to-pole) as the circulation reverses (see

e.g., *Hourdin et al.* [1995]; *Mitchell et al.* [2009]; *Newman et al.* [2011]), which led *Mitchell et al.* [2006] to describe Titan as having an “all tropics” climate. The single Hadley cell efficiently redistributes heat resulting in relatively small equator to pole temperature contrasts [*Jennings et al.*, 2009; *Schinder et al.*, 2011; *Cottini et al.*, 2012; *Schinder et al.*, 2012]. The surface temperature decreases asymmetrically from the equator to the poles with a decrease of 3 K toward the winter pole ( $60^{\circ}\text{N}$ ) and 1 K toward the summer pole ( $60^{\circ}\text{S}$ ) [*Cottini et al.*, 2012]. In terms of atmospheric circulation, Titan is intermediate to Earth and Venus as its atmospheric pressure is higher and rotation rate slower than Earth but lower and faster than Venus; however like Earth, Titan has a significant obliquity.

Most GCMs of Titan’s atmospheric dynamics predict the Hadley cell extends from the surface to the stratosphere. However, based on measurements of temperature and chemical tracers, *Teanby et al.* [2012] argue that the Hadley circulation may extend up as far as 600 km from the surface, above the top boundary of the GCMs. Limitations on the placement of the top boundary of GCMs are frequently invoked as the explanation for mismatches between models and a variety of observations. The winds near the surface have been interpreted as direct evidence of the surface branch of the Hadley circulation, which is predicted to extend to an altitude of a few km (see e.g., *Tokano* [2007]; *Friedson et al.* [2009]; *Mitchell et al.* [2011]; *Schneider et al.* [2012]; *Charnay and Lebonnois* [2012]); a reversal seen near 1 km in the Huygens data [*Karkoschka et al.*, 2007] may correspond to the upper boundary of the surface branch [*Lebonnois et al.*, 2014]. In addition to the main Hadley circulation, a number of GCMs find that a small tropospheric cell forms in the summer hemisphere [*Newman et al.*, 2011; *Lebonnois et al.*, 2012; *Lora et al.*, 2015]. The latitudinal extent of the global Hadley cell depends on certain aspects of the model (see

e.g., *Mitchell et al.* [2009]; *Lora et al.* [2011]; *Newman et al.* [2016]); *Lora et al.* [2011] find that the hottest point in the summer hemisphere does not reach the pole and the upwelling branch does not either. The latitude profile of the zonal winds is key for understanding horizontal angular momentum transport processes, but as discussed in Section 4.1, winds on Titan are often poorly constrained. Cloud tracking measurements tend to suggest higher wind speeds at the midlatitudes than at the poles, which potentially indicates that angular momentum is uniform with latitude and would be consistent with regions dominated by Hadley circulation [*Lebonnois et al.*, 2014].

Observations that Titan's spin rate differs from synchronous [*Lorenz et al.*, 2008a; *Stiles et al.*, 2008, 2010] have been explained by the exchange of angular momentum between Titan's massive atmosphere and its surface assuming the presence of a subsurface ocean [*Lorenz et al.*, 2008a]. This exchange may lead to seasonal variations in Titan's rotation rate because the seasonal reversal of the meridional circulation produces a torque; the exact details of this interaction are still being explored (see e.g., *Tokano and Neubauer* [2005]; *Karatekin et al.* [2008]; *Lorenz et al.* [2008a]; *Mitchell* [2009]; *Van Hoolst et al.* [2009]; *Goldreich and Mitchell* [2010]; *Tokano et al.* [2011]; *Richard et al.* [2014]; *Tokano et al.* [2014]).

In Titan's atmosphere the radiative time constant decreases rapidly with increasing altitude. In the troposphere, it is long compared to seasonal time scales (10 Titan years or longer, *Strobel et al.* [2009]). In the stratosphere and mesosphere, the radiative time constant is much shorter than a Titan season. The winter polar lower stratosphere ( $\sim$ 100-170 km) is an exception, as the radiative time constant there is comparable to the seasonal timescale [*Achterberg et al.*, 2011]. The shorter radiative time constant means that tem-

peratures adjust to seasonal forcing in the stratosphere as observed in CIRS data (see Section 5). Interestingly, *Cottini et al.* [2012] found a diurnal temperature variation of  $\sim 1.5$  K near the equator and seasonal changes in the surface temperature have also been observed [*Jennings et al.*, 2011] indicating that the thermal inertia of the surface must be low. It is important to note that Saturn's orbit is sufficiently eccentric (0.054) to result in seasonal asymmetries as the solar flux at Titan varies by  $\sim 20\%$  throughout Saturn's orbit. Currently Titan is closest to the sun at southern summer solstice. The orbital asymmetries are dominated by precession of perihelion which has a timescale of  $\sim 45,000$  yr [Roe, 2012].

Another timescale of interest for understanding Titan's atmospheric circulation is the dynamical timescale. For global circulation, the meridional overturning timescale, the meridional scale divided by the mean meridional velocity, is the timescale of interest. Estimations of these timescales require GCMs. Using Titan WRF, *Newman et al.* [2011] find that the shortest dynamical time constants (a few Titan days) exist in the upper stratosphere at low latitudes where the meridional winds are fastest and the longest (a few Titan years) in the upper troposphere and lower stratosphere at mid to high latitudes [*Lebonnois et al.*, 2014]. These estimates are consistent with the less complex model of *Flasar et al.* [1981] based on Voyager measurements.

A comparison of radiative and dynamical timescales indicates that the tropospheric and lower stratospheric radiative timescales are longer or comparable to the dynamical timescales, which is consistent with the observed efficiency of heat redistribution resulting in very small equator to pole temperatures variations in Titan's atmosphere. Higher up in the stratosphere, the meridional dynamical timescales are longer and radiative

processes should dominate, but the changes in heating also result in changes in zonal winds to maintain the thermal wind balance. As a result, seasonal changes in stratospheric temperatures and winds are expected and consistent with observations [*Lebonnois et al.*, 2014]

In addition to heat, the meridional circulation transports angular momentum resulting in high latitude, high altitude jets. In the stratosphere, this allows the centrifugal force to equilibrate the latitudinal pressure gradient force (PGF) in place of the Coriolis force and the atmosphere is in the cyclostrophic regime [*Flasar et al.*, 1981]. The troposphere is in the geostrophic regime (where pressure gradient force balances the Coriolis force) and the transition between the two regimes occurs somewhere mid-troposphere where the balance is between the PGF, Coriolis, and centrifugal forces [*Mitchell and Lora*, 2016].

One interesting feature of Titan's atmospheric structure is that the axis of symmetry for winds and temperatures is tilted 4 degrees with respect to the pole - tilted towards the sun in the northern hemisphere and shifted 76°W from the subsolar longitude [*Achterberg et al.*, 2008b]. A similar tilt (3.8 degrees, 79°W) is observed in the hemispheric brightness asymmetry seen in Cassini imaging data [*Roman et al.*, 2009] and is required to fit the measured HCN distribution from Cassini CIRS [*Teanby et al.*, 2010a]. The HCN ice cloud at Titan's south pole and distribution of trace species such as HC<sub>3</sub>N and C<sub>4</sub>H<sub>2</sub> also exhibit a 4 degree offset from the south pole [*Jennings et al.*, 2015]. *Tokano* [2010a] suggest that thermal tides may be responsible for the tilt but the explanation is not consistent with all of the observations at equinox when it predicts that the tilt decreases to 1 degree. Deeper investigation of the evolution of the tilt throughout the course of the Cassini mission should provide additional constraints on possible explanations [*Achterberg et al.*, 2008b].

### 4.3. Superrotation

As discussed above, one of the defining characteristics of Titan's atmospheric circulation is the presence of superrotating winds in the stratosphere including a strong jet near 0.1 mbar ( $\sim 300$  km) in the winter hemisphere. The first Titan GCM to successfully generate superrotation was *Hourdin et al.* [1995] demonstrating that numerical angular momentum conservation is important for generation of superrotation in models. However, other Titan GCMs, especially early on, have difficulties reproducing this superrotation [*Tokano et al.*, 1999; *Richardson et al.*, 2007; *Friedson et al.*, 2009; *Larson et al.*, 2014] and although a number of different GCMs can now reproduce superrotation (though not always strong enough) [*Newman et al.*, 2011; *Lebonnois et al.*, 2012; *Dias Pinto and Mitchell*, 2014; *Lora et al.*, 2015; *Newman et al.*, 2016], we lack consensus as to how to maintain it [*Lora et al.*, 2015]. Note the problems with generating and sustaining superrotation are not unique to Titan. The Venus atmospheric modeling community has faced similar difficulties (see e.g., *Del Genio and Zhou* [1996]; *Zhu* [2006]; *Lebonnois et al.* [2010]). Unlike Venus, Titan has a strong seasonal cycle, which complicates the atmospheric dynamics, and *Mitchell et al.* [2014] showed that strong seasonal effects act to prevent generation of superrotating winds and needed to adjust the Newtonian cooling time to achieve superrotation.

The results of models that generate superrotating winds (see e.g., *Hourdin et al.* [1995]; *Del Genio and Zhou* [1996]; *Newman et al.* [2011]; *Lebonnois et al.* [2012]) seem to support the idea that the mean meridional circulation transports excess angular momentum upward and poleward and that barotropic waves generated by instabilities on the edges of the high latitude jets transport momentum towards the equator [*Lebonnois et al.*, 2014], which is known as the GRW mechanism [*Gierasch*, 1975; *Rossow and Williams*, 1979].

For example, some models find that superrotation requires coupling between equatorial and high latitude waves but that generation and maintenance require equatorial Kelvin-like waves and Rossby-like waves, respectively [Dias Pinto and Mitchell, 2014; Wang and Mitchell, 2014]. Though waves play a key role in the atmospheric dynamics, they are difficult to constrain; observations of clouds may play a key role in revealing the characteristics of waves in Titan's atmosphere [Mitchell *et al.*, 2011].

Superrotation and zonal jets depend on the mean meridional circulation, which is determined by rotation rate, planetary radius, and solar heating but it is also affected by radiative transport and is therefore also related to the gas, haze, and cloud distributions. Models indicate that coupling of gas composition and dynamics is far less important than coupling of haze and dynamics [Lebonnois *et al.*, 2003; Hourdin *et al.*, 2004], though it is important to remember that the particle and gas phases are connected in Titan's atmosphere through photochemistry and condensation processes. Coupling with haze increases the maximum speeds achieved by zonal winds as transport of particles increases the equator to pole temperature variations thus strengthening the meridional circulation (see e.g., [Rannou *et al.*, 2002, 2004; Lora *et al.*, 2015]).

## 5. Seasonal change

Seasonal effects are important over a Titan year (29.5 Earth years) because of Saturn's axial tilt of almost  $27^\circ$ . Due to the length of the Cassini mission, seasonal changes can be investigated (see Figure 6). In addition, the seasonal overlap with Voyager allows for some investigation of inter-annual variability.

### 5.1. Composition and temperature

As shown in Figure 7, both Voyager IRIS and Cassini CIRS measurements show strong variations with latitude for stratospheric mixing ratios and in general hydrocarbons and nitriles are more abundant at the winter pole than at lower latitudes or in the summer hemisphere [Coustonis and Bézard, 1995; Coustonis et al., 2007; Vinatier et al., 2007; Teanby et al., 2008a, b, 2012; Vinatier et al., 2015; Coustonis et al., 2016]. This likely results from the winter polar vortex, which enhances abundances through subsidence of air from higher altitudes, where the molecules are produced and have larger mixing ratios, to deeper regions where they are protected from photolysis by the winter polar night (see e.g., Yung [1987]; Lebonnois et al. [2001]; Hourdin et al. [2004]; Crespin et al. [2008]; Teanby et al. [2008a]). This trend was observed when Cassini first arrived during northern winter, but has now been observed at the south pole as it moves into winter [Teanby et al., 2012; Bampasidis et al., 2012; Vinatier et al., 2015; Coustonis et al., 2016]. Equinox occurred on 11 August 2009 and evidence of seasonal changes in the form of increasing trace gas abundances and temperature changes at the south pole were first observed in June 2011 [Teanby et al., 2012]. The strength of the latitudinal variation depends on the chemical lifetime of the species (see e.g., Lavvas et al. [2008a]); short lived species (e.g.,  $\text{C}_2\text{H}_4$ ,  $\text{C}_3\text{H}_4$ ,  $\text{C}_4\text{H}_2$ ,  $\text{C}_6\text{H}_6$ ,  $\text{HC}_3\text{N}$ ) tend to exhibit stronger variations than long lived species (e.g.,  $\text{C}_2\text{H}_2$ ,  $\text{C}_2\text{H}_6$ ,  $\text{C}_3\text{H}_8$ ,  $\text{CO}_2$ ); short lived species also exhibit steeper gradients in their winter polar altitude profiles. Between January 2010 and September 2011, the mixing ratios of some molecules ( $\text{HC}_3\text{N}$ ,  $\text{C}_6\text{H}_6$ ,  $\text{C}_3\text{H}_4$ ,  $\text{C}_4\text{H}_2$ ,  $\text{C}_2\text{H}_4$ ,  $\text{HCN}$ ) increased by factors of 500 to 1000 between 0.02 mbar ( $\sim 365$  km) and 0.001 mbar ( $\sim 500$  km) as the south pole moved into winter [Vinatier et al., 2015]. By 2012, the hemispheric asymmetry in the

abundances of  $\text{HC}_3\text{N}$  and  $\text{C}_6\text{H}_6$  had flipped from the trend observed in 2010 at the poles [Coustonis *et al.*, 2016].

GCMs are generally consistent with the observed latitudinal and seasonal trends in mixing ratios, but they usually overestimate the latitudinal extent of enhancements at the winter pole and do not reproduce an observed depletion in species like  $\text{C}_2\text{H}_2$ ,  $\text{HCN}$ , and  $\text{C}_4\text{H}_2$  at 0.01 mbar and 50°N, which may result from residual circulation [Teanby *et al.*, 2008a].

Comparisons between Cassini CIRS and Voyager IRIS measurements indicate that for most molecules at similar latitudes and seasons the observed abundances are consistent with no inter-annual variability [Coustonis *et al.*, 2013, 2016]; small enhancements relative to Voyager are observed for  $\text{HC}_3\text{N}$  at 70°N [Coustonis *et al.*, 2016] and  $\text{C}_4\text{H}_2$  and  $\text{C}_3\text{H}_4$  at 50°N [Coustonis *et al.*, 2013], which may be explained by the observations not perfectly overlapping in season at a given latitude.

In addition to mixing ratio variations, seasonal variations in the temperature profile are also observed. The winter polar stratospheric temperature structure is consistent with subsidence and reminiscent of Earth's winter pole. In the lower stratosphere, temperatures are at least 25 K colder than the equator [Achterberg *et al.*, 2008a]. However, higher in the atmosphere the stratopause is ∼20 K warmer than at the equator and is about two scale heights higher; the temperatures exceed 200 K and it is the warmest region of Titan's atmosphere [Flasar *et al.*, 2005; Achterberg *et al.*, 2008a, 2011; Vinatier *et al.*, 2015]. The heating likely results from adiabatic heating from subsidence over the winter pole and has been predicted by GCMs (see e.g., Rannou *et al.* [2005]; Crespin *et al.* [2008]; Newman *et al.* [2011]). Additionally, as Achterberg *et al.* [2008a] point out, the combination of

higher polar altitudes in permanent sunlight and the increased aerosol abundance at the winter pole may result in additional heating from stratospheric aerosols. This temperature structure was first observed during northern hemisphere winter, but similar behavior has now been observed at the south pole, with temperatures of  $\sim$ 185 K seen at the stratopause [Achterberg *et al.*, 2011; Vinatier *et al.*, 2015]. Deeper in the atmosphere, temperature decreases attributed to radiative cooling have been observed as the south pole moves into winter; from 2010 to 2014, the temperature at 0.1 mbar at 70°S decreased by 40 K [Coustonis *et al.*, 2016], with very dramatic temperature changes beginning in February 2012 [Vinatier *et al.*, 2015].

Teanby *et al.* [2010b] found that there were no significant changes from 40°S to 30°N in composition from 2004 to 2010 and Coustonis *et al.* [2016] found that from 2010 to 2014 the mixing ratios did not change significantly at 50°N and until 2013 remained higher than the mixing ratios at 50°S. At the mid latitudes, Coustonis *et al.* [2016] found that the temperature does not vary significantly in the lower stratosphere (below 0.5 mbar) but higher up in the stratosphere it warmed by 10 K between 2010 and 2014 at 50°N while at 50°S it initially decreased from 2010 to 2012 before warming 8 to 10 K.

As a pole moves into summer, the downwelling decreases, resulting in a decrease in adiabatic heating and a decrease in temperature higher in the atmosphere, while the deeper atmosphere warms as the photon flux increases. The gas mixing ratio enhancements also begin to dissipate. At the north pole by 2014, the mixing ratios of some species were beginning to decrease and a 6 K increase in temperature was observed from February to September of 2014 [Coustonis *et al.*, 2016].

Models predict that for a brief period a few years after equinox there are two equator to pole Hadley cells as the main pole to pole circulation switches directions (see e.g., *Hourdin et al.* [1995, 2004]; *Newman et al.* [2011]; *Lebonnois et al.* [2012]). *Vinatier et al.* [2015] analyzed limb profiles (covering 150 to 500 km) from 2006 to 2013 and reported the first observational evidence of 2 short lived equator to pole Hadley cells in analyses of gases, aerosols, and temperature from Cassini CIRS. Their results, including increased aerosol abundance at the south pole and temperature changes, are compatible with two cells downwelling at the poles from at least January 2010 to at least June 2010. By June 2011, it appears that the circulation had reversed and was again a single Hadley cell with the downwelling branch now located at the south pole [*Vinatier et al.*, 2015]. Models also predict that the upwelling branches near the equator should cause a small temperature decrease from adiabatic cooling, but the temperature change may be too small to observe [*Vinatier et al.*, 2015]. CIRS observations in January 2012 indicate that there was an anomalously low aerosol concentration at the equator, which, if real, may indicate upwelling of air that is depleted in particles [*Vinatier et al.*, 2015].

## 5.2. Detached haze layer

The origin of the detached haze layer, shown in Figure 8, is not yet well understood. As mentioned above, before the discovery of very large ions in Titan's thermosphere, we assumed that the haze particles were produced at roughly the same altitude as the observed haze layers and that the detached haze layer was either the result of photochemistry [*Chassefière and Cabane*, 1995; *Clarke and Ferris*, 1997; *Rannou et al.*, 2000] or dynamics in which the detached haze layer is the result of large scale circulation in which particles are transported by meridional circulation to the winter pole where they grow,

settle, and mix in the stratosphere. In the summer hemisphere, particles are transported upward to maintain the detached haze layer and then transported horizontally by winds (see e.g. *Toon et al.* [1992]; *Rannou et al.* [2002, 2003, 2004]). The GCM of *Lebonnois et al.* [2012] accordingly predicts that the detached haze layer changes altitude because of the transient migration of the ascending branch of the Hadley cell. The Imaging Science Subsystem (ISS) and UVIS have detected a detached haze layer at 500 km, along with less pronounced layers above the main detached haze layer [*Porco et al.*, 2005; *Liang et al.*, 2007; *Koskinen et al.*, 2011]. This location is about 150 km higher than the detached haze layer observed by Voyager as shown in Figure 4. A temperature minimum in the region of the detached haze layer [*Fulchignoni et al.*, 2005; *Sicardy et al.*, 2006] has led to the suggestion that the detached layer is a result of condensation in the atmosphere [*Liang et al.*, 2007]. However, subsequent analyses by *Lavvas et al.* [2009] show that the detached haze layer is coincident with, and likely the cause of, a temperature maximum thus ruling out condensation as a source mechanism. *Lavvas et al.* [2009] suggested that the detached haze layer may result from the transition from 40 nm monomers to larger aggregates in the atmosphere, which would cause a decrease in the number density of aerosols. They also demonstrated that the mass flux out of the detached haze layer is sufficient to generate the main haze layer. Their explanation lacks a seasonal component, but the dynamical explanations do not reproduce some of the observations such as the spatial continuity of the detached haze layer at the summer pole [*West et al.*, 2014]. Given these difficulties, it seems likely that both dynamics and microphysics play a role in determining the structure and temporal evolution of the detached haze layer.

The layered structure observed above the detached haze layer may result from gravity waves [Strobel, 2006; Koskinen *et al.*, 2011]. Gravity waves have also been suggested as an explanation for similar layers observed in Pluto's atmospheric haze [Gladstone *et al.*, 2016].

From 2007 to 2010, the location of the detached haze layer dropped from 500 km to 380 km [West *et al.*, 2011] returning to the same altitude at which it was observed during the Voyager era at the same point in Titan's year. The apparent seasonal evolution in the presence and location of the detached haze layer strengthens the argument that atmospheric dynamics play a role in its origin. The drop in altitude was most rapid at equinox. Starting in late 2012 the detached haze layer was not detectable until early 2016 when it reappeared, with very low contrast, near 500 km [West *et al.*, 2016a].

Cours *et al.* [2011] find that the detached haze layer is composed of two populations of particles: particles less than 50 nm (81-87% small aerosols by mass), which are primarily responsible for absorption due to particles in that region of the atmosphere, and larger particles, although they are less abundant, which are responsible for 90% of the scattering at UV and visible wavelengths. The larger particles are too large to have formed at higher altitudes and therefore must have been transported from a reservoir of larger particles deeper in the atmosphere [Cours *et al.*, 2011]. Larson *et al.* [2015] find that the location of the detached haze layer represents the location where the upward velocity from dynamics equals the fall velocity due to gravity and thus represents the maximum combination of particles from above and below. They find that it varies seasonally because of seasonal changes in the vertical wind speeds and that it is relatively uniform with latitude because meridional motions are much faster than vertical motions. However, they predicted it

would reappear earlier than it has. Note that a few Titan GCMs qualitatively reproduce the seasonal variation in presence and altitude variation of the detached haze layer [*Rannou et al.*, 2002, 2004; *Lebonnois et al.*, 2012; *Larson et al.*, 2015] however the observed timing and locations have not been reproduced by models. The inability to reproduce the altitude is likely due to limitations imposed by the top of the model atmospheres, which is generally near the highest observed altitude of the detached haze layer [*Lebonnois et al.*, 2012; *Larson et al.*, 2015].

### 5.3. North-south haze asymmetry

Titan's north-south haze asymmetry, shown in Figure 8, has been observed from ground-[*Lockwood*, 1977; *Lockwood and Thompson*, 1979; *Gibbard et al.*, 2004a; *Lockwood and Thompson*, 2009] and space-based telescopes [*Lorenz et al.*, 1997, 2004; *Karkoschka*, 2016b], Pioneer 11 [*Tomasko and Smith*, 1982], Voyager 1 [*Sromovsky et al.*, 1981], and Cassini (see e.g., *Rannou et al.* [2010]; *Barnes et al.* [2013a]; *Hirtzig et al.* [2013]). The winter hemisphere is darker at short wavelengths and brighter in the near IR due to an increase in haze opacity (see e.g., *Toon et al.* [1992]; *Cours et al.* [2010]; *Larson et al.* [2014]), which is consistent with other measurements that show that haze is more abundant in the winter hemisphere (see e.g., *Rannou et al.* [2010]).

HST observations from 1992 to 1995 showed that the Voyager asymmetry had flipped hemispheres [*Lorenz et al.*, 1997] indicating that it is a seasonal asymmetry. The ground-based observations of *Lockwood and Thompson* [2009] suggest the reversal happened sometime in the mid 1980s. *Penteado et al.* [2010] demonstrated that variations in the aerosol optical depth above 80 km could be responsible for the change, but are unable to ascertain if it is a change in composition, size, and/or vertical distribution. Analysis of HST STIS

data from 1997 to 2004 using principal component analysis [Karkoschka, 2016b] shows that there are two principal components resulting in the asymmetry: one below 80 km and one above 150 km, which they attribute to condensation and dynamics, respectively. Between 80 and 150 km there was no change. The high altitudes were symmetric about equator in 2001 and then switched; at low altitudes the change happened later than at high altitudes and was latitude dependent [Karkoschka, 2016b], which is consistent with Lorenz *et al.* [2004]. Hirtzig *et al.* [2013] observed a decline in the asymmetry but it had not flipped by mid-2010; Karkoschka [2016b] predicted the next reversal might occur throughout 2017 and 2018. Inspection of publicly available Cassini ISS images in the MT3 (889 nm) filter suggests that the reversal is currently happening (late 2016). The long time baseline (greater than a Titan year) of the observations of Lockwood and Thompson [2009] allowed them to demonstrate inter-annual variability in Titan's brightness, indicating that Titan not only exhibits seasonal changes, but also annual variability.

#### 5.4. Polar hood

In addition to the detached haze layer and main haze layer, which although temporally and spatially varying, are global in extent, Titan's winter pole also has a layered haze structure between the main haze layer and the detached haze layer that resembles a polar hood, as shown in Figure 8. The polar hood is likely the result of transport of haze particles and downwelling at the winter pole [Rannou *et al.*, 2002, 2004; Lorenz *et al.*, 2006a], which is consistent with its presence at the north pole during the Voyager Era and disappearance from the south pole in 2002-2003 [Lorenz *et al.*, 2006a].

## 6. Clouds, rain, and Titan's methane cycle

Much like Earth, Titan exhibits a number of types of clouds resulting from different formation processes and conditions. Unlike Earth, Titan's clouds form from a number of different volatiles. *Tsai et al.* [2012] divided clouds into 3 categories: convective methane clouds [*Griffith et al.*, 1998, 2000; *Brown et al.*, 2002; *Roe et al.*, 2002; *Gibbard et al.*, 2004b; *Griffith et al.*, 2005; *Roe et al.*, 2005; *Schaller et al.*, 2006a, b; *Griffith et al.*, 2009; *Rodriguez et al.*, 2009; *Schaller et al.*, 2009; *Turtle et al.*, 2009; *Brown et al.*, 2010; *Rodriguez et al.*, 2011; *Turtle et al.*, 2011a], stratiform ethane clouds [*Griffith et al.*, 2006; *Brown et al.*, 2010; *Le Mouélic et al.*, 2012], and high altitude cirrus clouds (HCN, HC<sub>3</sub>N, etc.) [*Samuelson et al.*, 2007; *Anderson et al.*, 2010; *Anderson and Samuelson*, 2011]. In addition to those clouds, there is currently a large, high altitude HCN ice cloud, first observed in May 2012, that formed in the polar vortex at the south pole [*de Kok et al.*, 2014]. Figure 8 shows the polar HCN cloud and an example of methane clouds. Although there have been reports of detection of fog, *Charnay and Lebonnois* [2012] argue that those observations are more likely boundary layer clouds. In general, convective methane clouds are observed at the summer pole and mid-latitudes, while the other types of clouds are observed at the winter pole.

### 6.1. Convective methane storms

The GCMS aboard the Huygens Probe measured a methane relative humidity of approximately 50% at the surface [*Niemann et al.*, 2005, 2010]. However, cloud and thunderstorm models indicate that at least 60% surface relative humidity is required for convective cloud formation [*Lorenz et al.*, 2005] and 80% is required for thunderstorms capable of producing substantial rainfall [*Hueso and Sánchez-Lavega*, 2006]. It has therefore been argued that

there is not currently enough methane at the equator to produce rainfall necessary to form the channels observed at the Huygens landing site [Griffith *et al.*, 2008]. However, low latitude storms have been observed [Schaller *et al.*, 2009], including one that resulted in extensive alteration of the surface, presumably caused by large amounts of methane rainfall [Turtle *et al.*, 2011b]. These convective storms may produce fast surface winds that increase the lifetime of the storm and enhance precipitation [Hueso and Sánchez-Lavega, 2006; Rafkin and Barth, 2015; Charnay *et al.*, 2015].

The methane and temperature profiles at the Huygens landing site indicate that Titan's tropical atmosphere is highly stable; convection is weak and convective systems lie near or below 26 km [Barth and Rafkin, 2007; Griffith *et al.*, 2008]. Close to the surface (below 2 km) the temperature profile follows the dry lapse rate [Griffith *et al.*, 2008] and parcels of air from the surface need to reach the lifting condensation level (LCL) of 5 km before condensation will occur [Griffith *et al.*, 2008]. The level of free convection (LFC) is around 9 km and the level of neutral buoyancy (LNB) is around 24 km [Griffith *et al.*, 2008]. Many of the observed clouds that form and dissipate on short time scales are at altitudes near the LNB [Griffith *et al.*, 2000, 2005, 2009; Ádámkovics *et al.*, 2010] indicating that they are convective [Griffith *et al.*, 2000, 2005; Roe, 2012]. Interestingly, the clouds at higher latitudes also reach higher altitudes (up to 40 km), potentially indicating that the methane humidity profile varies latitudinally [Griffith *et al.*, 2005, 2009; Ádámkovics *et al.*, 2010; Griffith *et al.*, 2014] as discussed in Section 2.2.

Dynamical models of Titan's atmosphere indicate that there are four ways to produce clouds: updrafts (including the ascending branch of a Hadley cell) [Rannou *et al.*, 2006; Mitchell *et al.*, 2006; Mitchell, 2008; Mitchell *et al.*, 2009; Schneider *et al.*, 2012], solar

forcing at the summer poles, wave activity, and downwelling of photochemical species [Griffith *et al.*, 2014]. The clustering of clouds at 40°S during southern summer has been explained by either the location of slantwise convection [Rannou *et al.*, 2006] or the ascending branch of the Hadley cell [Mitchell *et al.*, 2006]. Planetary waves [Schaller *et al.*, 2009], Kelvin waves [Mitchell *et al.*, 2011; Turtle *et al.*, 2011b], and atmospheric tides [Rodriguez *et al.*, 2009, 2011] have all been used to explain the location, timing, and/or morphology of observed clouds. Clouds produced by waves are particularly important for the tropics near equinox [Mitchell *et al.*, 2011; Schneider *et al.*, 2012]. Barth and Toon [2004] predicted that optically thick clouds are most likely to form at the poles. Mountains, resulting in orographic clouds [Barth, 2010], and lakes and seas, resulting in sea breeze clouds [Brown *et al.*, 2009], may also play an important role in cloud formation on Titan.

It is generally assumed that haze particles produced higher in the atmosphere act as cloud condensation nuclei (see e.g., Griffith *et al.* [2006]; Bauerecker and Dartois [2009]); liquid and solid CH<sub>4</sub> nucleate easily on Titan haze analogs [Curtis *et al.*, 2008] but CH<sub>4</sub>-N<sub>2</sub> binary nucleation may also play an important role in cloud formation [Wang *et al.*, 2010; Tsai *et al.*, 2012].

Since clouds were first discovered using ground-based observations [Griffith *et al.*, 1998; Brown *et al.*, 2002; Roe *et al.*, 2002], observations of clouds have played an important role in improving our understanding of the dynamics of Titan's atmosphere. In addition to providing measurements of wind speeds, the powerful combination of long-term ground-based cloud monitoring campaigns (e.g., Roe *et al.* [2005]; Schaller *et al.* [2006a, b, 2009]; Ádámkovics *et al.* [2010]) and observations by Cassini (e.g., Porco *et al.* [2005]; Turtle

*et al.* [2009]; *Brown et al.* [2010]; *Rodriguez et al.* [2011]; *Turtle et al.* [2011a]) allow us to track seasonal changes in cloud cover, including location, extent, and duration, which provide important constraints on the global circulation of Titan's atmosphere and a test for GCMs. Clouds can also help us understand atmospheric waves and are particularly important for providing information about the troposphere, which is difficult to obtain from other types of remote sensing because of the large optical depth. The story of clouds on Titan is a particularly powerful demonstration of the synergy of ground and spacecraft based observations; Ground based observers have more consistent measurements, over a longer time baseline but are unable to detect smaller clouds. Cassini measurements can detect much smaller cloud features, but the frequency, consistency, and length of time baseline for the observations is better from the Earth; *Schaller et al.* [2009] found a storm from ground-based observations that was largely missed by Cassini.

Large cloud systems (covering up to  $\sim$ 10% of the disk) seem to occur every 3 to 18 months [Roe, 2012]. These large storms are capable of triggering Rossby waves, which result in formation of clouds elsewhere in the atmosphere [Schaller et al., 2009]. Despite the presence of large storms, lightning has not been detected in measurements of Titan's atmosphere from Cassini-Huygens [Béghin et al., 2007; Fischer et al., 2007; Fischer and Gurnett, 2011].

Cassini's RADAR should be capable of detecting raindrops, but a dedicated cloud backscatter observation during T30 did not detect droplets [Lorenz et al., 2008b]. Although raindrops have not been directly detected, a handful of probable rainfall events have been identified based on observed surface changes, some of which have been tied to specific observed storms [Turtle et al., 2009, 2011b; Dalba et al., 2012; Barnes et al.,

2013b]. On Titan, precipitation may be supply limited; if that is the case, we would expect frequent large storms during northern summer [Mitchell, 2012]. Since the average mixing ratio and atmospheric column mass of methane in Titan's atmosphere is much higher than that of water on Earth, when storms do produce rain, they are capable of significant amounts of precipitation [Hueso and Sánchez-Lavega, 2006; Barth and Toon, 2006; Barth and Rafkin, 2007; Barth, 2010]. Estimates of the average precipitation rate of methane to Titan's surface generally fall between 0.001 and 0.5 cm/terrestrial-year [Barth and Toon, 2006; Tokano *et al.*, 2006b].

The model of Mitchell *et al.* [2011] found that the “arrow storm” [Turtle *et al.*, 2011b] was caused by an equatorially trapped Kelvin wave, which is one of the dominant modes of dynamics in Titan's atmosphere. These waves result in large-scale storms (over 1000 km scale that produces several centimeters of precipitation, which is 20 times the average rate) indicating that it may rain more frequently in the equatorial region than previously thought.

## 6.2. Seasonal evolution of convective clouds

These storms tend to appear in the regions of maximum solar insolation, which results in seasonal variation in storm locations (see e.g., Brown *et al.* [2010]; Turtle *et al.* [2011a]) as the region of upwelling, similar to the intertropical convergence zone (ITCZ) on Earth, moves from pole to equator to pole. Near southern summer solstice (2002) most of the observed storms were near the south pole. As Titan moved through equinox (2009), clouds appeared at both poles. From 2013 to 2015, very few clouds were detected from Cassini or ground-based monitoring campaigns [Rodriguez *et al.*, 2014; Corlies *et al.*, 2015; Turtle, 2016], indicating that cloud activity may be less frequent post-equinox. In 2016,

small clouds started appearing more consistently; however, the 2016 clouds are still much smaller than some of the clouds observed near equinox at high northern latitudes [*Cassini Imaging Team*, 2016; *Turtle*, 2016]. The timing of clouds appearing at the north pole was not predicted by models and is an area of ongoing work.

In general GCMs reproduce the observed trends (see e.g., *Mitchell et al.* [2006, 2009]; *Schneider et al.* [2012]; *Lora et al.* [2015]; *Newman et al.* [2016]), although the presence and/or timing of mid-latitude clouds is not seen in every model leading *Lora et al.* [2015] to argue that the clouds observed at mid-latitudes are either not convective in origin or are generated by another mechanism like orographic gravity waves.

### 6.3. Ice clouds

Since the trace constituents in the atmosphere are produced by photochemistry, their abundances tend to decrease with decreasing altitude. Cloud formation from these species therefore requires transport of air parcels downward, from regions where the mixing ratio is higher. A number of opacity sources in Titan's atmosphere are consistent with particles that form from subsidence; some have been connected with specific species such as HC<sub>3</sub>N [*Coustenis et al.*, 1999; *Khanna*, 2005; *Anderson et al.*, 2010], HCN [*Samuelson et al.*, 1997; *Clark et al.*, 2010; *de Kok et al.*, 2014], C<sub>4</sub>N<sub>2</sub> [*Khanna et al.*, 1987; *Samuelson et al.*, 1997; *Coustenis et al.*, 1999], and C<sub>2</sub>H<sub>6</sub> [*Griffith et al.*, 2006; *Anderson and Samuelson*, 2011], while others remain unidentified. In general, particles formed are on the order of a few microns in size (see e.g., *Coustenis et al.* [1999]; *Mayo and Samuelson* [2005]; *Samuelson et al.* [2007]; *Griffith et al.* [2009]; *Anderson and Samuelson* [2011]; *de Kok et al.* [2014]).

In general nitriles condense at a higher altitude than hydrocarbons (see e.g., *Mayo and Samuelson* [2005]; *Anderson and Samuelson* [2011]; *Lavvas et al.* [2011b]). A feature at 160 cm<sup>-1</sup> observed at 90 km has been attributed to a mix of HCN and HC<sub>3</sub>N [*Anderson and Samuelson*, 2011], a region of the atmosphere where HCN and HC<sub>3</sub>N are expected to condense (see e.g., *Anderson and Samuelson* [2011]; *Lavvas et al.* [2011b]). This feature is observed from 58°S to 85°N (covering the full latitude range analyzed), is found at higher altitudes at higher latitudes, and the abundance increases from south to north [*Samuelson et al.*, 2007; *Anderson and Samuelson*, 2011].

No optically thick clouds were detected in DISR measurements [*Tomasko et al.*, 2005; *Doose et al.*, 2016b], however thin layers observed at 7, 11, and 21 km have been attributed to some combination of phase transitions, gas adsorption, and atmospheric mixing, resulting in a particle size increase of 5-10% [*Tomasko et al.*, 2005; *Tokano et al.*, 2006b; *Karkoschka and Tomasko*, 2009]. The layer at 21 km was also likely detected by HASI/PWA, which detected extremely low frequency noise possibly resulting from aerosols impacting the electrodes of the antenna [*Béghin et al.*, 2007].

*Lavvas et al.* [2011c] examined condensation processes at the Huygens landing site. Above 80 km, the DISR observations can be fit using only a model of particle coagulation and sedimentation. However, below 80 km condensation must be invoked to fit the observations. Between 30 and 80 km the aerosol opacity is dominated by a coating of HCN. Although HCN is removed from the atmosphere by this process, deposition of galactic cosmic rays (GCRs) results in production of HCN and replenishes the HCN that is lost allowing for continuous condensation onto aerosols. Below 30 km condensation of methane onto the particles explains their optical properties. They also note that while

ethane clouds are likely to form in the troposphere, the droplets would evaporate before they reach the surface. This may also happen with methane clouds [Lavvas *et al.*, 2011c].

### 6.3.1. The “Haystack” ( $220\text{ cm}^{-1}$ feature)

A far infrared feature, centered at  $220\text{ cm}^{-1}$  and sometimes referred to as “the haystack” [West *et al.*, 2014], was first observed in the data obtained by Voyager IRIS [Kunde *et al.*, 1981; Coustenis *et al.*, 1999]. It was present at northern high latitudes from 2004 to 2012 and observed frequently by CIRS; it is most likely due to the presence of solid particles from 80 to 150 km altitude (see e.g., Flasar *et al.* [2004]; de Kok *et al.* [2007, 2008]; Samuelson *et al.* [2007]; Jennings *et al.* [2012a, 2015]). From 2004 to 2012, the intensity of the feature decreased by a factor of four indicating seasonally varying processes (strength of downwelling, solar heating, photochemistry) are responsible for its formation [Jennings *et al.*, 2012a]. The variation in strength of the feature is similar to that of  $\text{HC}_3\text{N}$  leading Jennings *et al.* [2012a] to argue that it has a nitrile origin. Jennings *et al.* [2012b] reported the first observation of the feature in spectra of the south pole taken in July 2012 (it was not present in February 2012), indicating that it is a product of processes that occur at the winter pole. From the time it appeared the intensity has increased rapidly, doubling every year [Jennings *et al.*, 2015] as the temperature has decreased at the south pole [Teanby *et al.*, 2012; de Kok *et al.*, 2014; Vinatier *et al.*, 2015; Coustenis *et al.*, 2016]. The feature is offset 4 degrees from the pole, consistent with the other offsets as described in Section 4, and as of December 2013 it was confined to a ring south of  $80^\circ\text{S}$ . Nitriles and complex hydrocarbon gases are also offset but with a central peak at the pole, a minimum at  $80^\circ\text{S}$  and secondary maximum at  $70^\circ\text{S}$  [Jennings *et al.*, 2015]. By September 2014, the ring structure in the gases dissipated [Coustenis *et al.*, 2016].

### 6.3.2. Dicyanoacetylene ( $\text{C}_4\text{N}_2$ )

Although  $\text{C}_4\text{N}_2$  has not been detected in Titan's atmosphere [Samuelson *et al.*, 1997; Jolly *et al.*, 2015], a feature at  $478 \text{ cm}^{-1}$  has been attributed to a dicyanoacetylene ice cloud at high latitudes during northern winter below 90 km [Khanna *et al.*, 1987; Samuelson *et al.*, 1997; Coustenis *et al.*, 1999]. Anderson *et al.* [2016] argue that the  $\text{C}_4\text{N}_2$  is produced through solid-state photochemistry of HCN-HC<sub>3</sub>N mixtures, which would explain how  $\text{C}_4\text{N}_2$  could exist in the condensed phase and be undetectable in the gas phase.

### 6.3.3. Ethane ( $\text{C}_2\text{H}_6$ )

In addition to the large methane storms observed in Titan's atmosphere, an extensive polar ethane cloud has also been detected at an altitude 30 to 65 km poleward of 50°N [Griffith *et al.*, 2006; Rannou *et al.*, 2010], an altitude region where Barth and Toon [2003] demonstrated ethane ice clouds are stable. The cloud was present when Cassini arrived at Titan (from 51°N to 68°N, the highest latitude illuminated at the time) and persisted until 2009 when it began to dissipate as Titan approached spring equinox [Brown *et al.*, 2010; Le Mouélic *et al.*, 2012]. It appears to be the result of the descending branch of winter circulation and the extent and altitude is broadly consistent with GCMs [Rannou *et al.*, 2006, 2012]. Since the cloud appears to be a direct result of dynamical processes, the location, extent, and variation with season provides a useful test for models of Titan's atmospheric circulation. Interestingly, after the breakup of the cloud near equinox, the region north of 62°N is depleted in particles [Rannou *et al.*, 2012]. Anderson *et al.* [2014] argue that CH<sub>4</sub> ice particles formed from subsidence may contribute significantly to the opacity of this extensive cloud because the winter pole is cold enough to condense CH<sub>4</sub> ice.

#### 6.3.4. Hydrogen cyanide (HCN)

In 2012, at the location of what was previously a maximum in the atmospheric temperature profile at the south pole, a large cloud was observed in Cassini ISS data at an altitude of 300 km [*de Kok et al.*, 2014; *West et al.*, 2016b]. *de Kok et al.* [2014] used Cassini VIMS data to identify the cloud as a HCN ice cloud with particles of approximately 1  $\mu\text{m}$ . Cassini CIRS measurements indicate much more rapid cooling than GCMs predicted and the temperature would have to be  $\sim$ 100 K lower than predicted for HCN ice formation to occur [*de Kok et al.*, 2014]. The cloud has distinct boundaries, mottled texture, and is more yellow and brighter than the surrounding haze [*West et al.*, 2016b]. It is rotating offset 4.5° from the pole, which is consistent with *Achterberg et al.* [2008b], and exhibits zonal wind speeds of 87 to 89 m/s [*West et al.*, 2016b]. *West et al.* [2016b] point out that the morphology is reminiscent of open cell convection on Earth. They suggest that on Titan it may form as the pole approaches winter and begins cooling to space, the radiative relaxation time decreases with increasing altitude and the condensable species (HCN) comes from above creating a destabilization that results in the texture. Interestingly, the cloud formed at the same altitude as the detached haze layer but the relationship, if any, between these two features remains to be explored [*West et al.*, 2016b].

#### 6.4. Methane cycle

Although there are numerous analogies between Earth's hydrological and Titan's volatile cycle, it is important to remember that unlike water on Earth, methane can be transported through the cold trap at the tropopause, which allows it to play an important role in the radiation balance and chemistry in other regions of the atmosphere including allowing it to be destroyed in the upper atmosphere [*Roe, 2012*]. Thus although

methane does cycle back and forth between the atmosphere and the surface, it is also lost in significant amounts from the atmosphere and the cycle is only stable over geologic timescales if there is a source of methane. Another difference is that on Titan, most of the methane is in the atmosphere rather than on the surface. If all of the methane currently in Titan's atmosphere condensed onto the surface, it would form a global layer 4-5 m deep [Penteado *et al.*, 2010]. For a more detailed discussion of clouds and Titan's methane cycle, see the excellent reviews by Lunine and Atreya [2008] and Roe [2012].

Over the years a number of possible methane sources have been suggested including outgassing of a deep reservoir [Tobie *et al.*, 2005, 2006], interior chemistry involving organic material [Atreya *et al.*, 2006], seepage of methane from a shallow subsurface reservoir [Soderblom *et al.*, 2007a; Hayes *et al.*, 2008; Griffith *et al.*, 2012a], and cryovolcanism. Our lack of understanding about the near surface and subsurface reservoirs of methane and other hydrocarbons limits our ability to fully understand the methane cycle on Titan. Aside from the information from the Huygen's landing site about volatiles in the surface, discussed below, there is other evidence that replenishment from the subsurface may play an important role in Titan's volatile budget. Neish and Lorenz [2014] find that Titan's crater distribution indicates widespread wetlands of liquid hydrocarbons at low elevations over much of geologic time. As the north pole moves into summer, the warming is lagging predictions potentially indicating that the north polar region is saturated with liquid [Jennings *et al.*, 2016; Le Gall *et al.*, 2016]. Additionally, there is some evidence of low latitude lakes, which are not stable and would require subsurface replenishment [Griffith *et al.*, 2012a].

One additional outstanding issue with Titan's methane is whether or not it is escaping from Titan's upper atmosphere. The measured profile in the thermosphere defies explanation. If methane is escaping, it represents only a small fraction of the total methane budget and therefore does not significantly impact the methane lifetime mentioned above [Strobel and Cui, 2014].

## 7. Connection with surface

Titan's surface possesses a variety of environments including lakes, mountains, and dunes as shown in Figure 9. As discussed below, the surface has been shaped by aeolian and fluvial processes and the connection between Titan's surface and atmosphere allows us to test theories developed for Earth in completely different environment.

### 7.1. Surface composition

Despite analysis of data obtained *in situ* by the GCMS carried by Huygens and remote sensing data from DISR, VIMS, and RADAR, the composition of Titan's surface remains poorly understood. Chemical and physical processes occurring in the atmosphere result in the formation of organic liquids and solids that are eventually deposited on the surface; the surface composition is uniquely tied to its atmosphere. Based on Titan's bulk density ( $\sim 1.88 \text{ g/cm}^3$ , Jacobson *et al.* [2006]) water ice makes up a large fraction of Titan's mass and is therefore another likely candidate surface material. Evidence for water ice on Titan's surface was first obtained by ground-based telescopes [Griffith *et al.*, 1991, 2003] and has also been seen in VIMS [McCord *et al.*, 2006; Griffith *et al.*, 2012a; Hayne *et al.*, 2014] and DISR data [Tomasko *et al.*, 2005; Rannou *et al.*, 2016]. Others have argued that these features can be explained by other hydrocarbons or nitriles [Clark *et al.*, 2010]. Other

suggested surface constituents from interpretation of VIMS data include CO<sub>2</sub> [Barnes *et al.*, 2005; McCord *et al.*, 2008], C<sub>6</sub>H<sub>6</sub>, C<sub>2</sub>H<sub>6</sub>, and HC<sub>3</sub>N [Clark *et al.*, 2010]. Our ability to constrain the composition of Titan's surface is fundamentally limited by the resolution of VIMS and the small wavelength windows where it is possible to observe the surface from orbit. VIMS data can be used to identify distinct units on the surface [Barnes *et al.*, 2007; Soderblom *et al.*, 2007a], but conclusive identification of the composition of the units is probably not possible without another mission given the constraints of the instrument. For example, Xanadu, one of Titan's most prominent features and the first surface feature seen from earth [Lemmon *et al.*, 1993; Smith *et al.*, 1996], is a “bright” terrain unit. Other units include “dark brown”, which seems to be dominated by dunes, and “dark blue”, which seems to be richer in water ice than the dark brown unit [Barnes *et al.*, 2007]. Neish *et al.* [2015] examined spectra of Titan's craters as a function of degradation state and concluded that impacts expose water ice and organics and then rainfall removes the soluble organics, leaving behind water ice and insoluble organics.

Measurements from Cassini RADAR provide constraints on the dielectric constant of the surface and Janssen *et al.* [2016] found that the radar bright regions ( $\sim 10\%$  of Titan's surface) are consistent with near subsurface water ice, while the radar dark regions are consistent with organics. The orbital measurements agree with measurements made by HASI/PWA of the surface at the Huygens landing site, which found a dielectric constant of  $2.5 \pm 0.3$  and a conductivity of  $1.2 \pm 0.6$  nS/m; values consistent with photochemically produced organic material in the first meter of the surface [Grard *et al.*, 2006; Hamelin *et al.*, 2016].

Analyses of measurements taken by the Huygens Probe and assessment of its behavior upon landing indicate that the surface at the Huygens landing site was fine-grained, relatively soft, and possibly covered in a 7 mm thick “fluffy” layer [Zarnecki *et al.*, 2005; Lorenz, 2006; Karkoschka *et al.*, 2007; Atkinson *et al.*, 2010; Schröder *et al.*, 2012]. The surface also contained volatiles as indicated by the increase in abundance of CH<sub>4</sub> after the Huygens Probe landed, most likely resulting from the heating of liquid CH<sub>4</sub> that was present on the surface[Niemann *et al.*, 2005, 2010], attenuation of acoustic signals after landing [Lorenz *et al.*, 2014b], a change in the PWA-MIP observations 11 minutes after landing [Hamelin *et al.*, 2016], and modeling of DISR spectra [Rannou *et al.*, 2016]. Located in a dry region of Titan, Williams *et al.* [2012] interpret the moisture detected at the Huygens landing site as evidence of a recent local precipitation event or the result of recharging from a precipitation event located farther away because the surface should dry relatively rapidly.

Only 11% of the sunlight incident at the top of Titan’s atmosphere reaches the surface [Tomasko *et al.*, 2005], which means there is very little solar energy available for further chemical processing on the surface. However, the molecules produced in the atmosphere, in particular those that possess triple bonds (like acetylene), carry chemical energy to the surface that could potentially be released [Lunine and Hörst, 2011]. Some laboratory work indicates that GCRs may induce chemistry on the surface [Zhou *et al.*, 2010], but the majority are deposited near 65 km and more work is required to characterize the surface energetic particle flux.

## 7.2. Fluvial transport and lakes and seas

In addition to methane, a number of products of Titan's atmospheric photochemistry are also liquid at Titan surface conditions; of these ethane is the most abundant. Based on photochemical considerations, *Lunine et al.* [1983] argued that the surface might be covered in vast seas or oceans of ethane. Prior to Cassini-Huygens, Earth-based measurements revealed that Titan's surface is heterogeneous [*Muhleman et al.*, 1990; *Lemmon et al.*, 1993; *Griffith*, 1993; *Lemmon et al.*, 1995; *Smith et al.*, 1996]. As the Huygens Probe descended through Titan's atmosphere, images taken by DISR revealed a network of channels flowing into a plain reminiscent of flood plains [*Tomasko et al.*, 2005]. The complex dendritic drainage systems observed are likely indicative of a distributed source and possibly formed by rapid erosion that creates deeply incised valleys [*Perron et al.*, 2006; *Soderblom et al.*, 2007a]. Rounded cobbles at the landing site provided additional evidence of fluvial erosion [*Tomasko et al.*, 2005]. Channel morphology can be used to constrain formation mechanisms. For example, the presence of dry valleys, found only at mid-latitudes, indicates strong episodic events [*Langhans et al.*, 2012]. Well-developed drowned river valleys indicate periods when rising fluid levels outpaced sediment deposition [*Stofan et al.*, 2007]. The spatial distribution of different channel types provides information about spatial variation in the strength and frequency of rainfall.

Although the Huygens Probe only found evidence of past fluvial activity, RADAR data obtained during T16 revealed numerous lakes and seas near the north pole [*Stofan et al.*, 2007]. For a review of the lakes and seas, see *Hayes* [2016]. The surprising ability to use Cassini RADAR to measure the depths of the lakes and seas has resulted in the production of the first extraterrestrial bathymetric maps [*Mastrogiuseppe et al.*, 2014; *Le*

*Gall et al.*, 2016; *Hayes*, 2016]; Ligeia Mare is up to 160 m deep, while Ontario Lacus is 90 m deep. Titan's lakes and seas cover  $\sim$ 1% of Titan's surface [*Hayes et al.*, 2008; *Hayes*, 2016] and contain liquids that represent a global ocean depth of about 1 m [*Hayes*, 2016], significantly less than predicated by photochemical models as discussed in Section 3.2.

Although Titan's entire surface has not been mapped, there appears to be a north-south asymmetry in the distribution of the lakes, which may be the result of Titanian Croll-Milankovitch cycles [*Aharonson et al.*, 2009; *Schneider et al.*, 2012; *Lora and Mitchell*, 2015]. As discussed previously, Titan GCMs agree that methane is efficiently transported away from the equator, drying out the low and mid-latitudes and depositing liquid at the poles [*Mitchell et al.*, 2006; *Mitchell*, 2008; *Mitchell et al.*, 2009; *Schneider et al.*, 2012; *Mitchell*, 2012; *Lora et al.*, 2014, 2015]. Although the southern hemisphere appears to be almost entirely devoid of currently filled lakes, there is some geomorphological evidence of paleoseas [*Aharonson et al.*, 2009; *Hayes et al.*, 2011; *Moore and Pappalardo*, 2011], with the most equatorward candidates located at  $39^{\circ}$  and  $42^{\circ}$ S [*Vixie et al.*, 2015].

*Lora et al.* [2014] simulated Titan's paleoclimate over the past 42,000 years looking at four characteristic configurations and found that all four result in efficient transport of methane to the poles; the present day configuration and 14 kyr configuration favor transport to the north pole, the 28 kyr configuration favors the south pole, and the 42 kyr configuration is symmetric. This work demonstrates that the lakes may preferentially form at one pole based on orbital configuration, but also shows that the low and mid-latitudes have likely been dry for a long time, and that the asymmetry would reverse with a period of  $\sim$ 125 kyr [*Lora et al.*, 2014].

Due to the length of the Cassini mission, it might be possible to detect seasonal changes in lake level by looking for shoreline changes [Mitri *et al.*, 2007]. While some shoreline changes have been reported there are conflicting interpretations of the data and it remains an open question whether Cassini has detected changes in the liquid level of the lakes and seas [Barnes *et al.*, 2009; Turtle *et al.*, 2009; Moriconi *et al.*, 2010; Hayes *et al.*, 2011; Turtle *et al.*, 2011a, b; Cornet *et al.*, 2012a; Sotin *et al.*, 2012; Lucas *et al.*, 2014a; Hayes, 2016]. Regardless of whether the lake levels have changed over the past decade, there is evidence for deposits of evaporites on the surface, created by cycles of evaporation and refilling, including around Ontario Lacus [Barnes *et al.*, 2009; Moriconi *et al.*, 2010; Barnes *et al.*, 2011a; Cornet *et al.*, 2012b; MacKenzie *et al.*, 2014]. These putative evaporite deposits are anomalously bright at 5  $\mu\text{m}$  in the VIMS data and  $\sim 1\%$  of the surface exhibits this spectral behavior [MacKenzie *et al.*, 2014]. The signal attributed to evaporites near Ligeia Mare would require it to have covered 9% greater area indicating lake level changes of unknown timescales [MacKenzie *et al.*, 2014]. The southern paleoseas do not exhibit this signature, indicating burial, erasure, lack of formation in the first place, or some other unknown process [MacKenzie *et al.*, 2014]. The distribution and composition of evaporites contain information about Titan's climate history, but will require composition measurements that cannot be obtained with Cassini. Measurements [Le Gall *et al.*, 2016] and recent models [Glein and Shock, 2013; Tan *et al.*, 2013, 2015] agree that the northern lakes and seas appear to be methane rich, contrary to prior predictions that they should be dominated by ethane [Cordier *et al.*, 2009, 2012]. Ethane has been detected in Ontario Lacus from VIMS measurements [Brown *et al.*, 2008] and from RADAR Ontario Lacus appears to contain a greater fraction of ethane than the northern lakes and seas [Hayes,

2016]. It is likely that a combination of spatial/temporal variation in precipitation rates (and composition of precipitation), transport [Lorenz, 2014a; Tokano and Lorenz, 2016], and thermodynamic considerations will be required to explain the composition of the lakes. Even so, considering that ethane is the most abundant product of Titan's photochemistry, it is surprising that so little liquid ethane has been detected on the surface. Mousis *et al.* [2016] showed that ethane could be preferentially pulled into clathrates that are in contact with the lakes and/or an alcanofer, resulting in predominantly methane rich lakes and trapping significant amounts of ethane in clathrates thus explaining the observed lack of liquid ethane on the surface.

The so-called "cookie-cutter" lakes found near the north pole have steep walls and are 100s of meters deep [Hayes *et al.*, 2008; Stiles *et al.*, 2009], morphology that is consistent with dissolution karst [Cornet *et al.*, 2015]. Since methane does not dissolve water ice but it can dissolve organics like solid acetylene [Glein and Shock, 2013; Malaska and Hodyss, 2014], the presence of dissolution karst would indicate that there are 100s of meters of organics at the north pole, which has implications for atmospheric chemical and dynamical processes that would result in such a significant deposit of organics.

The lakes and seas represent a region of particular astrobiological interest for Titan. Some fraction of the complex organics produced in the atmosphere will end up in the lakes and seas either directly through sedimentation from the atmosphere (dry removal), washout from rain (wet removal), or from subsequent transport processes once they are deposited on the surface. Some of the compounds are soluble in liquid hydrocarbons, but others are not thus the lakes will partition the organics produced in the atmosphere potentially resulting in subsequent chemistry. Stevenson *et al.* [2015] suggested that nitrogen

compounds could act as a lipid bilayer in the lakes. In addition to solubility, density also plays a role in the fate of materials in the lakes and seas; ice formed during the winter would likely float [*Roe and Grundy*, 2012; *Hofgartner and Lunine*, 2013] and experimental simulations of haze formation indicate the possibility that the haze particles would also float [*Hörst and Tolbert*, 2013]. However, hydrocarbon solids are generally more dense than their corresponding liquids and will sink forming deposits on the sea floor [*Tokano*, 2009]. For example, *Le Gall et al.* [2016] see evidence that the bottom of the Ligeia Mare is coated in a layer of nitriles. An improved understanding of the chemistry of the lakes requires experimental investigations and additional measurements from a future mission.

### 7.3. Winds and waves

The lakes and seas are of particular atmospheric interest because waves can be used to constrain the wind speeds, which as previously mentioned are very difficult to measure directly. For most of the mission, vertical deviations were less than a few mm [*Wye et al.*, 2009; *Stephan et al.*, 2010; *Barnes et al.*, 2011b; *Zebker et al.*, 2014]. The size of the wave depends on wind speed and liquid viscosity, both of which are ultimately determined by the atmosphere. *Lorenz and Hayes* [2012] showed that the 2 m/s maximum wind speeds predicted by GCMs would produce 1 m waves. *Hayes et al.* [2013] argue that the lack of detections for most of the mission are not surprising based on GCMs [*Schneider et al.*, 2012; *Lora et al.*, 2015] as the wind speeds should be below the threshold for generating waves at equinox but should exceed it moving into summer solstice. As we move into northern summer there have been a few reports of potential wave activity [*Barnes et al.*, 2014; *Hofgartner et al.*, 2014, 2016] and one hopes definitive detections of waves will occur before the end of the mission.

#### 7.4. Aeolian transport and dunes

Although pre-Cassini-Huygens predictions indicated that Titan is not a favorable location for dune formation [Lorenz *et al.*, 1995], data from Cassini RADAR revealed widespread regions of equatorial dunes ( $\pm 30^\circ$ ) covering 10-20% of Titan's surface [Elachi *et al.*, 2005; Lorenz *et al.*, 2006b; Radebaugh *et al.*, 2008; Lorenz and Radebaugh, 2009; Le Gall *et al.*, 2011; Rodriguez *et al.*, 2014]. The dunes are likely composed of 100-300  $\mu\text{m}$  particles [Lorenz *et al.*, 2006b] and analyses of RADAR and VIMS data indicate that they are composed of pure organic or organic coated materials [McCord *et al.*, 2006; Soderblom *et al.*, 2007b; Barnes *et al.*, 2008; Clark *et al.*, 2010; Le Gall *et al.*, 2011; Hirtzig *et al.*, 2013; Rodriguez *et al.*, 2014]. The dune particles are much larger than the aerosols measured by DISR near the surface and it is not yet clear whether the dune sands are composed of haze material and if so, how the larger particles formed. Barnes *et al.* [2015] discussed a number of possible formation mechanisms including sintering, lithification/erosion, flocculation, and evaporitic precipitation.

Titan's dunes are eastward propagating longitudinal dunes  $\sim$ 100 m tall, 1 km wide, and on average 30-50 km long [Lorenz *et al.*, 2006b; Radebaugh *et al.*, 2008; Barnes *et al.*, 2008; Neish *et al.*, 2010b; Le Gall *et al.*, 2011]. The observed 1-3 km spacing [Lorenz *et al.*, 2006b; Radebaugh *et al.*, 2008; Savage *et al.*, 2014] is approximately the same height as the boundary layer indicating that the dunes are mature, and have therefore stopped growing [Griffith *et al.*, 2008; Lorenz *et al.*, 2010; Lorenz, 2014b]. Dune orientation and morphology are determined by wind patterns; given the difficulties in measuring Titan's winds remotely, the dunes provide some of our only constraints on the wind speed and direction at the surface. Although initial GCM wind predictions were inconsistent with the

dune orientations [*Tokano*, 2008], more recent works demonstrate that conditions around equinox, either a reversal of the prevailing winds (to strong westerly (eastward) winds) [*Tokano*, 2010b] or the generation of strong, westerly wind gusts by the observed equinoctial storms (because their momentum comes from higher altitudes where strong westerlies are present) [*Lucas et al.*, 2014b; *Charnay et al.*, 2015], control the dune elongation rather than the prevailing easterlies (westward).

This interpretation is supported by experiments done using the Titan Wind Tunnel that show that threshold wind speeds are higher than previously predicted for Titan and faster than the prevailing easterlies [*Burr et al.*, 2015]. As with the channels observed at the Huygens landing site, it seems that many of the observed surface features may form during brief, intense periods rather than under the prevailing conditions. There is evidence that the dunes are active and therefore record the relatively recent climate conditions [*Barnes et al.*, 2008; *Neish et al.*, 2010b; *Lorenz*, 2014b; *Savage et al.*, 2014]. *Lorenz* [2014b] estimated a reorientation timescale of  $\sim$ 50,000 years, which is a similar timescale to climate forcing so the dunes could potentially be out of equilibrium with the present winds [*Lorenz*, 2014b; *Ewing et al.*, 2015]. Through an inter-GCM comparison *McDonald et al.* [2016] showed that orbital forcing is important and must be considered when evaluating dune orientations.

In addition to dune formation, aeolian processes may be responsible for the formation of the so-called "blandlands", Titan's undifferentiated plains [*Lopes et al.*, 2016]. Since the blandlands appear to be the most prevalent geomorphologic unit on Titan (covering  $\sim$ 17%), with dunes coming in a close second [*Lopes et al.*, 2016], an aeolian formation mechanism would mean that aeolian processes play a dominant role in shaping Titan's

landscape. An analysis of material transport directions indicates that aeolian transport is the dominant transport mechanism at the equator and mid-latitudes [Malaska *et al.*, 2016].

## 7.5. Craters

The dearth of craters on Titan's surface indicates that it is geologically young. The largest crater observed thus far is Menrva with a diameter of 450 km [Elachi *et al.*, 2006]. The craters are not distributed uniformly; Xanadu is the most heavily cratered region and the equatorial dune regions and north pole have lower crater densities than average [Wood *et al.*, 2010]. Well-preserved craters seem to be found only at low latitudes [Lopes *et al.*, 2010]. Based on the crater size distribution, the age of the surface has been estimated to be between 200 Myr and 1 Gyr, which is quite similar to the age of Earth's surface and indicates that Titan's surface has undergone some amount of resurfacing [Lorenz *et al.*, 2007; Neish and Lorenz, 2012]. The craters that have been investigated in greater detail, including Sinlap and Selk craters, show evidence of fluvial and aeolian erosion [Le Mouélic *et al.*, 2008; Soderblom *et al.*, 2010; Wood *et al.*, 2010]. Neish *et al.* [2013] found that craters on Titan are shallower than comparable size craters on Ganymede; they argue that the craters have been filled in from aeolian transport.

## 7.6. Cryovolcanism

In addition to mountains (see e.g., Radebaugh *et al.* [2007, 2011]), a number of potential cryovolcanic features have been identified through the use of RADAR and VIMS measurements. The general trend in investigation of cryovolcanic features on Titan seems to be that as more data become available for a particular feature, the less likely it seems that

it is cryovolcanic. Both Ganesa Macula and Tortola Facula were initially believed to be cryovolcanic features based on RADAR [Neish *et al.*, 2006; Lopes *et al.*, 2007] and VIMS measurements respectively [Sotin *et al.*, 2005], but data from the other instruments did not support that interpretation [Hansen *et al.*, 2010]. Tui Regio is extremely bright at 5  $\mu\text{m}$ , leading to the suggestion that it may be a region of cryovolcanic activity [Barnes *et al.*, 2006, 2011a]; measurements from RADAR may support this interpretation [Mitchell *et al.*, 2010], but it has been suggested that Tui Regio is actually the site of an ancient sea [Moore and Howard, 2010].

Currently, the two most probable candidate cryovolcanic features are Hotei Regio and the complex that includes Sotra Patera, Doom Mons, Mohini Fluctus, and Erebor Mons (shown in Figure 9) [Lopes *et al.*, 2013]. Measurements from VIMS indicate that Hotei Regio is unusually bright at 5  $\mu\text{m}$  [Barnes *et al.*, 2005], is not fluvial in origin [Soderblom *et al.*, 2009], and may have exhibited spectrophotometric variability in the VIMS measurements during the Cassini mission [Nelson *et al.*, 2009]. Additionally, the flow features appear to be lobate based on RADAR mapping [Wall *et al.*, 2009]. Others interpret the available data as an indication of a fluvial origin [Moore and Pappalardo, 2011]. The Sotra Patera region consists of mountains, non-circular pits, and flow-like lobes [Kirk *et al.*, 2010; Lopes *et al.*, 2013]. The large scale flow deposits known as Mohini Fluctus appear to originate from Doom Mons. Erebor Mons also has lobate deposits associated with it. Sotra Patera is 1.7 km deep, making it the deepest local depression identified thus far on Titan [Lopes *et al.*, 2013]. The existence of cryovolcanism on Titan remains an open question, one whose answer has important implications for the origin and resupply of CH<sub>4</sub> in Titan's atmosphere, as discussed in Section 8.

## 8. The Age and Origin of Titan's Atmosphere

Prior to Cassini-Huygens, the origin and age of Titan's atmosphere were poorly constrained. The mostly likely sources of nitrogen in Titan's atmosphere are either N<sub>2</sub> or NH<sub>3</sub> (see e.g., *Strobel* [1982]), which were incorporated during formation or delivered after formation. If the original nitrogen bearing molecule was NH<sub>3</sub>, then subsequent photolysis [Lewis, 1971; Atreya *et al.*, 1978] or reactions in Titan's interior [Glein *et al.*, 2009; Glein, 2015] are required to form the current N<sub>2</sub> atmosphere. The abundances of primordial noble gases are particularly important for constraining the origin of Titan's atmosphere, but could not be measured prior to Cassini-Huygens. The GCMS carried by Huygens detected <sup>36</sup>Ar, <sup>22</sup>Ne, and set upper limits on the abundances of Kr and Xe. The ratio of <sup>36</sup>Ar to <sup>14</sup>N is orders of magnitude below solar [Niemann *et al.*, 2005, 2010] and it is therefore unlikely that large amounts of N<sub>2</sub> accreted during formation [Bar-Nun *et al.*, 1988; Niemann *et al.*, 2005]. The presence of radiogenic <sup>40</sup>Ar, outgassed from Titan's rocky interior, indicates that the interior and atmosphere are connected [Niemann *et al.*, 2005]. The non-detection of Kr and Xe is not particularly surprising; the upper limits are consistent with solar abundances and a number of other atmospheres in the solar system [Owen and Niemann, 2009]. Additionally there are a number of possible noble gas sequestration mechanisms, both prior to and after formation: H<sub>3</sub><sup>+</sup> complexes [Pauzat *et al.*, 2013], trapping in hazes [Jacovi and Bar-Nun, 2008], dissolution in lakes and seas [Cordier *et al.*, 2010; Hodyss *et al.*, 2013], and trapping in clathrate hydrates [Mousis *et al.*, 2011; Tobie *et al.*, 2012]. However, Glein [2015] recently suggested the Kr upper limit is sufficiently restrictive to indicate that Titan's CH<sub>4</sub> formed in Titan's interior from CO<sub>2</sub>, rather than CH<sub>4</sub> clathrates that would efficiently trap Kr [Niemann *et al.*, 2005;

*Atreya et al.*, 2006]. Additional measurements of primordial and radiogenic noble gases are required.

The  $^{14}\text{N}/^{15}\text{N}$  measurement in  $\text{N}_2$  from GCMS ( $167.7 \pm 0.6$ , *Niemann et al.* [2005, 2010]), is the lowest measured atmospheric value in the solar system and similar to a range of cometary measurements [*Rousselot et al.*, 2014; *Shinnaka et al.*, 2014]. Figure 10 places the measurements of Titan's H, C, N, and O isotopes into solar system context. Conversion of  $\text{NH}_3$  to  $\text{N}_2$  by photolysis [*Atreya et al.*, 1978], shock chemistry [*McKay et al.*, 1988], and thermal decomposition in the interior [*Glein et al.*, 2009] do not significantly alter the  $^{14}\text{N}/^{15}\text{N}$  ratio [*Berezhnoi*, 2010]. *Sekine et al.* [2011] also suggested that impacts into ammonium hydrate in the crust could convert  $\text{NH}_3$  into  $\text{N}_2$ ; however, *Marounina et al.* [2015] showed that impact erosion of Titan's atmosphere would be very efficient. Escape processes (Jean's, sputtering, and/or hydrodynamic) are not efficient enough to fractionate Titan's  $\text{N}_2$  over the age of the solar system [*Mandt et al.*, 2009, 2014]. The Ar isotopes combined with  $^{14}\text{N}/^{15}\text{N}$  indicate that Titan's nitrogen originated as ammonia from the protosolar nebula, not the subsaturnian nebula [*Mandt et al.*, 2014], and may have undergone conversion to  $\text{N}_2$  in Titan's interior rather than its atmosphere [*Glein*, 2015]. Ground-based observations have set a lower limit on  $^{14}\text{N}/^{15}\text{N}$  in  $\text{NH}_3$  in Saturn's atmosphere [*Fletcher et al.*, 2014], which is significantly higher than for Titan indicating that the nitrogen in the atmospheres of Titan and Saturn came from different reservoirs.

The  $\text{CH}_4$  in Titan's atmosphere is irreversibly destroyed by photolysis because one of the most abundant photolysis products,  $\text{H}_2$ , escapes. Photochemical models agree that the current abundance of  $\text{CH}_4$  would be destroyed by the present day atmospheric chemistry in  $\sim 30$  Myr [*Yung et al.*, 1984; *Wilson and Atreya*, 2004], implying that the  $\text{CH}_4$  has a

continuous or episodic resupply mechanism, the models were missing important processes, and/or the atmosphere is not the age of the solar system, but we lacked information required to begin to answer these questions. Measurements of  $^{12}\text{C}/^{13}\text{C}$  in  $\text{CH}_4$  from the INMS and CIRS agree with the measurement from GCMS [Niemann *et al.*, 2010; Nixon *et al.*, 2012; Mandt *et al.*, 2012], and are consistent with an assumed possible range of primordial values. Models of atmospheric escape and fractionation by chemistry (which vary in relative importance depending on the process), combined with the carbon isotope observations indicate that either no significant fractionating loss process is occurring, the methane present is very recent, or that there is a production/loss mechanism that is balancing escape over geologic timescales [Nixon *et al.*, 2012; Mandt *et al.*, 2012]. Even if replenishment is occurring, the  $^{12}\text{C}/^{13}\text{C}$  still points to an atmospheric age of less than 1 Gyr.

The issue of  $\text{CH}_4$  resupply remains an outstanding question. The lakes and seas do not represent a large enough reservoir to maintain the current atmospheric abundance over the age of the solar system. If the atmospheric methane is resupplied, methane in the subsurface ocean and/or methane clathrate hydrates in the crust are presumably the source. If the crust is methane clathrate, diffusion of  $\text{C}_2\text{H}_6$  into the clathrate pushes  $\text{CH}_4$  out, resupplying half of the necessary methane [Choukroun and Sotin, 2012]. It is also possible that a substantial amount of liquid hydrocarbons is present in the subsurface, perhaps in the form of an alkanofer, which could also resupply the atmosphere. The possible detection of tropical lakes [Griffith *et al.*, 2012b] supports the existence of a subsurface reservoir.

Titan's D/H ratio remains poorly understood. Higher than Saturn, but lower than cometary water and Enceladus ( $2.9^{+1.5}_{-0.7} \times 10^{-4}$ , *Waite et al.* [2009]), it is difficult to explain the evolution of D/H from either of those reservoirs to Titan's present value. A measurement of D/H in cometary CH<sub>4</sub> and/or Titan's water ice crust would hopefully explain Titan's D/H, in the process determining if Titan's CH<sub>4</sub> is primordial or if it comes from conversion of CO<sub>2</sub> to CH<sub>4</sub> in Titan's interior [*Niemann et al.*, 2010].

Another puzzle relating to the origin of Titan's atmosphere, dating back to the Voyager era, is the abundance of carbon monoxide (CO) in Titan's atmosphere, as discussed in Section 3.2. The primordial CO abundance in Titans atmosphere represents an additional constraint on models of Titan's formation and evolution and the thermochemical conditions where Titan's building blocks formed [*Tobie et al.*, 2012], which in turn constrains whether those building blocks formed in the protosolar nebula or the subsaturnian nebula. The detection of O<sup>+</sup> precipitating into Titan's atmosphere by the Cassini Plasma Spectrometer (CAPS) [*Hartle et al.*, 2006], combined with photochemical modeling of Titan's oxygen chemistry, demonstrates that Titan's oxygen has an exogenic source, Enceladus. The oxygen isotope measurements from Titan [*Serigano et al.*, 2016] and Enceladus [*Waite et al.*, 2009] are consistent. Given CO's extremely long lifetime in Titan's atmosphere, it is unlikely that Titan's primordial atmosphere contained significant amounts of CO [*Hörst et al.*, 2008]. This result supports the conclusion that Titan's nitrogen was originally NH<sub>3</sub>.

There are other possible constraints on the age of Titan's atmosphere in addition to the atmospheric composition measurements and models as shown in Figure 11. Interior models suggest that major outgassing episodes were likely to occur for the past 1 Gyr [*Tobie et al.*, 2006; *Castillo-Rogez and Lunine*, 2010] and the crater populations point

to a surface age of  $\sim$ 200-1000 Myr [Lorenz *et al.*, 2007; Neish and Lorenz, 2012]. The current observable organic inventory on the surface requires  $\sim$ 135 Myr to accumulate [Lorenz *et al.*, 2008c; Nixon *et al.*, 2012], which is significantly less than the age of the solar system, requiring either an efficient burial mechanism or implying that the current organic deposition rates have not existed for the entire age of the solar system. Taken together, these lines of evidence make it difficult to envision a scenario in which Titan's atmosphere has existed as we see it today for the entire age of the Solar system. Additionally, overlap in these different estimates occurs around  $\sim$ 300-500 Myr ago (without assuming CH<sub>4</sub> has been replenished) indicating that there is likely something fundamental about that period in Titan's history.

There are a number of different possible scenarios if Titan's present-day atmosphere has only existed as such for  $\sim$ 500 Myr. Many of the age constraints mentioned above and shown in Figure 11 constrain only the age of the CH<sub>4</sub> and period of active CH<sub>4</sub> photochemistry. It may be possible that prior to that time a different atmosphere, such as a pure N<sub>2</sub> atmosphere, existed. Charnay *et al.* [2014] explored the behavior of a pure N<sub>2</sub> atmosphere, including a paleo-nitrogen cycle in which liquid nitrogen lakes and seas modified Titan's surface. This case is particularly interesting given that without a resupply mechanism, Titan's atmospheric methane will be depleted within the next 10s of Myr resulting in an N<sub>2</sub> atmosphere. For the future Titan case, they found that without methane, Titan's mean surface temperature would be  $\sim$ 86.5-89.5 (depending on cloud properties) and although thin clouds would exist, the surface would be very dry [Charnay *et al.*, 2014].

## 9. Outstanding questions and the future

On the eve of the Voyager encounter, *Caldwell* [1981] wrote “Titan is therefore also unique in being the object in the Solar System for which the atmosphere is least well understood.” As we enter the post-Cassini-Huygens era, it is clear that Titan’s atmosphere is no longer the “least well understood.” Nonetheless, as discussed above, a number of outstanding questions remain including:

1. What are the very heavy ions in the ionosphere, how do they form, and what are the implications for complexity of prebiotic chemistry?
2. What is the connection between the plumes of Enceladus and Titan’s atmosphere?
3. What is the composition of the haze and how does it vary spatially and temporally?
4. How do the organic compounds produced in the atmosphere evolve once reaching the surface?
5. What are the dynamics of Titan’s troposphere and how does that affect the evolution of the surface?
6. How variable is Titan’s weather from year to year and how variable is the climate over longer timescales?
7. How old is Titan’s current atmosphere?
8. What happened on Titan 300-500 Myrs ago?
9. Is Titan’s atmospheric methane cyclic and/or episodic and if so, what are the implications of those timescales on habitability?
10. Where is the origin of Titan’s methane and what is the fate of the photochemically produced ethane?

11. What is controlling Titan's H<sub>2</sub> profile and potential spatial variations?
12. What is the composition of the surface and on what scales is it spatially variable?
13. What is the composition of the lakes and seas and what chemistry occurs there?
14. What is the circulation in the lakes and seas and how is it affected by the atmospheric dynamics?
15. What is the composition of the dune particles and how are they produced?
16. Does cryovolcanism occur on Titan?

Finding answers to many of these questions will require future missions to Titan; *Tobie et al.* [2014] and *Mitri et al.* [2014] provide excellent reviews of science goals and mission concepts for future exploration of Titan. The presence of both a subsurface water ocean [*Béghin et al.*, 2010; *Baland et al.*, 2011; *Bills and Nimmo*, 2011; *Béghin et al.*, 2012; *Iess et al.*, 2012] and extensive hydrocarbon seas on the surface make Titan a prime target for NASA's renewed interest in exploring "Ocean Worlds". Titan's diverse oceans serve as a test for the ubiquity and diversity of life [*Lunine*, 2009].

The wealth of data obtained by Cassini-Huygens and Earth-based observations in support of our quest to understand Titan will take many years to fully synthesize into an increased understanding of Titan's atmosphere and climate and will require additional insights from laboratory experiments and models. With the highly successful New Horizons flyby of Pluto, we now have a rich atmospheric dataset for another hazy N<sub>2</sub>/CH<sub>4</sub>/CO atmosphere; comparative planetology investigations in the coming years should improve our understanding of both atmospheres. Additionally, since a large number of exoplanets appear to have an aerosol absorber in their atmospheres (see e.g., *Kreidberg et al.* [2014]; *Knutson et al.* [2014a, b]), which may be photochemically produced [*Marley et al.*, 2013],

there is increasing interest in using Titan as an exoplanet analogue [Lunine, 2010; Bazzon *et al.*, 2014; Robinson *et al.*, 2014].

Since the Voyager era, we, as a community, have made significant progress in understanding Titan's atmosphere and climate; we have transformed Titan from an enigmatic moon into a dynamic world. This transformation required the persistent and sustained effort of an international, multidisciplinary community that leveraged ground and space based observing, spacecraft measurements, laboratory experiments, and models in pursuit of one overarching goal: to understand Titan as a world. In the process, we have pushed our understanding of terrestrial processes like fluvial and aeolian erosion into completely new phase space allowing us to begin to determine the underlying fundamental physics and chemistry that drive a number of planetary processes. We unveiled a beautiful world that holds so many pieces to the puzzle of how planets form and evolve. We revealed atmospheric organic chemistry that is so complex we are forced to rethink our ideas about how atmospheres work. As discussed above, our work is not yet finished, many unanswered questions remain. Answering those questions will require a similar effort that will lead to even greater rewards.

**Acknowledgments.** This work is dedicated to my dad, Dr. William Peter Horst, who passed away unexpectedly around the time that I agreed to write this review. He still inspires me to “slam back” every day. I would like to thank two anonymous referees for their time and energy. The paper benefited greatly from their expertise and contributions. As a review paper, all the data shown and discussed here are in the cited references and/or in NASA’s Planetary Data System (PDS) <http://pds.nasa.gov>.

## References

- Ågren, K., J.-E. Wahlund, P. Garnier, R. Modolo, J. Cui, M. Galand, and I. Müller-Wodarg (2009), On the ionospheric structure of Titan, *Planet. Space Sci.*, **57**, 1821–1827, doi:10.1016/j.pss.2009.04.012.
- Ågren, K., N. J. T. Edberg, and J.-E. Wahlund (2012), Detection of negative ions in the deep ionosphere of Titan during the Cassini T70 flyby, *Geophys. Res. Lett.*, **39**, L10201, doi:10.1029/2012GL051714.
- Aboudan, A., G. Colombatti, F. Ferri, and F. Angrilli (2008), Huygens probe entry trajectory and attitude estimated simultaneously with Titan atmospheric structure by Kalman filtering, *Planet. Space Sci.*, **56**, 573–585, doi:10.1016/j.pss.2007.10.006.
- Achterberg, R. K., B. J. Conrath, P. J. Gierasch, F. M. Flasar, and C. A. Nixon (2008a), Titan's middle-atmospheric temperatures and dynamics observed by the Cassini Composite Infrared Spectrometer, *Icarus*, **194**, 263–277, doi:10.1016/j.icarus.2007.09.029.
- Achterberg, R. K., B. J. Conrath, P. J. Gierasch, F. M. Flasar, and C. A. Nixon (2008b), Observation of a tilt of Titan's middle-atmospheric superrotation, *Icarus*, **197**, 549–555, doi:10.1016/j.icarus.2008.05.014.
- Achterberg, R. K., P. J. Gierasch, B. J. Conrath, F. Michael Flasar, and C. A. Nixon (2011), Temporal variations of Titan's middle-atmospheric temperatures from 2004 to 2009 observed by Cassini/CIRS, *Icarus*, **211**, 686–698, doi:10.1016/j.icarus.2010.08.009.
- Ádámkovics, M., J. W. Barnes, M. Hartung, and I. de Pater (2010), Observations of a stationary mid-latitude cloud system on Titan, *Icarus*, **208**, 868–877, doi:10.1016/j.icarus.2010.03.006.
- Ádámkovics, M., J. L. Mitchell, A. G. Hayes, P. M. Rojo, P. Corlies, J. W. Barnes,

- V. D. Ivanov, R. H. Brown, K. H. Baines, B. J. Buratti, R. N. Clark, P. D. Nicholson, and C. Sotin (2016), Meridional variation in tropospheric methane on Titan observed with AO spectroscopy at Keck and VLT, *Icarus*, 270, 376–388, doi: 10.1016/j.icarus.2015.05.023.
- Adriani, A., B. M. Dinelli, M. López-Puertas, M. García-Comas, M. L. Moriconi, E. D'Aversa, B. Funke, and A. Coradini (2011), Distribution of HCN in Titan's upper atmosphere from Cassini/VIMS observations at 3  $\mu\text{m}$ , *Icarus*, 214, 584–595, doi: 10.1016/j.icarus.2011.04.016.
- Aharonson, O., A. G. Hayes, J. I. Lunine, R. D. Lorenz, M. D. Allison, and C. Elachi (2009), An asymmetric distribution of lakes on Titan as a possible consequence of orbital forcing, *Nature Geoscience*, 2, 851–854, doi:10.1038/ngeo698.
- Ajello, J. M., M. H. Stevens, I. Stewart, K. Larsen, L. Esposito, J. Colwell, W. McClintock, G. Holsclaw, J. Gustin, and W. Pryor (2007), Titan airglow spectra from Cassini Ultraviolet Imaging Spectrograph (UVIS): EUV analysis, *Geophys. Res. Lett.*, 34, L24204, doi:10.1029/2007GL031555.
- Ajello, J. M., J. Gustin, I. Stewart, K. Larsen, L. Esposito, W. Pryor, W. McClintock, M. H. Stevens, C. P. Malone, and D. Dziczek (2008), Titan airglow spectra from the Cassini Ultraviolet Imaging Spectrograph: FUV disk analysis, *Geophys. Res. Lett.*, 35, L06,102, doi:10.1029/2007GL032315.
- Allen, M., Y. L. Yung, and J. P. Pinto (1980), Titan - Aerosol photochemistry and variations related to the sunspot cycle, *ApJL*, 242, L125–L128, doi:10.1086/183416.
- Anderson, C. M., and R. E. Samuelson (2011), Titan's aerosol and stratospheric ice opacities between 18 and 500  $\mu\text{m}$ : Vertical and spectral characteristics from Cassini CIRS,

*Icarus*, 212, 762–778, doi:10.1016/j.icarus.2011.01.024.

Anderson, C. M., R. E. Samuelson, G. L. Bjoraker, and R. K. Achterberg (2010), Particle size and abundance of HC<sub>3</sub>N ice in Titan's lower stratosphere at high northern latitudes, *Icarus*, 207, 914–922, doi:10.1016/j.icarus.2009.12.024.

Anderson, C. M., R. E. Samuelson, R. K. Achterberg, J. W. Barnes, and F. M. Flasar (2014), Subsidence-induced methane clouds in Titan's winter polar stratosphere and upper troposphere, *Icarus*, 243, 129–138, doi:10.1016/j.icarus.2014.09.007.

Anderson, C. M., R. E. Samuelson, Y. L. Yung, and J. L. McLain (2016), Solid-state photochemistry as a formation mechanism for Titan's stratospheric C<sub>4</sub>N<sub>2</sub> ice clouds, *Geophys. Res. Lett.*, 43, 3088–3094, doi:10.1002/2016GL067795.

Atkinson, K. R., J. C. Zarnecki, M. C. Towner, T. J. Ringrose, A. Hagermann, A. J. Ball, M. R. Leese, G. Kargl, M. D. Paton, R. D. Lorenz, and S. F. Green (2010), Penetrometry of granular and moist planetary surface materials: Application to the Huygens landing site on Titan, *Icarus*, 210, 843–851, doi:10.1016/j.icarus.2010.07.019.

Atreya, S. K., T. M. Donahue, and W. R. Kuhn (1978), Evolution of a nitrogen atmosphere on Titan, *Science*, 201, 611–613.

Atreya, S. K., E. Y. Adams, H. B. Niemann, J. E. Demick-Montelara, T. C. Owen, M. Fulchignoni, F. Ferri, and E. H. Wilson (2006), Titan's methane cycle, *Planet. Space. Sci.*, 54, 1177–1187, doi:10.1016/j.pss.2006.05.028.

Backes, H., F. M. Neubauer, M. K. Dougherty, N. Achilleos, N. André, C. S. Arridge, C. Bertucci, G. H. Jones, K. K. Khurana, C. T. Russell, and A. Wennmacher (2005), Titan's Magnetic Field Signature During the First Cassini Encounter, *Science*, 308, 992–995, doi:10.1126/science.1109763.

Bakes, E. L. O., S. é. Lebonnois, C. W. Bauschlicher, and C. P. McKay (2003), The role of submicrometer aerosols and macromolecules in H<sub>2</sub> formation in the titan haze, *Icarus*, **161**, 468–473, doi:10.1016/S0019-1035(02)00040-4.

Baland, R.-M., T. van Hoolst, M. Yseboodt, and Ö. Karatekin (2011), Titan's obliquity as evidence of a subsurface ocean?, *Astronomy and Astrophysics*, **530**, A141, doi: 10.1051/0004-6361/201116578.

Bampasidis, G., A. Coustenis, R. K. Achterberg, S. Vinatier, P. Lavvas, C. A. Nixon, D. E. Jennings, N. A. Teanby, F. M. Flasar, R. C. Carlson, X. Moussas, P. Preka-Papadema, P. N. Romani, E. A. Guandique, and S. Stamogiorgos (2012), Thermal and Chemical Structure Variations in Titan's Stratosphere during the Cassini Mission, *ApJ*, **760**, 144, doi:10.1088/0004-637X/760/2/144.

Bar-Nun, A., I. Kleinfeld, and E. Ganor (1988), Shape and optical properties of aerosols formed by photolysis of acetylene, ethylene, and hydrogen cyanide, *J. Geophys. Res.*, **93**, 8383–8387, doi:10.1029/JD093iD07p08383.

Bar-Nun, A., I. Kleinfeld, and E. Kochavi (1988), Trapping of gas mixtures by amorphous water ice, *Phys. Rev. B*, **38**, 7749–7754, doi:10.1103/PhysRevB.38.7749.

Barnes, J. W., R. H. Brown, E. P. Turtle, A. S. McEwen, R. D. Lorenz, M. Janssen, E. L. Schaller, M. E. Brown, B. J. Buratti, C. Sotin, C. Griffith, R. Clark, J. Perry, S. Fussner, J. Barbara, R. West, C. Elachi, A. H. Bouchez, H. G. Roe, K. H. Baines, G. Bellucci, J. Bibring, F. Capaccioni, P. Cerroni, M. Combes, A. Coradini, D. P. Cruikshank, P. Drossart, V. Formisano, R. Jaumann, Y. Langevin, D. L. Matson, T. B. McCord, P. D. Nicholson, and B. Sicardy (2005), A 5-Micron-Bright Spot on Titan: Evidence for Surface Diversity, *Science*, **310**, 92–95, doi:10.1126/science.1117075.

Barnes, J. W., R. H. Brown, J. Radebaugh, B. J. Buratti, C. Sotin, S. Le Mouelic, S. Rodriguez, E. P. Turtle, J. Perry, R. Clark, K. H. Baines, and P. D. Nicholson (2006), Cassini observations of flow-like features in western Tui Regio, Titan, *Geophys. Res. Lett.*, 33, L16,204, doi:10.1029/2006GL026843.

Barnes, J. W., R. H. Brown, L. Soderblom, B. J. Buratti, C. Sotin, S. Rodriguez, S. Le Mouelic, K. H. Baines, R. Clark, and P. Nicholson (2007), Global-scale surface spectral variations on Titan seen from Cassini/VIMS, *Icarus*, 186, 242–258, doi: 10.1016/j.icarus.2006.08.021.

Barnes, J. W., R. H. Brown, L. Soderblom, C. Sotin, S. Le Mouelic, S. Rodriguez, R. Jaumann, R. A. Beyer, B. J. Buratti, K. Pitman, K. H. Baines, R. Clark, and P. Nicholson (2008), Spectroscopy, morphometry, and photoclinometry of Titan's dunefields from Cassini/VIMS, *Icarus*, 195, 400–414, doi:10.1016/j.icarus.2007.12.006.

Barnes, J. W., R. H. Brown, J. M. Soderblom, L. A. Soderblom, R. Jaumann, B. Jackson, S. Le Mouélic, C. Sotin, B. J. Buratti, K. M. Pitman, K. H. Baines, R. N. Clark, P. D. Nicholson, E. P. Turtle, and J. Perry (2009), Shoreline features of Titan's Ontario Lacus from Cassini/VIMS observations, *Icarus*, 201, 217–225, doi: 10.1016/j.icarus.2008.12.028.

Barnes, J. W., J. Bow, J. Schwartz, R. H. Brown, J. M. Soderblom, A. G. Hayes, G. Vixie, S. Le Mouélic, S. Rodriguez, C. Sotin, R. Jaumann, K. Stephan, L. A. Soderblom, R. N. Clark, B. J. Buratti, K. H. Baines, and P. D. Nicholson (2011a), Organic sedimentary deposits in Titan's dry lakebeds: Probable evaporite, *Icarus*, 216, 136–140, doi:10.1016/j.icarus.2011.08.022.

Barnes, J. W., J. M. Soderblom, R. H. Brown, L. A. Soderblom, K. Stephan, R. Jaumann, S. L. Mouélic, S. Rodriguez, C. Sotin, B. J. Buratti, K. H. Baines, R. N. Clark, and P. D. Nicholson (2011b), Wave constraints for Titan's Jingpo Lacus and Kraken Mare from VIMS specular reflection lightcurves, *Icarus*, 211, 722–731, doi: 10.1016/j.icarus.2010.09.022.

Barnes, J. W., R. N. Clark, C. Sotin, M. Ádámkovics, T. Appéré, S. Rodriguez, J. M. Soderblom, R. H. Brown, B. J. Buratti, K. H. Baines, S. Le Mouélic, and P. D. Nicholson (2013a), A Transmission Spectrum of Titan's North Polar Atmosphere from a Specular Reflection of the Sun, *ApJ*, 777, 161, doi:10.1088/0004-637X/777/2/161.

Barnes, J. W., B. J. Buratti, E. P. Turtle, J. Bow, P. A. Dalba, J. Perry, R. H. Brown, S. Rodriguez, S. L. Mouélic, K. H. Baines, C. Sotin, R. D. Lorenz, M. J. Malaska, T. B. McCord, R. N. Clark, R. Jaumann, P. O. Hayne, P. D. Nicholson, J. M. Soderblom, and L. A. Soderblom (2013b), Precipitation-induced surface brightenings seen on Titan by Cassini VIMS and ISS, *Planetary Science*, 2, 1, doi:10.1186/2191-2521-2-1.

Barnes, J. W., C. Sotin, J. M. Soderblom, R. H. Brown, A. G. Hayes, M. Donelan, S. Rodriguez, S. Le Mouelic, K. H. Baines, and T. B. McCord (2014), Cassini/VIMS Observes Rough Surfaces on Titan's Punga Mare in Specular Reflection, *Planetary Science*, 3, 3, doi:10.1186/s13535-014-0003-4.

Barnes, J. W., R. D. Lorenz, J. Radebaugh, A. G. Hayes, K. Arnold, and C. Chandler (2015), Production and global transport of Titan's sand particles, *Planetary Science*, 4, 1, doi:10.1186/s13535-015-0004-y.

Barth, E. L. (2010), Cloud formation along mountain ridges on Titan, *Planet. Space Sci.*, 58, 1740–1747, doi:10.1016/j.pss.2010.07.013.

Barth, E. L., and S. C. R. Rafkin (2007), TRAMS: A new dynamic cloud model for Titan's methane clouds, *Geophys. Res. Lett.*, *34*, L03203, doi:10.1029/2006GL028652.

Barth, E. L., and O. B. Toon (2003), Microphysical modeling of ethane ice clouds in titan's atmosphere, *Icarus*, *162*, 94–113, doi:10.1016/S0019-1035(02)00067-2.

Barth, E. L., and O. B. Toon (2004), Properties of methane clouds on Titan: Results from microphysical modeling, *Geophys. Res. Lett.*, *31*, L17S07, doi:10.1029/2004GL019825.

Barth, E. L., and O. B. Toon (2006), Methane, ethane, and mixed clouds in Titan's atmosphere: Properties derived from microphysical modeling, *Icarus*, *182*, 230–250, doi:10.1016/j.icarus.2005.12.017.

Bauerecker, S., and E. Dartois (2009), Ethane aerosol phase evolution in Titan's atmosphere, *Icarus*, *199*, 564–567, doi:10.1016/j.icarus.2008.09.014.

Bazzon, A., H. M. Schmid, and E. Buenzli (2014), HST observations of the limb polarization of Titan, *Astronomy and Astrophysics*, *572*, A6, doi:10.1051/0004-6361/201323139.

Béghin, C., F. Simões, V. Krasnoselskikh, K. Schwingenschuh, J. J. Berthelier, B. P. Besser, C. Bettanini, R. Grard, M. Hamelin, J. J. López-Moreno, G. J. Molina-Cuberos, and T. Tokano (2007), A Schumann-like resonance on Titan driven by Saturn's magnetosphere possibly revealed by the Huygens Probe, *Icarus*, *191*, 251–266, doi:10.1016/j.icarus.2007.04.005.

Béghin, C., C. Sotin, and M. Hamelin (2010), Titan's native ocean revealed beneath some 45km of ice by a Schumann-like resonance, *Comptes Rendus Geoscience*, *342*, 425–433, doi:10.1016/j.crte.2010.03.003.

Béghin, C., O. Randriamboarison, M. Hamelin, E. Karkoschka, C. Sotin, R. C. Whitten, J.-J. Berthelier, R. Grard, and F. Simões (2012), Analytic theory of Titan's Schumann

- resonance: Constraints on ionospheric conductivity and buried water ocean, *Icarus*, 218, 1028–1042, doi:10.1016/j.icarus.2012.02.005.
- Bell, J. M., S. W. Bougher, J. H. Waite, A. J. Ridley, B. A. Magee, K. E. Mandt, J. Westlake, A. D. DeJong, A. Bar-Nun, R. Jacovi, G. Toth, and V. De La Haye (2010), Simulating the one-dimensional structure of Titan's upper atmosphere: 1. Formulation of the Titan Global Ionosphere-Thermosphere Model and benchmark simulations, *Journal of Geophysical Research (Planets)*, 115, E12002, doi:10.1029/2010JE003636.
- Bellucci, A., B. Sicardy, P. Drossart, P. Rannou, P. D. Nicholson, M. Hedman, K. H. Baines, and B. Buratti (2009), Titan solar occultation observed by Cassini/VIMS: Gas absorption and constraints on aerosol composition, *Icarus*, 201, 198–216, doi:10.1016/j.icarus.2008.12.024.
- Berezhnoi, A. A. (2010), The role of photochemical processes in evolution of the isotopic composition of the atmosphere of Titan, *Solar System Research*, 44, 498–506, doi:10.1134/S0038094610060031.
- Bernard, J.-M., E. Quirico, O. Brissaud, G. Montagnac, B. Reynard, P. McMillan, P. Coll, M. Nguyen, F. Raulin, and B. Schmitt (2006), Reflectance spectra and chemical structure of Titan's tholins: Application to the analysis of Cassini Huygens observations, *Icarus*, 185, 301–307, doi:10.1016/j.icarus.2006.06.004.
- Bézard, B. (2009), Composition and chemistry of titan's stratosphere, *Philosophical Transactions of the Royal Society of London A: Mathematical, Physical and Engineering Sciences*, 367(1889), 683–695.
- Bézard, B. (2014), The methane mole fraction in Titan's stratosphere from DISR measurements during the Huygens probe's descent, *Icarus*, 242, 64–73, doi:

10.1016/j.icarus.2014.07.013.

Bezard, B., J. P. Balauteau, A. Marten, and N. Coron (1987), The C-12/C-13 and O-16/O-18 ratios in the atmosphere of Venus from high-resolution 10-micron spectroscopy, *Icarus*, 72, 623–634, doi:10.1016/0019-1035(87)90057-1.

Bézard, B., A. Marten, and G. Paubert (1993), Detection of Acetonitrile on Titan, in *AAS/Division for Planetary Sciences Meeting Abstracts #25, Bulletin of the American Astronomical Society*, vol. 25, p. 1100.

Biemann, K. (2006), Astrochemistry: Complex organic matter in Titan's aerosols?, *Nature*, 444, 6, doi:10.1038/nature05417.

Bills, B. G., and F. Nimmo (2011), Rotational dynamics and internal structure of Titan, *Icarus*, 214, 351–355, doi:10.1016/j.icarus.2011.04.028.

Bird, M. K., M. Allison, S. W. Asmar, D. H. Atkinson, I. M. Avruch, R. Dutta-Roy, Y. Dzierma, P. Edenhofer, W. M. Folkner, L. I. Gurvits, D. V. Johnston, D. Plettemeier, S. V. Pogrebenko, R. A. Preston, and G. L. Tyler (2005), The vertical profile of winds on Titan, *Nature*, 438, 800–802, doi:10.1038/nature04060.

Bockelée-Morvan, D., U. Calmonte, S. Charnley, J. Duprat, C. Engrand, A. Gicquel, M. Hässig, E. Jehin, H. Kawakita, B. Marty, et al. (2015), Cometary isotopic measurements, *Space Science Reviews*, 197(1-4), 47–83.

Borucki, W. J., and R. C. Whitten (2008), Influence of high abundances of aerosols on the electrical conductivity of the Titan atmosphere, *Planet. Space Sci.*, 56, 19–26, doi:10.1016/j.pss.2007.03.013.

Borucki, W. J., Z. Levin, R. C. Whitten, R. G. Keesee, L. A. Capone, A. L. Summers, O. B. Toon, and J. Dubach (1987), Predictions of the electrical conductivity and

charging of the aerosols in Titan's atmosphere, *Icarus*, *72*, 604–622, doi:10.1016/0019-1035(87)90056-X.

Bouchez, A. H. (2004), Seasonal trends in Titan's atmosphere: Haze, wind, and clouds, Ph.D. thesis, CALIFORNIA INSTITUTE OF TECHNOLOGY.

Bouchez, A. H., and M. E. Brown (2005), Statistics of Titan's South Polar Tropospheric Clouds, *ApJL*, *618*, L53–L56, doi:10.1086/427693.

Brassé, C., O. Muñoz, P. Coll, and F. Raulin (2015), Optical constants of Titan aerosols and their tholins analogs: Experimental results and modeling/observational data, *Planet. Space Sci.*, *109*, 159–174, doi:10.1016/j.pss.2015.02.012.

Broadfoot, A. L., B. R. Sandel, D. E. Shemansky, J. B. Holberg, G. R. Smith, D. F. Strobel, J. C. McConnell, S. Kumar, D. M. Hunten, S. K. Atreya, T. M. Donahue, H. W. Moos, J. L. Bertaux, J. E. Blamont, R. B. Pomphrey, and S. Linick (1981), Extreme ultraviolet observations from Voyager 1 encounter with Saturn, *Science*, *212*, 206–211, doi:10.1126/science.212.4491.206.

Brown, M. E., A. H. Bouchez, and C. A. Griffith (2002), Direct detection of variable tropospheric clouds near Titan's south pole, *Nature*, *420*, 795–797.

Brown, M. E., E. L. Schaller, H. G. Roe, C. Chen, J. Roberts, R. H. Brown, K. H. Baines, and R. N. Clark (2009), Discovery of lake-effect clouds on Titan, *Geophys. Res. Lett.*, *36*, L01,103, doi:10.1029/2008GL035964.

Brown, M. E., J. E. Roberts, and E. L. Schaller (2010), Clouds on Titan during the Cassini prime mission: A complete analysis of the VIMS data, *Icarus*, *205*, 571–580, doi:10.1016/j.icarus.2009.08.024.

- Brown, R. H., L. A. Soderblom, J. M. Soderblom, R. N. Clark, R. Jaumann, J. W. Barnes, C. Sotin, B. Buratti, K. H. Baines, and P. D. Nicholson (2008), The identification of liquid ethane in Titan's Ontario Lacus, *Nature*, *454*, 607–610, doi:10.1038/nature07100.
- Burr, D. M., N. T. Bridges, J. R. Marshall, J. K. Smith, B. R. White, and J. P. Emery (2015), Higher-than-predicted saltation threshold wind speeds on Titan, *Nature*, *517*, 60–63, doi:10.1038/nature14088.
- Cabane, M., P. Rannou, E. Chassefiere, and G. Israel (1993), Fractal aggregates in Titan's atmosphere, *Planet. Space Sci.*, *41*, 257–267, doi:10.1016/0032-0633(93)90021-S.
- Cable, M. L., S. M. Hörst, R. Hodyss, P. M. Beauchamp, M. A. Smith, and P. A. Willis (2012), Titan tholins: Simulating titan organic chemistry in the cassini-huygens era, *Chemical Reviews*, *112*(3), 1882–1909, doi:10.1021/cr200221x.
- Caldwell, J. (1975), Ultraviolet observations of small bodies in the solar system by OAO-2, *Icarus*, *25*, 384–396, doi:10.1016/0019-1035(75)90003-2.
- Caldwell, J. (1981), Titan on the eve of Voyager encounter, *Advances in Space Research*, *1*, 87–91, doi:10.1016/0273-1177(81)90223-4.
- Capalbo, F. J., Y. Bénilan, R. V. Yelle, T. T. Koskinen, B. R. Sandel, G. M. Holsclaw, and W. E. McClintock (2013), Solar Occultation by Titan Measured by Cassini/UVIS, *ApJL*, *766*, L16, doi:10.1088/2041-8205/766/2/L16.
- Capalbo, F. J., Y. Bénilan, R. V. Yelle, and T. T. Koskinen (2015), Titan's Upper Atmosphere from Cassini/UVIS Solar Occultations, *ApJ*, *814*, 86, doi:10.1088/0004-637X/814/2/86.
- Capone, L. A., R. C. Whitten, J. Dubach, S. S. Prasad, and W. T. Huntress, Jr. (1976), The lower ionosphere of Titan, *Icarus*, *28*, 367–378, doi:10.1016/0019-1035(76)90150-0.

Carrasco, N., S. Plessis, M. Dobrijevic, and P. Pernot (2008), Toward a reduction of the bimolecular reaction model for titan's ionosphere, *International Journal of Chemical Kinetics*, 40(11), 699–709.

Cassini Imaging Team (2016), Pia21051: Watching summer clouds on titan.

Castillo-Rogez, J. C., and J. I. Lunine (2010), Evolution of Titan's rocky core constrained by Cassini observations, *Geophys. Res. Lett.*, 37, L20205, doi:10.1029/2010GL044398.

Charnay, B., and S. Lebonnois (2012), Two boundary layers in Titan's lower troposphere inferred from a climate model, *Nature Geoscience*, 5, 106–109, doi:10.1038/ngeo1374.

Charnay, B., F. Forget, G. Tobie, C. Sotin, and R. Wordsworth (2014), Titan's past and future: 3D modeling of a pure nitrogen atmosphere and geological implications, *Icarus*, 241, 269–279, doi:10.1016/j.icarus.2014.07.009.

Charnay, B., E. Barth, S. Rafkin, C. Narteau, S. Lebonnois, S. Rodriguez, S. Courrech Du Pont, and A. Lucas (2015), Methane storms as a driver of Titan's dune orientation, *Nature Geoscience*, 8, 362–366, doi:10.1038/ngeo2406.

Chassefière, E., and M. Cabane (1995), Two formation regions for Titan's hazes: indirect clues and possible synthesis mechanisms, *Planet. Space Sci.*, 43, 91–103, doi: 10.1016/0032-0633(94)00138-H.

Choukroun, M., and C. Sotin (2012), Is Titan's shape caused by its meteorology and carbon cycle?, *Geophys. Res. Lett.*, 39, L04201, doi:10.1029/2011GL050747.

Clark, R. N., J. M. Curchin, J. W. Barnes, R. Jaumann, L. Soderblom, D. P. Cruikshank, R. H. Brown, S. Rodriguez, J. Lunine, K. Stephan, T. M. Hoefen, S. Le Mouélic, C. Sotin, K. H. Baines, B. J. Buratti, and P. D. Nicholson (2010), Detection and mapping of hydrocarbon deposits on Titan, *J. Geophys. Res.*, 115(E14), E10,005, doi:

10.1029/2009JE003369.

Clarke, D. W., and J. P. Ferris (1997), Titan Haze: Structure and Properties of Cyanoacetylene and Cyanoacetylene-Acetylene Photopolymers, *Icarus*, 127, 158–172, doi:10.1006/icar.1996.5667.

Coates, A. J., F. J. Crary, G. R. Lewis, D. T. Young, J. H. Waite, and E. C. Sittler (2007), Discovery of heavy negative ions in Titan's ionosphere, *Geophys. Res. Lett.*, 34, 22,103–+, doi:10.1029/2007GL030978.

Coates, A. J., A. Wellbrock, G. R. Lewis, G. H. Jones, D. T. Young, F. J. Crary, and J. H. Waite (2009), Heavy negative ions in Titan's ionosphere: Altitude and latitude dependence, *Planet. Space Sci.*, 57, 1866–1871, doi:10.1016/j.pss.2009.05.009.

Coates, A. J., A. Wellbrock, G. R. Lewis, G. H. Jones, D. T. Young, F. J. Crary, J. H. Waite, R. E. Johnson, T. W. Hill, and E. C. Sittler, Jr. (2010), Negative ions at Titan and Enceladus: recent results, *Faraday Discussions*, 147, 293, doi:10.1039/c004700g.

Coll, P., S. I. Ramírez, R. Navarro-González, and F. Raulin (2001), Chemical and optical behaviour of tholins, laboratory analogues of Titan aerosols, *Adv. Space Res.*, 27, 289–297, doi:10.1016/S0273-1177(01)00060-6.

Comas Solà, J. (1908), Observations des satellites principaux de Jupiter et de Titan, *Astronomische Nachrichten*, pp. 289–290.

Cordier, D., O. Mousis, J. I. Lunine, P. Lavvas, and V. Vuitton (2009), An Estimate of the Chemical Composition of Titan's Lakes, *ApJL*, 707, L128–L131, doi:10.1088/0004-637X/707/2/L128.

Cordier, D., O. Mousis, J. I. Lunine, S. Lebonnois, P. Lavvas, L. Q. Lobo, and A. G. M. Ferreira (2010), About the Possible Role of Hydrocarbon Lakes in the Origin of Ti-

tan's Noble Gas Atmospheric Depletion, *ApJL*, 721, L117–L120, doi:10.1088/2041-8205/721/2/L117.

Cordier, D., O. Mousis, J. I. Lunine, S. Lebonnois, P. Rannou, P. Lavvas, L. Q. Lobo, and A. G. M. Ferreira (2012), Titan's lakes chemical composition: Sources of uncertainties and variability, *Planet. Space Sci.*, 61, 99–107, doi:10.1016/j.pss.2011.05.009.

Cordiner, M. A., C. A. Nixon, N. A. Teanby, P. G. J. Irwin, J. Serigano, S. B. Charnley, S. N. Milam, M. J. Mumma, D. C. Lis, G. Villanueva, L. Paganini, Y.-J. Kuan, and A. J. Remijan (2014), ALMA Measurements of the HNC and HC<sub>3</sub>N Distributions in Titan's Atmosphere, *ApJL*, 795, L30, doi:10.1088/2041-8205/795/2/L30.

Cordiner, M. A., M. Y. Palmer, C. A. Nixon, P. G. J. Irwin, N. A. Teanby, S. B. Charnley, M. J. Mumma, Z. Kisiel, J. Serigano, Y.-J. Kuan, Y.-L. Chuang, and K.-S. Wang (2015), Ethyl Cyanide On Titan: Spectroscopic Detection and Mapping Using Alma, *ApJL*, 800, L14, doi:10.1088/2041-8205/800/1/L14.

Corlies, P., A. G. Hayes, S. Rodriguez, M. Adamkovics, P. Rojo, and E. P. Turtle (2015), Using the VIMS Dataset to Understand Titan's Hydrologic Cycle Through Cloud Characterization, in *AAS/Division for Planetary Sciences Meeting Abstracts*, *AAS/Division for Planetary Sciences Meeting Abstracts*, vol. 47, p. 300.07.

Cornet, T., O. Bourgeois, S. Le Mouélic, S. Rodriguez, C. Sotin, J. W. Barnes, R. H. Brown, K. H. Baines, B. J. Buratti, R. N. Clark, and P. D. Nicholson (2012a), Edge detection applied to Cassini images reveals no measurable displacement of Ontario Lacus' margin between 2005 and 2010, *Journal of Geophysical Research (Planets)*, 117, E07005, doi:10.1029/2012JE004073.

Cornet, T., O. Bourgeois, S. Le Mouélic, S. Rodriguez, T. Lopez Gonzalez, C. Sotin, G. Tobie, C. Fleurant, J. W. Barnes, R. H. Brown, K. H. Baines, B. J. Buratti, R. N. Clark, and P. D. Nicholson (2012b), Geomorphological significance of Ontario Lacus on Titan: Integrated interpretation of Cassini VIMS, ISS and RADAR data and comparison with the Etosha Pan (Namibia), *Icarus*, 218, 788–806, doi:10.1016/j.icarus.2012.01.013.

Cornet, T., D. Cordier, T. L. Bahers, O. Bourgeois, C. Fleurant, S. L. Mouélic, and N. Altobelli (2015), Dissolution on Titan and on Earth: Toward the age of Titan's karstic landscapes, *Journal of Geophysical Research (Planets)*, 120, 1044–1074, doi: 10.1002/2014JE004738.

Cottini, V., C. A. Nixon, D. E. Jennings, R. de Kok, N. A. Teanby, P. G. J. Irwin, and F. M. Flasar (2012), Spatial and temporal variations in Titan's surface temperatures from Cassini CIRS observations, *Planet. Space Sci.*, 60, 62–71, doi: 10.1016/j.pss.2011.03.015.

Cours, T., P. Rannou, A. Coustenis, and A. Hamdouni (2010), A new analysis of the ESO Very Large Telescope (VLT) observations of Titan at 2  $\mu\text{m}$ , *Planet. Space Sci.*, 58, 1708–1714, doi:10.1016/j.pss.2009.12.009.

Cours, T., J. Burgalat, P. Rannou, S. Rodriguez, A. Brahic, and R. A. West (2011), Dual Origin of Aerosols in Titan's Detached Haze Layer, *ApJL*, 741, L32, doi:10.1088/2041-8205/741/2/L32.

Courtin, R., D. Gautier, and C. P. McKay (1995), Titan's thermal emission spectrum: Reanalysis of the Voyager infrared measurements., *Icarus*, 114, 144–162, doi: 10.1006/icar.1995.1050.

Courtin, R., B. M. Swinyard, R. Moreno, T. Fulton, E. Lellouch, M. Rengel, and P. Hartogh (2011), First results of Herschel-SPIRE observations of Titan, *Astronomy and Astrophysics*, 536, L2, doi:10.1051/0004-6361/201118304.

Courtin, R., C. K. Sim, S. J. Kim, and D. Gautier (2012), The abundance of H<sub>2</sub> in Titan's troposphere from the Cassini CIRS investigation, *Planet. Space Sci.*, 69, 89–99, doi:10.1016/j.pss.2012.03.012.

Courtin, R., S. J. Kim, and A. Bar-Nun (2015), Three-micron extinction of the Titan haze in the 250–700 km altitude range: Possible evidence of a particle-aging process, *Astronomy and Astrophysics*, 573, A21, doi:10.1051/0004-6361/201424977.

Courtin, R., H. Feuchtgruber, S.-j. Kim, and E. Lellouch (2016), The 6–7 μm spectrum of Titan from ISO/SWS observations, *Icarus*, 270, 389–398, doi:10.1016/j.icarus.2015.07.021.

Courtin, R. D., C. K. Sim, S. J. Kim, and D. Gautier (2007), The Tropospheric Abundance of H<sub>2</sub> on Titan from the Cassini CIRS Investigation, in *BAAS, Bulletin of the American Astronomical Society*, vol. 38, pp. 529–+.

Coustenis, A., and B. Bézard (1995), Titan's atmosphere from Voyager infrared observations. 4: Latitudinal variations of temperature and composition, *Icarus*, 115, 126–140, doi:10.1006/icar.1995.1084.

Coustenis, A., A. Salama, E. Lellouch, T. Encrenaz, G. L. Bjoraker, R. E. Samuelson, T. de Graauw, H. Feuchtgruber, and M. F. Kessler (1998), Evidence for water vapor in Titan's atmosphere from ISO/SWS data, *Astron. Astrophys.*, 336, L85–L89.

Coustenis, A., B. Schmitt, R. K. Khanna, and F. Trotta (1999), Plausible condensates in Titan's stratosphere from Voyager infrared spectra, *Planet. Space Sci.*, 47, 1305–1329,

doi:10.1016/S0032-0633(99)00053-7.

Coustenis, A., A. Salama, B. Schulz, S. Ott, E. Lellouch, T. H. Encrenaz, D. Gautier, and H. Feuchtgruber (2003), Titan's atmosphere from ISO mid-infrared spectroscopy, *Icarus*, 161, 383–403, doi:10.1016/S0019-1035(02)00028-3.

Coustenis, A., R. K. Achterberg, B. J. Conrath, D. E. Jennings, A. Marten, D. Gautier, C. A. Nixon, F. M. Flasar, N. A. Teanby, B. Bézard, R. E. Samuelson, R. C. Carlson, E. Lellouch, G. L. Bjoraker, P. N. Romani, F. W. Taylor, P. G. J. Irwin, T. Fouchet, A. Hubert, G. S. Orton, V. G. Kunde, S. Vinatier, J. Mondellini, M. M. Abbas, and R. Courtin (2007), The composition of Titan's stratosphere from Cassini/CIRS mid-infrared spectra, *Icarus*, 189, 35–62, doi:10.1016/j.icarus.2006.12.022.

Coustenis, A., D. E. Jennings, C. A. Nixon, R. K. Achterberg, P. Lavvas, S. Vinatier, N. A. Teanby, G. L. Bjoraker, R. C. Carlson, L. Piani, G. Bampasidis, F. M. Flasar, and P. N. Romani (2010), Titan trace gaseous composition from CIRS at the end of the Cassini-Huygens prime mission, *Icarus*, 207, 461–476, doi:10.1016/j.icarus.2009.11.027.

Coustenis, A., G. Bampasidis, R. K. Achterberg, P. Lavvas, D. E. Jennings, C. A. Nixon, N. A. Teanby, S. Vinatier, F. M. Flasar, R. C. Carlson, G. Orton, P. N. Romani, E. A. Guandique, and S. Stamogiorgos (2013), Evolution of the Stratospheric Temperature and Chemical Composition over One Titanian Year, *ApJ*, 779, 177, doi:10.1088/0004-637X/779/2/177.

Coustenis, A., D. E. Jennings, R. K. Achterberg, G. Bampasidis, P. Lavvas, C. A. Nixon, N. A. Teanby, C. M. Anderson, V. Cottini, and F. M. Flasar (2016), Titan's temporal evolution in stratospheric trace gases near the poles, *Icarus*, 270, 409–420, doi:10.1016/j.icarus.2015.08.027.

Crary, F. J., B. A. Magee, K. Mandt, J. H. Waite, J. Westlake, and D. T. Young (2009), Heavy ions, temperatures and winds in Titan's ionosphere: Combined Cassini CAPS and INMS observations, *Planet. Space Sci.*, *57*, 1847–1856, doi: 10.1016/j.pss.2009.09.006.

Cravens, T. E., I. P. Robertson, S. A. Ledvina, D. Mitchell, S. M. Krimigis, and J. H. Waite (2008), Energetic ion precipitation at Titan, *Geophys. Res. Lett.*, *35*, L03103, doi:10.1029/2007GL032451.

Crespin, A., S. Lebonnois, S. Vinatier, B. Bézard, A. Coustenis, N. A. Teanby, R. K. Achterberg, P. Rannou, and F. Hourdin (2008), Diagnostics of Titan's stratospheric dynamics using Cassini/CIRS data and the 2-dimensional IPSL circulation model, *Icarus*, *197*, 556–571, doi:10.1016/j.icarus.2008.05.010.

Cui, J., R. V. Yelle, V. Vuitton, J. H. Waite, W. T. Kasprzak, D. A. Gell, H. B. Niemann, I. C. F. Müller-Wodarg, N. Borggren, G. G. Fletcher, E. L. Patrick, E. Raaen, and B. A. Magee (2009), Analysis of Titan's neutral upper atmosphere from Cassini Ion Neutral Mass Spectrometer measurements, *Icarus*, *200*, 581–615, doi: 10.1016/j.icarus.2008.12.005.

Cui, J., R. V. Yelle, D. F. Strobel, I. C. F. Müller-Wodarg, D. S. Snowden, T. T. Koskinen, and M. Galand (2012), The CH<sub>4</sub> structure in Titan's upper atmosphere revisited, *Journal of Geophysical Research (Planets)*, *117*, E11006, doi:10.1029/2012JE004222.

Curtis, D. B., C. D. Hatch, C. A. Hasenkopf, O. B. Toon, M. A. Tolbert, C. P. McKay, and B. N. Khare (2008), Laboratory studies of methane and ethane adsorption and nucleation onto organic particles: Application to Titan's clouds, *Icarus*, *195*, 792–801, doi:10.1016/j.icarus.2008.02.003.

- Dalba, P. A., B. J. Buratti, R. H. Brown, J. W. Barnes, K. H. Baines, C. Sotin, R. N. Clark, K. J. Lawrence, and P. D. Nicholson (2012), Cassini VIMS Observations Show Ethane is Present in Titan's Rainfall, *ApJL*, 761, L24, doi:10.1088/2041-8205/761/2/L24.
- Danielson, R. E., J. J. Caldwell, and D. R. Larach (1973), An Inversion in the Atmosphere of Titan, *Icarus*, 20, 437–+, doi:10.1016/0019-1035(73)90016-X.
- de Kok, R., P. G. J. Irwin, N. A. Teanby, C. A. Nixon, D. E. Jennings, L. Fletcher, C. Howett, S. B. Calcutt, N. E. Bowles, F. M. Flasar, and F. W. Taylor (2007), Characteristics of Titan's stratospheric aerosols and condensate clouds from Cassini CIRS far-infrared spectra, *Icarus*, 191, 223–235, doi:10.1016/j.icarus.2007.04.003.
- de Kok, R., P. G. J. Irwin, and N. A. Teanby (2008), Condensation in Titan's stratosphere during polar winter, *Icarus*, 197, 572–578, doi:10.1016/j.icarus.2008.05.024.
- de Kok, R. J., N. A. Teanby, L. Maltagliati, P. G. J. Irwin, and S. Vinatier (2014), HCN ice in Titan's high-altitude southern polar cloud, *Nature*, 514, 65–67, doi:10.1038/nature13789.
- de La Haye, V., J. H. Waite, R. E. Johnson, R. V. Yelle, T. E. Cravens, J. G. Luhmann, W. T. Kasprzak, D. A. Gell, B. Magee, F. Leblanc, M. Michael, S. Jurac, and I. P. Robertson (2007), Cassini Ion and Neutral Mass Spectrometer data in Titan's upper atmosphere and exosphere: Observation of a suprathermal corona, *Journal of Geophysical Research (Space Physics)*, 112, A07309, doi:10.1029/2006JA012222.
- Del Genio, A. D., and W. Zhou (1996), Simulations of Superrotation on Slowly Rotating Planets: Sensitivity to Rotation and Initial Condition, *Icarus*, 120, 332–343, doi:10.1006/icar.1996.0054.

Delitsky, M. L., and C. P. McKay (2010), The photochemical products of benzene in Titan's upper atmosphere, *Icarus*, *207*, 477–484, doi:10.1016/j.icarus.2009.11.002.

Dias Pinto, J. R., and J. L. Mitchell (2014), Atmospheric superrotation in an idealized GCM: Parameter dependence of the eddy response, *Icarus*, *238*, 93–109, doi:10.1016/j.icarus.2014.04.036.

Dinelli, B. M., M. López-Puertas, A. Adriani, M. L. Moriconi, B. Funke, M. García-Comas, and E. D'Aversa (2013), An unidentified emission in Titan's upper atmosphere, *Geophys. Res. Lett.*, *40*, 1489–1493, doi:10.1002/grl.50332.

Dobrijevic, M., E. Hébrard, J. C. Loison, and K. M. Hickson (2014), Coupling of oxygen, nitrogen, and hydrocarbon species in the photochemistry of Titan's atmosphere, *Icarus*, *228*, 324–346, doi:10.1016/j.icarus.2013.10.015.

Dobrijevic, M., J. C. Loison, K. M. Hickson, and G. Gronoff (2016), 1D-coupled photochemical model of neutrals, cations and anions in the atmosphere of Titan, *Icarus*, *268*, 313–339, doi:10.1016/j.icarus.2015.12.045.

Donahue, T. M., J. H. Hoffman, R. R. Hodges, and A. J. Watson (1982), Venus was wet - A measurement of the ratio of deuterium to hydrogen, *Science*, *216*, 630–633, doi:10.1126/science.216.4546.630.

Doose, L. R., E. Karkoschka, M. G. Tomasko, and C. M. Anderson (2016a), Vertical structure and optical properties of Titan's aerosols from radiance measurements made inside and outside the atmosphere, *Icarus*, *270*, 355–375, doi:10.1016/j.icarus.2015.09.039.

Doose, L. R., E. Karkoschka, M. G. Tomasko, and C. M. Anderson (2016b), Vertical structure and optical properties of Titan's aerosols from radiance measurements made inside and outside the atmosphere, *Icarus*, *270*, 355–375, doi:10.1016/j.icarus.2015.09.039.

Elachi, C., S. Wall, M. Allison, Y. Anderson, R. Boehmer, P. Callahan, P. Encrenaz, E. Flamini, G. Franceschetti, Y. Gim, G. Hamilton, S. Hensley, M. Janssen, W. Johnson, K. Kelleher, R. Kirk, R. Lopes, R. Lorenz, J. Lunine, D. Muhleman, S. Ostro, F. Paganelli, G. Picardi, F. Posa, L. Roth, R. Seu, S. Shaffer, L. Soderblom, B. Stiles, E. Stofan, S. Vetrella, R. West, C. Wood, L. Wye, and H. Zebker (2005), Cassini Radar Views the Surface of Titan, *Science*, 308, 970–974, doi:10.1126/science.1109919.

Elachi, C., S. Wall, M. Janssen, E. Stofan, R. Lopes, R. Kirk, R. Lorenz, J. Lunine, F. Paganelli, L. Soderblom, C. Wood, L. Wye, H. Zebker, Y. Anderson, S. Ostro, M. Allison, R. Boehmer, P. Callahan, P. Encrenaz, E. Flamini, G. Francescetti, Y. Gim, G. Hamilton, S. Hensley, W. Johnson, K. Kelleher, D. Muhleman, G. Picardi, F. Posa, L. Roth, R. Seu, S. Shaffer, B. Stiles, S. Vetrella, and R. West (2006), Titan Radar Mapper observations from Cassini's T<sub>3</sub> fly-by, *Nature*, 441, 709–713, doi:10.1038/nature04786.

Ewing, R. C., A. G. Hayes, and A. Lucas (2015), Sand dune patterns on titan controlled by long-term climate cycles, *Nature Geoscience*, 8(1), 15–19.

Fischer, G., and D. A. Gurnett (2011), The search for Titan lightning radio emissions, *Geophys. Res. Lett.*, 38, L08206, doi:10.1029/2011GL047316.

Fischer, G., D. A. Gurnett, W. S. Kurth, W. M. Farrell, M. L. Kaiser, and P. Zarka (2007), Nondetection of Titan lightning radio emissions with Cassini/RPWS after 35 close Titan flybys, *Geophys. Res. Lett.*, 34, L22104, doi:10.1029/2007GL031668.

Flasar, F. M., R. E. Samuelson, and B. J. Conrath (1981), Titan's atmosphere - Temperature and dynamics, *Nature*, 292, 693–698.

Flasar, F. M., V. G. Kunde, M. M. Abbas, R. K. Achterberg, P. Ade, A. Barucci, B. B'ezard, G. L. Bjoraker, J. C. Brasunas, S. Calcutt, R. Carlson, C. J. C'esarsky,

B. J. Conrath, A. Coradini, R. Courtin, A. Coustenis, S. Edberg, S. Edgington, C. Ferrari, T. Fouchet, D. Gautier, P. J. Gierasch, K. Grossman, P. Irwin, D. E. Jennings, E. Lellouch, A. A. Mamoutkine, A. Marten, J. P. Meyer, C. A. Nixon, G. S. Orton, T. C. Owen, J. C. Pearl, R. Prang'e, F. Raulin, P. L. Read, P. N. Romani, R. E. Samuelson, M. E. Segura, M. R. Showalter, A. A. Simon-Miller, M. D. Smith, J. R. Spencer, L. J. Spilker, and F. W. Taylor (2004), Exploring The Saturn System In The Thermal Infrared: The Composite Infrared Spectrometer, *Space Science Reviews*, 115, 169–297, doi:10.1007/s11214-004-1454-9.

Flasar, F. M., R. K. Achterberg, B. J. Conrath, P. J. Gierasch, V. G. Kunde, C. A. Nixon, G. L. Bjoraker, D. E. Jennings, P. N. Romani, A. A. Simon-Miller, B. Bézard, A. Coustenis, P. G. J. Irwin, N. A. Teanby, J. Brasunas, J. C. Pearl, M. E. Segura, R. C. Carlson, A. Mamoutkine, P. J. Schinder, A. Barucci, R. Courtin, T. Fouchet, D. Gautier, E. Lellouch, A. Marten, R. Prangé, S. Vinatier, D. F. Strobel, S. B. Calcutt, P. L. Read, F. W. Taylor, N. Bowles, R. E. Samuelson, G. S. Orton, L. J. Spilker, T. C. Owen, J. R. Spencer, M. R. Showalter, C. Ferrari, M. M. Abbas, F. Raulin, S. Edgington, P. Ade, and E. H. Wishnow (2005), Titan's Atmospheric Temperatures, Winds, and Composition, *Science*, 308, 975–978, doi:10.1126/science.1111150.

Flasar, F. M., R. K. Achterberg, and P. J. Schinder (2014), *Thermal Structure of Titan's Troposphere and Middle Atmosphere*, pp. 102–121.

Fletcher, L. N., G. S. Orton, N. A. Teanby, P. G. J. Irwin, and G. L. Bjoraker (2009), Methane and its isotopologues on Saturn from Cassini/CIRS observations, *Icarus*, 199, 351–367, doi:10.1016/j.icarus.2008.09.019.

Fletcher, L. N., T. K. Greathouse, G. S. Orton, P. G. J. Irwin, O. Mousis, J. A. Sinclair, and R. S. Giles (2014), The origin of nitrogen on Jupiter and Saturn from the  $^{15}\text{N}/^{14}\text{N}$  ratio, *Icarus*, 238, 170–190, doi:10.1016/j.icarus.2014.05.007.

Folkner, W. M., S. W. Asmar, J. S. Border, G. W. Franklin, S. G. Finley, J. Gorelik, D. V. Johnston, V. V. Kerzhanovich, S. T. Lowe, R. A. Preston, M. K. Bird, R. Dutta-Roy, M. Allison, D. H. Atkinson, P. Edenhofer, D. Plettemeier, and G. L. Tyler (2006), Winds on Titan from ground-based tracking of the Huygens probe, *Journal of Geophysical Research (Planets)*, 111, E07S02, doi:10.1029/2005JE002649.

Friedson, A. J., R. A. West, E. H. Wilson, F. Oyafuso, and G. S. Orton (2009), A global climate model of Titan's atmosphere and surface, *Planet. Space Sci.*, 57, 1931–1949, doi:10.1016/j.pss.2009.05.006.

Fulchignoni, M., F. Ferri, F. Angrilli, A. J. Ball, A. Bar-Nun, M. A. Barucci, C. Bettanini, G. Bianchini, W. Borucki, G. Colombatti, M. Coradini, A. Coustenis, S. Debei, P. Falkner, G. Fanti, E. Flamini, V. Gaborit, R. Grard, M. Hamelin, A. M. Harri, B. Hathi, I. Jernej, M. R. Leese, A. Lehto, P. F. Lion Stoppato, J. J. López-Moreno, T. Mäkinen, J. A. M. McDonnell, C. P. McKay, G. Molina-Cuberos, F. M. Neubauer, V. Pirronello, R. Rodrigo, B. Saggin, K. Schwingenschuh, A. Seiff, F. Simões, H. Svedhem, T. Tokano, M. C. Towner, R. Trautner, P. Withers, and J. C. Zarnecki (2005), In situ measurements of the physical characteristics of Titan's environment, *Nature*, 438, 785–791, doi:10.1038/nature04314.

Galand, M., R. Yelle, J. Cui, J.-E. Wahlund, V. Vuitton, A. Wellbrock, and A. Coates (2010), Ionization sources in Titan's deep ionosphere, *Journal of Geophysical Research (Space Physics)*, 115, A07312, doi:10.1029/2009JA015100.

Gautier, T., N. Carrasco, A. Mahjoub, S. Vinatier, A. Giuliani, C. Szopa, C. M. Anderson, J.-J. Correia, P. Dumas, and G. Cernogora (2012), Mid- and far-infrared absorption spectroscopy of Titan's aerosols analogues, *Icarus*, 221, 320–327, doi:10.1016/j.icarus.2012.07.025.

Gibbard, S. G., I. de Pater, B. A. Macintosh, H. G. Roe, C. E. Max, E. F. Young, and C. P. McKay (2004a), Titan's 2  $\mu\text{m}$  surface albedo and haze optical depth in 1996–2004, *Geophys. Res. Lett.*, 31, L17S02, doi:10.1029/2004GL019803.

Gibbard, S. G., B. Macintosh, D. Gavel, C. E. Max, I. de Pater, H. G. Roe, A. M. Ghez, E. F. Young, and C. P. McKay (2004b), Speckle imaging of Titan at 2 microns: surface albedo, haze optical depth, and tropospheric clouds 1996–1998, *Icarus*, 169, 429–439, doi:10.1016/j.icarus.2003.12.026.

Gierasch, P. J. (1975), Meridional circulation and the maintenance of the Venus atmospheric rotation, *Journal of Atmospheric Sciences*, 32, 1038–1044, doi:10.1175/1520-0469(1975)032;1038:MCATMO;2.0.CO;2.

Gillett, F. C. (1975), Further observations of the 8–13 micron spectrum of Titan, *ApJL*, 201, L41–L43, doi:10.1086/181937.

Gillett, F. C., W. J. Forrest, and K. M. Merrill (1973), 8–13 Micron Observations of Titan, *ApJL*, 184, L93, doi:10.1086/181296.

Gladstone, G. R., S. A. Stern, K. Ennico, C. B. Olkin, H. A. Weaver, L. A. Young, M. E. Summers, D. F. Strobel, D. P. Hinson, J. A. Kammer, A. H. Parker, A. J. Steffl, I. R. Linscott, J. W. Parker, A. F. Cheng, D. C. Slater, M. H. Versteeg, T. K. Greathouse, K. D. Rutherford, H. Throop, N. J. Cunningham, W. W. Woods, K. N. Singer, C. C. C. Tsang, E. Schindhelm, C. M. Lisso, M. L. Wong, Y. L. Yung, X. Zhu, W. Curdt,

P. Lavvas, E. F. Young, G. L. Tyler, F. Bagenal, W. M. Grundy, W. B. McKinnon, J. M. Moore, J. R. Spencer, T. Andert, J. Andrews, M. Banks, B. Bauer, J. Bauman, O. S. Barnouin, P. Bedini, K. Beisser, R. A. Beyer, S. Bhaskaran, R. P. Binzel, E. Birath, M. Bird, D. J. Bogan, A. Bowman, V. J. Bray, M. Brozovic, C. Bryan, M. R. Buckley, M. W. Buie, B. J. Buratti, S. S. Bushman, A. Calloway, B. Carcich, S. Conard, C. A. Conrad, J. C. Cook, D. P. Cruikshank, O. S. Custodio, C. M. D. Ore, C. Deboy, Z. J. B. Dischner, P. Dumont, A. M. Earle, H. A. Elliott, J. Ercol, C. M. Ernst, T. Finley, S. H. Flanigan, G. Fountain, M. J. Freeze, J. L. Green, Y. Guo, M. Hahn, D. P. Hamilton, S. A. Hamilton, J. Hanley, A. Harch, H. M. Hart, C. B. Hersman, A. Hill, M. E. Hill, M. E. Holdridge, M. Horanyi, A. D. Howard, C. J. A. Howett, C. Jackman, R. A. Jacobson, D. E. Jennings, H. K. Kang, D. E. Kaufmann, P. Kollmann, S. M. Krimigis, D. Kusnierzewicz, T. R. Lauer, J. E. Lee, K. L. Lindstrom, A. W. Lunsford, V. A. Mallder, N. Martin, D. J. McComas, R. L. McNutt, D. Mehoke, T. Mehoke, E. D. Melin, M. Mutchler, D. Nelson, F. Nimmo, J. I. Nunez, A. Ocampo, W. M. Owen, M. Paetzold, B. Page, F. Pelletier, J. Peterson, N. Pinkine, M. Piquette, S. B. Porter, S. Protopapa, J. Redfern, H. J. Reitsema, D. C. Reuter, J. H. Roberts, S. J. Robbins, G. Rogers, D. Rose, K. Runyon, M. G. Ryschkewitsch, P. Schenk, B. Sepan, M. R. Showalter, M. Soluri, D. Stanbridge, T. Stryk, J. R. Szalay, M. Tapley, A. Taylor, H. Taylor, O. M. Umurhan, A. J. Verbiscer, M. H. Versteeg, M. Vincent, R. Webbert, S. Weidner, G. E. Weigle, O. L. White, K. Whittenburg, B. G. Williams, K. Williams, S. Williams, A. M. Zangari, and E. Zirnstein (2016), The atmosphere of Pluto as observed by New Horizons, *Science*, 351, aad8866, doi:10.1126/science.aad8866.

Glein, C. R. (2015), Noble gases, nitrogen, and methane from the deep interior to the atmosphere of Titan, *Icarus*, 250, 570–586, doi:10.1016/j.icarus.2015.01.001.

Glein, C. R., and E. L. Shock (2013), A geochemical model of non-ideal solutions in the methane-ethane-propane-nitrogen-acetylene system on Titan, *Geochimica et Cosmochimica Acta*, 115, 217–240, doi:10.1016/j.gca.2013.03.030.

Glein, C. R., S. J. Desch, and E. L. Shock (2009), The absence of endogenic methane on Titan and its implications for the origin of atmospheric nitrogen, *Icarus*, 204, 637–644, doi:10.1016/j.icarus.2009.06.020.

Goldreich, P. M., and J. L. Mitchell (2010), Elastic ice shells of synchronous moons: Implications for cracks on Europa and non-synchronous rotation of Titan, *Icarus*, 209, 631–638, doi:10.1016/j.icarus.2010.04.013.

Grard, R., M. Hamelin, J. J. López-Moreno, K. Schwingenschuh, I. Jernej, G. J. Molina-Cuberos, F. Simões, R. Trautner, P. Falkner, F. Ferri, M. Fulchignoni, R. Rodrigo, H. Svedhem, C. Béghin, J.-J. Berthelier, V. J. G. Brown, M. Chabassière, J. M. Jeronimo, L. M. Lara, and T. Tokano (2006), Electric properties and related physical characteristics of the atmosphere and surface of Titan, *Planet. Space Sci.*, 54, 1124–1136, doi:10.1016/j.pss.2006.05.036.

Griffith, C., S. Rafkin, P. Rannou, and C. McKay (2014), Storms, clouds, and weather, *Titan: Interior, surface, atmosphere, and space environment, I. Müller-Wodarg, CA Griffith, E. Lellouch, and TE Cravens, Eds., Cambridge University Press, Cambridge.*

Griffith, C. A. (1993), Evidence for surface heterogeneity on Titan, *Nature*, 364, 511–514, doi:10.1038/364511a0.

Griffith, C. A., T. Owen, and R. Wagener (1991), Titan's surface and troposphere, investigated with ground-based, near-infrared observations, *Icarus*, *93*, 362–378, doi: 10.1016/0019-1035(91)90219-J.

Griffith, C. A., T. Owen, G. A. Miller, and T. Geballe (1998), Transient clouds in Titan's lower atmosphere, *Nature*, *395*, 575–578, doi:10.1038/26920.

Griffith, C. A., J. L. Hall, and T. R. Geballe (2000), Detection of Daily Clouds on Titan, *Science*, *290*, 509–513, doi:10.1126/science.290.5491.509.

Griffith, C. A., T. Owen, T. R. Geballe, J. Rayner, and P. Rannou (2003), Evidence for the Exposure of Water Ice on Titan's Surface, *Science*, *300*, 628–630, doi: 10.1126/science.1081897.

Griffith, C. A., P. Penteado, K. Baines, P. Drossart, J. Barnes, G. Bellucci, J. Bibring, R. Brown, B. Buratti, F. Capaccioni, P. Cerroni, R. Clark, M. Combes, A. Coradini, D. Cruikshank, V. Formisano, R. Jaumann, Y. Langevin, D. Matson, T. McCord, V. Mennella, R. Nelson, P. Nicholson, B. Sicardy, C. Sotin, L. A. Soderblom, and R. Kursinski (2005), The Evolution of Titan's Mid-Latitude Clouds, *Science*, *310*, 474–477, doi:10.1126/science.1117702.

Griffith, C. A., P. Penteado, P. Rannou, R. Brown, V. Boudon, K. H. Baines, R. Clark, P. Drossart, B. Buratti, P. Nicholson, C. P. McKay, A. Coustenis, A. Negrao, and R. Jaumann (2006), Evidence for a Polar Ethane Cloud on Titan, *Science*, *313*, 1620–1622, doi:10.1126/science.1128245.

Griffith, C. A., C. P. McKay, and F. Ferri (2008), Titan's Tropical Storms in an Evolving Atmosphere, *ApJL*, *687*, L41–L44, doi:10.1086/593117.

Griffith, C. A., P. Penteado, S. Rodriguez, S. Le Mouélic, K. H. Baines, B. Buratti, R. Clark, P. Nicholson, R. Jaumann, and C. Sotin (2009), Characterization of Clouds in Titan's Tropical Atmosphere, *ApJL*, 702, L105–L109, doi:10.1088/0004-637X/702/2/L105.

Griffith, C. A., L. Doose, M. G. Tomasko, P. F. Penteado, and C. See (2012a), Radiative transfer analyses of Titan's tropical atmosphere, *Icarus*, 218, 975–988, doi:10.1016/j.icarus.2011.11.034.

Griffith, C. A., J. M. Lora, J. Turner, P. F. Penteado, R. H. Brown, M. G. Tomasko, L. Doose, and C. See (2012b), Possible tropical lakes on Titan from observations of dark terrain, *Nature*, 486, 237–239, doi:10.1038/nature11165.

Gronoff, G., J. Lilensten, L. Desorgher, and E. Flückiger (2009), Ionization processes in the atmosphere of Titan. I. Ionization in the whole atmosphere, *Astronomy and Astrophysics*, 506, 955–964, doi:10.1051/0004-6361/200912371.

Gurwell, M. A. (2004), Submillimeter Observations of Titan: Global Measures of Stratospheric Temperature, CO, HCN, HC<sub>3</sub>N, and the Isotopic Ratios <sup>12</sup>C/<sup>13</sup>C and <sup>14</sup>N/<sup>15</sup>N, *ApJ*, 616, L7–L10, doi:10.1086/423954.

Hadamcik, E., J.-B. Renard, A. Mahjoub, T. Gautier, N. Carrasco, G. Cernogora, and C. Szopa (2013), Optical properties of analogs of Titan's aerosols produced by dusty plasma, *Earth, Planets, and Space*, 65, 1175–1184, doi:10.5047/eps.2013.05.019.

Hamelin, M., C. Béghin, R. Grard, J. J. López-Moreno, K. Schwingenschuh, F. Simões, R. Trautner, J. J. Berthelier, V. J. G. Brown, M. Chabassière, P. Falkner, F. Ferri, M. Fulchignoni, I. Jernej, J. M. Jeronimo, G. J. Molina-Cuberos, R. Rodrigo, and T. Tokano (2007), Electron conductivity and density profiles derived from the mutual

impedance probe measurements performed during the descent of Huygens through the atmosphere of Titan, *Planet. Space Sci.*, 55, 1964–1977, doi:10.1016/j.pss.2007.04.008.

Hamelin, M., A. Lethuillier, A. Le Gall, R. Grard, C. Béghin, K. Schwingenschuh, I. Jernej, J.-J. López-Moreno, V. Brown, R. D. Lorenz, F. Ferri, and V. Ciarletti (2016), The electrical properties of Titan's surface at the Huygens landing site measured with the PWA-HASI Mutual Impedance Probe. New approach and new findings, *Icarus*, 270, 272–290, doi:10.1016/j.icarus.2015.11.035.

Hanel, R., B. Conrath, F. M. Flasar, V. Kunde, W. Maguire, J. C. Pearl, J. Pirraglia, R. Samuelson, L. Herath, M. Allison, D. P. Cruikshank, D. Gautier, P. J. Gierasch, L. Horn, R. Koppany, and C. Ponnampерuma (1981), Infrared observations of the Saturnian system from Voyager 1, *Science*, 212, 192–200.

Hansen, C. J., J. H. Waite, and S. J. Bolton (2010), *Titan in the Cassini-Huygens Extended Mission*, pp. 455–477.

Hartle, R. E., E. C. Sittler, F. M. Neubauer, R. E. Johnson, H. T. Smith, F. Crary, D. J. McComas, D. T. Young, A. J. Coates, D. Simpson, S. Bolton, D. Reisenfeld, K. Szego, J. J. Berthelier, A. Rymer, J. Vilppola, J. T. Steinberg, and N. Andre (2006), Preliminary interpretation of Titan plasma interaction as observed by the Cassini Plasma Spectrometer: Comparisons with Voyager 1, *Geophys. Res. Lett.*, 33, 8201–+, doi: 10.1029/2005GL024817.

Hasenkopf, C. A., M. R. Beaver, M. G. Trainer, H. Langley Dewitt, M. A. Freedman, O. B. Toon, C. P. McKay, and M. A. Tolbert (2010), Optical properties of Titan and early Earth haze laboratory analogs in the mid-visible, *Icarus*, 207, 903–913, doi: 10.1016/j.icarus.2009.12.015.

Hayes, A., O. Aharonson, P. Callahan, C. Elachi, Y. Gim, R. Kirk, K. Lewis, R. Lopes, R. Lorenz, J. Lunine, K. Mitchell, G. Mitri, E. Stofan, and S. Wall (2008), Hydrocarbon lakes on Titan: Distribution and interaction with a porous regolith, *Geophys. Res. Lett.*, 35, L09204, doi:10.1029/2008GL033409.

Hayes, A. G. (2016), The lakes and seas of titan, *Annual Review of Earth and Planetary Sciences*, 44(1), null, doi:10.1146/annurev-earth-060115-012247.

Hayes, A. G., O. Aharonson, J. I. Lunine, R. L. Kirk, H. A. Zebker, L. C. Wye, R. D. Lorenz, E. P. Turtle, P. Paillou, G. Mitri, S. D. Wall, E. R. Stofan, K. L. Mitchell, C. Elachi, and the Cassini RADAR Team (2011), Transient surface liquid in Titan's polar regions from Cassini, *Icarus*, 211, 655–671, doi:10.1016/j.icarus.2010.08.017.

Hayes, A. G., R. D. Lorenz, M. A. Donelan, M. Manga, J. I. Lunine, T. Schneider, M. P. Lamb, J. M. Mitchell, W. W. Fischer, S. D. Graves, H. L. Tolman, O. Aharonson, P. J. Encrenaz, B. Ventura, D. Casarano, and C. Notarnicola (2013), Wind driven capillary-gravity waves on Titan's lakes: Hard to detect or non-existent?, *Icarus*, 225, 403–412, doi:10.1016/j.icarus.2013.04.004.

Hayne, P. O., T. B. McCord, and C. Sotin (2014), Titan's surface composition and atmospheric transmission with solar occultation measurements by Cassini VIMS, *Icarus*, 243, 158–172, doi:10.1016/j.icarus.2014.08.045.

Hébrard, E., Y. Bénilan, and F. Raulin (2005), Sensitivity effects of photochemical parameters uncertainties on hydrocarbon production in the atmosphere of Titan, *Advances in Space Research*, 36, 268–273, doi:10.1016/j.asr.2005.03.093.

Hébrard, E., M. Dobrijevic, J. C. Loison, A. Bergeat, K. M. Hickson, and F. Caralp (2013), Photochemistry of  $C_3H_p$  hydrocarbons in Titan's stratosphere revisited, *Astronomy and*

*Astrophysics*, 552, A132, doi:10.1051/0004-6361/201220686.

Hickson, K. M., J. C. Loison, T. Cavalié, E. Hébrard, and M. Dobrijevic (2014), The evolution of infalling sulfur species in Titan's atmosphere, *Astronomy and Astrophysics*, 572, A58, doi:10.1051/0004-6361/201424703.

Hirtzig, M., B. Bézard, E. Lellouch, A. Coustenis, C. de Bergh, P. Drossart, A. Campagne, V. Boudon, V. Tyuterev, P. Rannou, T. Cours, S. Kassi, A. Nikitin, D. Monadelain, S. Rodriguez, and S. Le Mouélic (2013), Titan's surface and atmosphere from Cassini/VIMS data with updated methane opacity, *Icarus*, 226, 470–486, doi: 10.1016/j.icarus.2013.05.033.

Hodyss, R., M. Choukroun, C. Sotin, and P. Beauchamp (2013), The solubility of  $^{40}\text{Ar}$  and  $^{84}\text{Kr}$  in liquid hydrocarbons: Implications for Titan's geological evolution, *Geophys. Res. Lett.*, 40, 2935–2940, doi:10.1002/grl.50630.

Hoffman, J. H., R. R. Hodges, M. B. McElroy, T. M. Donahue, and M. Kolpin (1979), Composition and structure of the Venus atmosphere - Results from Pioneer Venus, *Science*, 205, 49–52, doi:10.1126/science.205.4401.49.

Hoffman, J. H., V. I. Oyama, and U. von Zahn (1980), Measurement of the Venus lower atmosphere composition - A comparison of results, *J. Geophys. Res.*, 85, 7871–7881, doi:10.1029/JA085iA13p07871.

Hofgartner, J. D., and J. I. Lunine (2013), Does ice float in Titan's lakes and seas?, *Icarus*, 223, 628–631, doi:10.1016/j.icarus.2012.11.028.

Hofgartner, J. D., A. G. Hayes, J. I. Lunine, H. Zebker, B. W. Stiles, C. Sotin, J. W. Barnes, E. P. Turtle, K. H. Baines, R. H. Brown, B. J. Buratti, R. N. Clark, P. Encrenaz, R. D. Kirk, A. Le Gall, R. M. Lopes, R. D. Lorenz, M. J. Malaska, K. L. Mitchell, P. D.

- Nicholson, P. Paillou, J. Radebaugh, S. D. Wall, and C. Wood (2014), Transient features in a Titan sea, *Nature Geoscience*, 7, 493–496, doi:10.1038/ngeo2190.
- Hofgartner, J. D., A. G. Hayes, J. I. Lunine, H. Zebker, R. D. Lorenz, M. J. Malaska, M. Mastrogiovanni, C. Notarnicola, and J. M. Soderblom (2016), Titan's "Magic Islands": Transient features in a hydrocarbon sea, *Icarus*, 271, 338–349, doi:10.1016/j.icarus.2016.02.022.
- Hörst, S. M., and M. A. Tolbert (2013), In Situ Measurements of the Size and Density of Titan Aerosol Analogs, *ApJL*, 770, L10, doi:10.1088/2041-8205/770/1/L10.
- Hörst, S. M., and M. A. Tolbert (2014), The Effect of Carbon Monoxide on Planetary Haze Formation, *ApJ*, 781, 53, doi:10.1088/0004-637X/781/1/53.
- Hörst, S. M., V. Vuitton, and R. V. Yelle (2008), Origin of oxygen species in Titan's atmosphere, *Journal of Geophysical Research (Planets)*, 113(E12), 10,006–+, doi:10.1029/2008JE003135.
- Hörst, S. M., R. V. Yelle, A. Buch, N. Carrasco, G. Cernogora, O. Dutuit, E. Quirico, E. Sciamma-O'Brien, M. A. Smith, Á. Somogyi, C. Szopa, R. Thissen, and V. Vuitton (2012), Formation of Amino Acids and Nucleotide Bases in a Titan Atmosphere Simulation Experiment, *Astrobiology*, 12, 809–817, doi:10.1089/ast.2011.0623.
- Hourdin, F., O. Talagrand, R. Sadourny, R. Courtin, D. Gautier, and C. P. McKay (1995), Numerical simulation of the general circulation of the atmosphere of Titan., *Icarus*, 117, 358–374, doi:10.1006/icar.1995.1162.
- Hourdin, F., S. Lebonnois, D. Luz, and P. Rannou (2004), Titan's stratospheric composition driven by condensation and dynamics, *Journal of Geophysical Research (Planets)*, 109, 12,005–+, doi:10.1029/2004JE002282.

- Hubbard, W. B., D. M. Hunten, H. J. Reitsema, N. Brosch, Y. Nevo, E. Carreira, F. Rossi, and L. H. Wasserman (1990), Results for Titan's atmosphere from its occultation of 28 Sagittarii, *Nature*, 343, 353–355, doi:10.1038/343353a0.
- Hubbard, W. B., B. Sicardy, R. Miles, A. J. Hollis, R. W. Forrest, I. K. M. Nicolson, G. Appleby, W. Beisker, C. Bittner, H.-J. Bode, M. Bruns, H. Denzau, M. Nezel, E. Riedel, H. Struckmann, J. E. Arlot, F. Roques, F. Sevre, W. Thuillot, M. Hoffmann, E. H. Geyer, C. Buil, F. Colas, J. Lecacheux, A. Klotz, E. Thouvenot, J. L. Vidal, E. Carreira, F. Rossi, C. Blanco, S. Cristaldi, Y. Nevo, H. J. Reitsema, N. Brosch, K. Cernis, K. Zdanavicius, L. H. Wasserman, D. M. Hunten, D. Gautier, E. Lellouch, R. V. Yelle, B. Rizk, F. M. Flasar, C. C. Porco, D. Toublanc, and G. Corugedo (1993), The occultation of 28 SGR by Titan, *Astronomy and Astrophysics*, 269, 541–563.
- Hueso, R., and A. Sánchez-Lavega (2006), Methane storms on Saturn's moon Titan, *Nature*, 442, 428–431, doi:10.1038/nature04933.
- Hunten, D. M., M. G. Tomasko, F. M. Flasar, R. E. Samuelson, D. F. Strobel, and D. J. Stevenson (1984), *Titan*, pp. 671–759.
- Iess, L., R. A. Jacobson, M. Ducci, D. J. Stevenson, J. I. Lunine, J. W. Armstrong, S. W. Asmar, P. Racioppa, N. J. Rappaport, and P. Tortora (2012), The Tides of Titan, *Science*, 337, 457, doi:10.1126/science.1219631.
- Imanaka, H., and M. A. Smith (2007), Role of photoionization in the formation of complex organic molecules in Titan's upper atmosphere, *Geophys. Res. Lett.*, 34, 2204–+, doi:10.1029/2006GL028317.
- Imanaka, H., and M. A. Smith (2010), Formation of nitrogenated organic aerosols in the Titan Upper Atmosphere, *PNAS*, 28, 12,423–12,428, doi:10.1073/pnas.0913353107.

Imanaka, H., B. N. Khare, J. E. Elsila, E. L. O. Bakes, C. P. McKay, D. P. Cruikshank, S. Sugita, T. Matsui, and R. N. Zare (2004), Laboratory experiments of Titan tholin formed in cold plasma at various pressures: implications for nitrogen-containing polycyclic aromatic compounds in Titan haze, *Icarus*, *168*, 344–366, doi: 10.1016/j.icarus.2003.12.014.

Imanaka, H., D. P. Cruikshank, B. N. Khare, and C. P. McKay (2012), Optical constants of Titan tholins at mid-infrared wavelengths (2.5–25  $\mu\text{m}$ ) and the possible chemical nature of Titan's haze particles, *Icarus*, *218*, 247–261, doi:10.1016/j.icarus.2011.11.018.

Israël, G., C. Szopa, F. Raulin, M. Cabane, H. B. Niemann, S. K. Atreya, S. J. Bauer, J. Brun, E. Chassefière, P. Coll, E. Condé, D. Coscia, A. Hauchecorne, P. Millian, M. Nguyen, T. Owen, W. Riedler, R. E. Samuelson, J. Siguier, M. Steller, R. Sternberg, and C. Vidal-Madjar (2005), Complex organic matter in Titan's atmospheric aerosols from in situ pyrolysis and analysis, *Nature*, *438*, 796–799, doi:10.1038/nature04349.

Israël, G., C. Szopa, F. Raulin, M. Cabane, H. B. Niemann, S. K. Atreya, S. J. Bauer, J.-F. Brun, E. Chassefière, P. Coll, E. Condé, D. Coscia, A. Hauchecorne, P. Millian, M. J. Nguyen, T. Owen, W. Riedler, R. E. Samuelson, J.-M. Siguier, M. Steller, R. Sternberg, and C. Vidal-Madjar (2006), Astrochemistry: Complex organic matter in Titan's aerosols? (Reply), *Nature*, *444*, doi:10.1038/nature05418.

Jacobson, R. A., P. G. Antreasian, J. J. Bordi, K. E. Criddle, R. Ionasescu, J. B. Jones, R. A. Mackenzie, M. C. Meek, D. Parcher, F. J. Pelletier, W. M. Owen, Jr., D. C. Roth, I. M. Roundhill, and J. R. Stauch (2006), The Gravity Field of the Saturnian System from Satellite Observations and Spacecraft Tracking Data, *AJ*, *132*, 2520–2526, doi:10.1086/508812.

Jacovi, R., and A. Bar-Nun (2008), Removal of Titan's noble gases by their trapping in its haze, *Icarus*, 196, 302–304, doi:10.1016/j.icarus.2008.02.014.

Jacquemart, D., E. Lellouch, B. Bézard, C. de Bergh, A. Coustenis, N. Lacome, B. Schmitt, and M. Tomasko (2008), New laboratory measurements of CH<sub>4</sub> in Titan's conditions and a reanalysis of the DISR near-surface spectra at the Huygens landing site, *Planet. Space Sci.*, 56, 613–623, doi:10.1016/j.pss.2007.10.008.

Janssen, M. A., A. Le Gall, R. M. Lopes, R. D. Lorenz, M. J. Malaska, A. G. Hayes, C. D. Neish, A. Solomonidou, K. L. Mitchell, J. Radebaugh, S. J. Keihm, M. Choukroun, C. Leyrat, P. J. Encrenaz, and M. Mastrogiovanni (2016), Titan's surface at 2.18-cm wavelength imaged by the Cassini RADAR radiometer: Results and interpretations through the first ten years of observation, *Icarus*, 270, 443–459, doi:10.1016/j.icarus.2015.09.027.

Jennings, D. E., F. M. Flasar, V. G. Kunde, R. E. Samuelson, J. C. Pearl, C. A. Nixon, R. C. Carlson, A. A. Mamoutkine, J. C. Brasunas, E. Guandique, R. K. Achterberg, G. L. Bjorkaker, P. N. Romani, M. E. Segura, S. A. Albright, M. H. Elliott, J. S. Tingley, S. Calcutt, A. Coustenis, and R. Courtin (2009), Titan's Surface Brightness Temperatures, *ApJL*, 691, L103–L105, doi:10.1088/0004-637X/691/2/L103.

Jennings, D. E., V. Cottini, C. A. Nixon, F. M. Flasar, V. G. Kunde, R. E. Samuelson, P. N. Romani, B. E. Hesman, R. C. Carlson, N. J. P. Gorius, A. Coustenis, and T. Tokano (2011), Seasonal Changes in Titan's Surface Temperatures, *ApJL*, 737, L15, doi:10.1088/2041-8205/737/1/L15.

Jennings, D. E., C. M. Anderson, R. E. Samuelson, F. M. Flasar, C. A. Nixon, V. G. Kunde, R. K. Achterberg, V. Cottini, R. de Kok, A. Coustenis, S. Vinatier, and S. B.

- Calcutt (2012a), Seasonal Disappearance of Far-infrared Haze in Titan's Stratosphere, *ApJL*, 754, L3, doi:10.1088/2041-8205/754/1/L3.
- Jennings, D. E., C. M. Anderson, R. E. Samuelson, F. M. Flasar, C. A. Nixon, G. L. Bjoraker, P. N. Romani, R. K. Achterberg, V. Cottini, B. E. Hesman, V. G. Kunde, R. C. Carlson, R. de Kok, A. Coustenis, S. Vinatier, G. Bampasidis, N. A. Teanby, and S. B. Calcutt (2012b), First Observation in the South of Titan's Far-infrared 220 cm<sup>-1</sup> Cloud, *ApJL*, 761, L15, doi:10.1088/2041-8205/761/1/L15.
- Jennings, D. E., R. K. Achterberg, V. Cottini, C. M. Anderson, F. M. Flasar, C. A. Nixon, G. L. Bjoraker, V. G. Kunde, R. C. Carlson, E. Guandique, M. S. Kaelberer, J. S. Tingley, S. A. Albright, M. E. Segura, R. de Kok, A. Coustenis, S. Vinatier, G. Bampasidis, N. A. Teanby, and S. Calcutt (2015), Evolution of the Far-infrared Cloud at Titan's South Pole, *ApJL*, 804, L34, doi:10.1088/2041-8205/804/2/L34.
- Jennings, D. E., V. Cottini, C. A. Nixon, R. K. Achterberg, F. M. Flasar, V. G. Kunde, P. N. Romani, R. E. Samuelson, A. Mamoutkine, N. J. P. Gorius, A. Coustenis, and T. Tokano (2016), Surface Temperatures on Titan during Northern Winter and Spring, *ApJL*, 816, L17, doi:10.3847/2041-8205/816/1/L17.
- Jolly, A., V. Cottini, A. Fayt, L. Manceron, F. Kwabia-Tchana, Y. Benilan, J.-C. Guillemin, C. Nixon, and P. Irwin (2015), Gas phase dicyanoacetylene (C<sub>4</sub>N<sub>2</sub>) on Titan: New experimental and theoretical spectroscopy results applied to Cassini CIRS data, *Icarus*, 248, 340–346, doi:10.1016/j.icarus.2014.10.049.
- Kammer, J. A., D. E. Shemansky, X. Zhang, and Y. L. Yung (2013), Composition of Titan's upper atmosphere from Cassini UVIS EUV stellar occultations, *Planet. Space Sci.*, 88, 86–92, doi:10.1016/j.pss.2013.08.003.

Karatekin, Ö., T. Van Hoolst, and T. Tokano (2008), Effect of internal gravitational coupling on Titan's non-synchronous rotation, *Geophys. Res. Lett.*, 35, L16202, doi: 10.1029/2008GL034744.

Karkoschka, E. (2016a), Titan's meridional wind profile and Huygens' orientation and swing inferred from the geometry of DISR imaging, *Icarus*, 270, 326–338, doi: 10.1016/j.icarus.2015.06.012.

Karkoschka, E. (2016b), Seasonal variation of Titan's haze at low and high altitudes from HST-STIS spectroscopy, *Icarus*, 270, 339–354, doi:10.1016/j.icarus.2015.07.007.

Karkoschka, E., and M. G. Tomasko (2009), Rain and dewdrops on titan based on in situ imaging, *Icarus*, 199(2), 442–448.

Karkoschka, E., M. G. Tomasko, L. R. Doose, C. See, E. A. McFarlane, S. E. Schröder, and B. Rizk (2007), DISR imaging and the geometry of the descent of the Huygens probe within Titan's atmosphere, *Planet. Space Sci.*, 55, 1896–1935, doi: 10.1016/j.pss.2007.04.019.

Keller, C. N., V. G. Anicich, and T. E. Cravens (1998), Model of Titan's ionosphere with detailed hydrocarbon ion chemistry, *Planet. Space Sci.*, 46, 1157–1174, doi: 10.1016/S0032-0633(98)00053-1.

Khanna, R., M. Perera-Jarmer, and M. Ospina (1987), Vibrational infrared and raman spectra of dicyanoacetylene, *Spectrochimica Acta Part A: Molecular Spectroscopy*, 43(3), 421–425.

Khanna, R. K. (2005), Condensed species in Titan's stratosphere: Confirmation of crystalline cyanoacetylene ( $\text{HC}_3\text{N}$ ) and evidence for crystalline acetylene ( $\text{C}_2\text{H}_2$ ) on Titan, *Icarus*, 178, 165–170, doi:10.1016/j.icarus.2005.03.011.

Khare, B. N., C. Sagan, W. R. Thompson, E. T. Arakawa, F. Suits, T. A. Callcott, M. W. Williams, S. Shrader, H. Ogino, T. O. Willingham, and B. Nagy (1984), The organic aerosols of Titan, *Adv. Space Res.*, 4, 59–68, doi:10.1016/0273-1177(84)90545-3.

Kim, S. J., and R. Courtin (2013), Spectral characteristics of the Titanian haze at 1–5 micron from Cassini/VIMS solar occultation data, *Astronomy and Astrophysics*, 557, L6, doi:10.1051/0004-6361/201322173.

Kim, S. J., A. Jung, C. K. Sim, R. Courtin, A. Bellucci, B. Sicardy, I. O. Song, and Y. C. Minh (2011), Retrieval and tentative identification of the 3  $\mu\text{m}$  spectral feature in Titan's haze, *Planet. Space Sci.*, 59, 699–704, doi:10.1016/j.pss.2011.02.002.

Kirk, R. L., E. Howington-Kraus, J. W. Barnes, A. G. Hayes, R. M. Lopes, R. D. Lorenz, J. I. Lunine, K. L. Mitchell, E. R. Stofan, and S. D. Wall (2010), La Sotra y las otras: Topographic evidence for (and against) cryovolcanism on Titan (Invited), *AGU Fall Meeting Abstracts*, pp. A3+.

Kliore, A. J., A. F. Nagy, E. A. Marouf, R. G. French, F. M. Flasar, N. J. Rappaport, A. Anabtawi, S. W. Asmar, D. S. Kahann, E. Barbinis, G. L. Goltz, D. U. Fleischman, and D. J. Rochblatt (2008), First results from the Cassini radio occultations of the Titan ionosphere, *Journal of Geophysical Research (Space Physics)*, 113, A09317, doi: 10.1029/2007JA012965.

Knutson, H. A., D. Dragomir, L. Kreidberg, E. M.-R. Kempton, P. R. McCullough, J. J. Fortney, J. L. Bean, M. Gillon, D. Homeier, and A. W. Howard (2014a), Hubble Space Telescope Near-IR Transmission Spectroscopy of the Super-Earth HD 97658b, *Astrophysical Journal*, 794, 155, doi:10.1088/0004-637X/794/2/155.

Knutson, H. A., B. Benneke, D. Deming, and D. Homeier (2014b), A featureless transmission spectrum for the Neptune-mass exoplanet GJ436b, *Nature*, *505*, 66–68, doi: 10.1038/nature12887.

Koskinen, T. T., R. V. Yelle, D. S. Snowden, P. Lavvas, B. R. Sandel, F. J. Capalbo, Y. Benilan, and R. A. West (2011), The mesosphere and lower thermosphere of Titan revealed by Cassini/UVIS stellar occultations, *Icarus*, *216*, 507–534, doi: 10.1016/j.icarus.2011.09.022.

Kostiuk, T., K. E. Fast, T. A. Livengood, T. Hewagama, J. J. Goldstein, F. Espenak, and D. Buhl (2001), Direct measurement of winds on Titan, *Geophys. Res. Lett.*, *28*, 2361–2364, doi:10.1029/2000GL012617.

Kostiuk, T., T. A. Livengood, T. Hewagama, G. Sonnabend, K. E. Fast, K. Murakawa, A. T. Tokunaga, J. Annen, D. Buhl, and F. Schmülling (2005), Titan's stratospheric zonal wind, temperature, and ethane abundance a year prior to Huygens insertion, *Geophys. Res. Lett.*, *32*, L22205, doi:10.1029/2005GL023897.

Kostiuk, T., T. A. Livengood, G. Sonnabend, K. E. Fast, T. Hewagama, K. Murakawa, A. T. Tokunaga, J. Annen, D. Buhl, F. Schmülling, D. Luz, and O. Witasse (2006), Stratospheric global winds on Titan at the time of Huygens descent, *Journal of Geophysical Research (Planets)*, *111*, E07S03, doi:10.1029/2005JE002630.

Kostiuk, T., T. Hewagama, K. E. Fast, T. A. Livengood, J. Annen, D. Buhl, G. Sonnabend, F. Schmülling, J. D. Delgado, and R. Achterberg (2010), High spectral resolution infrared studies of Titan: Winds, temperature, and composition, *Planet. Space Sci.*, *58*, 1715–1723, doi:10.1016/j.pss.2010.08.004.

Krasnopolsky, V. A. (2009), A photochemical model of Titan's atmosphere and ionosphere, *Icarus*, *201*, 226–256, doi:10.1016/j.icarus.2008.12.038.

Krasnopolsky, V. A. (2012), Titan's photochemical model: Further update, oxygen species, and comparison with Triton and Pluto, *Planet. Space Sci.*, *73*, 318–326, doi:10.1016/j.pss.2012.08.013.

Kreidberg, L., J. L. Bean, J.-M. Désert, B. Benneke, D. Deming, K. B. Stevenson, S. Seager, Z. Berta-Thompson, A. Seifahrt, and D. Homeier (2014), Clouds in the atmosphere of the super-Earth exoplanet GJ1214b, *Nature*, *505*, 69–72, doi:10.1038/nature12888.

Kuiper, G. P. (1944), Titan: a Satellite with an Atmosphere., *ApJ*, *100*, 378–+, doi:10.1086/144679.

Kunde, V. G., A. C. Aikin, R. A. Hanel, D. E. Jennings, W. C. Maguire, and R. E. Samuelson (1981), C<sub>4</sub>H<sub>2</sub>, HC<sub>3</sub>N and C<sub>2</sub>N<sub>2</sub> in Titan's atmosphere, *Nature*, *292*, 686–688, doi:10.1038/292686a0.

Langhans, M. H., R. Jaumann, K. Stephan, R. H. Brown, B. J. Buratti, R. N. Clark, K. H. Baines, P. D. Nicholson, R. D. Lorenz, L. A. Soderblom, J. M. Soderblom, C. Sotin, J. W. Barnes, and R. Nelson (2012), Titan's fluvial valleys: Morphology, distribution, and spectral properties, *Planet. Space Sci.*, *60*, 34–51, doi:10.1016/j.pss.2011.01.020.

Lara, L. M., E. Lellouch, J. J. López-Moreno, and R. Rodrigo (1996), Vertical distribution of Titan's atmospheric neutral constituents, *J. Geophys. Res.*, *101*, 23,261–23,283, doi:10.1029/96JE02036.

Lara, L.-M., E. Lellouch, and V. Shematovich (1999), Titan's atmospheric haze: the case for HCN incorporation, *Astron. Astrophys.*, *341*, 312–317.

Lara, L. M., E. Lellouch, M. González, R. Moreno, and M. Rengel (2014), A time-dependent photochemical model for Titan's atmosphere and the origin of H<sub>2</sub>O, *Astronomy and Astrophysics*, 566, A143, doi:10.1051/0004-6361/201323085.

Larson, E. J. L., O. B. Toon, and A. J. Friedson (2014), Simulating Titan's aerosols in a three dimensional general circulation model, *Icarus*, 243, 400–419, doi:10.1016/j.icarus.2014.09.003.

Larson, E. J. L., O. B. Toon, R. A. West, and A. J. Friedson (2015), Microphysical modeling of Titan's detached haze layer in a 3D GCM, *Icarus*, 254, 122–134, doi:10.1016/j.icarus.2015.03.010.

Lavvas, P., R. V. Yelle, and V. Vuitton (2009), The detached haze layer in Titan's mesosphere, *Icarus*, 201, 626–633, doi:10.1016/j.icarus.2009.01.004.

Lavvas, P., R. V. Yelle, and C. A. Griffith (2010), Titan's vertical aerosol structure at the Huygens landing site: Constraints on particle size, density, charge, and refractive index, *Icarus*, 210, 832–842, doi:10.1016/j.icarus.2010.07.025.

Lavvas, P., M. Galand, R. V. Yelle, A. N. Heays, B. R. Lewis, G. R. Lewis, and A. J. Coates (2011a), Energy deposition and primary chemical products in Titan's upper atmosphere, *Icarus*, 213, 233–251, doi:10.1016/j.icarus.2011.03.001.

Lavvas, P., M. Sander, M. Kraft, and H. Imanaka (2011b), Surface Chemistry and Particle Shape: Processes for the Evolution of Aerosols in Titan's Atmosphere, *ApJ*, 728, 80–+, doi:10.1088/0004-637X/728/2/80.

Lavvas, P., C. A. Griffith, and R. V. Yelle (2011c), Condensation in Titan's atmosphere at the Huygens landing site, *Icarus*, 215, 732–750, doi:10.1016/j.icarus.2011.06.040.

Lavvas, P., R. V. Yelle, T. Koskinen, A. Bazin, V. Vuitton, E. Vigren, M. Galand, A. Wellbrock, A. J. Coates, J.-E. Wahlund, et al. (2013), Aerosol growth in titans ionosphere, *Proceedings of the National Academy of Sciences*, 110(8), 2729–2734.

Lavvas, P. P., A. Coustenis, and I. M. Vardavas (2008a), Coupling photochemistry with haze formation in Titan's atmosphere, Part I: Model description, *Planet. Space Sci.*, 56, 27–66, doi:10.1016/j.pss.2007.05.026.

Lavvas, P. P., A. Coustenis, and I. M. Vardavas (2008b), Coupling photochemistry with haze formation in Titan's atmosphere, Part II: Results and validation with Cassini/Huygens data, *Planet. Space Sci.*, 56, 67–99, doi:10.1016/j.pss.2007.05.027.

Le Gall, A., M. A. Janssen, L. C. Wye, A. G. Hayes, J. Radebaugh, C. Savage, H. Zebker, R. D. Lorenz, J. I. Lunine, R. L. Kirk, R. M. C. Lopes, S. Wall, P. Callahan, E. R. Stofan, T. Farr, and the Cassini Radar Team (2011), Cassini SAR, radiometry, scatterometry and altimetry observations of Titan's dune fields, *Icarus*, 213, 608–624, doi:10.1016/j.icarus.2011.03.026.

Le Gall, A., M. J. Malaska, R. D. Lorenz, M. A. Janssen, T. Tokano, A. G. Hayes, M. Mastrogiovanni, J. I. Lunine, G. Veyssiére, P. Encrénaz, and O. Karatekin (2016), Composition, seasonal change, and bathymetry of Ligeia Mare, Titan, derived from its microwave thermal emission, *Journal of Geophysical Research (Planets)*, 121, 233–251, doi:10.1002/2015JE004920.

Le Mouélic, S., P. Paillou, M. A. Janssen, J. W. Barnes, S. Rodriguez, C. Sotin, R. H. Brown, K. H. Baines, B. J. Buratti, R. N. Clark, M. Crapeau, P. J. Encrénaz, R. Jaumann, D. Geudtner, F. Paganelli, L. Soderblom, G. Tobie, and S. Wall (2008), Mapping and interpretation of Sinlap crater on Titan using Cassini VIMS

and RADAR data, *Journal of Geophysical Research (Planets)*, 113(E12), E04,003, doi: 10.1029/2007JE002965.

Le Mouélic, S., P. Rannou, S. Rodriguez, C. Sotin, C. A. Griffith, L. Le Corre, J. W. Barnes, R. H. Brown, K. H. Baines, B. J. Buratti, R. N. Clark, P. D. Nicholson, and G. Tobie (2012), Dissipation of Titan's north polar cloud at northern spring equinox, *Planet. Space Sci.*, 60, 86–92, doi:10.1016/j.pss.2011.04.006.

Lebonnois, S. (2005), Benzene and aerosol production in Titan and Jupiter's atmospheres: a sensitivity study, *Planet. Space Sci.*, 53, 486–497, doi:10.1016/j.pss.2004.11.004.

Lebonnois, S., D. Toublanc, F. Hourdin, and P. Rannou (2001), Seasonal Variations of Titan's Atmospheric Composition, *Icarus*, 152, 384–406, doi:10.1006/icar.2001.6632.

Lebonnois, S., E. L. O. Bakes, and C. P. McKay (2002), Transition from Gaseous Compounds to Aerosols in Titan's Atmosphere, *Icarus*, 159, 505–517, doi: 10.1006/icar.2002.6943.

Lebonnois, S., F. Hourdin, V. Eymet, A. Crespin, R. Fournier, and F. Forget (2010), Superrotation of Venus' atmosphere analyzed with a full general circulation model, *Journal of Geophysical Research (Planets)*, 115, E06006, doi:10.1029/2009JE003458.

Lebonnois, S., J. Burgalat, P. Rannou, and B. Charnay (2012), Titan global climate model: A new 3-dimensional version of the IPSL Titan GCM, *Icarus*, 218, 707–722, doi:10.1016/j.icarus.2011.11.032.

Lebonnois, S., F. M. Flasar, T. Tokano, and C. E. Newman (2014), *The general circulation of Titan's lower and middle atmosphere*, pp. 122–157.

Lebonnois, S. É., E. L. O. Bakes, and C. P. McKay (2003), Atomic and molecular hydrogen budget in Titan's atmosphere, *Icarus*, 161, 474–485, doi:10.1016/S0019-1035(02)00039-

8.

- Lellouch, E., B. Bézard, F. M. Flasar, S. Vinatier, R. Achterberg, C. A. Nixon, G. L. Bjoraker, and N. Gorius (2014), The distribution of methane in Titan's stratosphere from Cassini/CIRS observations, *Icarus*, 231, 323–337, doi:10.1016/j.icarus.2013.12.016.
- Lemmon, M. T., E. Karkoschka, and M. Tomasko (1993), Titan's rotation - Surface feature observed, *Icarus*, 103, 329–332, doi:10.1006/icar.1993.1074.
- Lemmon, M. T., E. Karkoschka, and M. Tomasko (1995), Titan's rotational light-curve, *Icarus*, 113, 27–38, doi:10.1006/icar.1995.1003.
- Lewis, J. S. (1971), Satellites of the Outer Planets: Their Physical and Chemical Nature, *Icarus*, 15, 174–+, doi:10.1016/0019-1035(71)90072-8.
- Li, C., X. Zhang, J. A. Kammer, M.-C. Liang, R.-L. Shia, and Y. L. Yung (2014), A non-monotonic eddy diffusivity profile of Titan's atmosphere revealed by Cassini observations, *Planet. Space Sci.*, 104, 48–58, doi:10.1016/j.pss.2013.10.009.
- Li, C., X. Zhang, P. Gao, and Y. Yung (2015), Vertical Distribution of C<sub>3</sub>-hydrocarbons in the Stratosphere of Titan, *ApJL*, 803, L19, doi:10.1088/2041-8205/803/2/L19.
- Li, J., D. Liu, A. Coustenis, and X. Liu (2012), Possible physical cause of the zonal wind collapse on Titan, *Planet. Space Sci.*, 63, 150–157, doi:10.1016/j.pss.2011.09.011.
- Liang, M., Y. L. Yung, and D. E. Shemansky (2007), Photolytically Generated Aerosols in the Mesosphere and Thermosphere of Titan, *ApJL*, 661, L199–L202, doi:10.1086/518785.
- Lindal, G. F., G. E. Wood, H. B. Hotz, D. N. Sweetnam, V. R. Eshleman, and G. L. Tyler (1983), The atmosphere of Titan - an analysis of the Voyager 1 radio occultation measurements, *Icarus*, 53, 348–363, doi:10.1016/0019-1035(83)90155-0.

Lockwood, G. W. (1977), Secular brightness increases of Titan, Uranus, and Neptune, 1972-1976, *Icarus*, 32, 413–430, doi:10.1016/0019-1035(77)90012-4.

Lockwood, G. W., and D. T. Thompson (1979), A relationship between solar activity and planetary albedos, *Nature*, 280, 43–45, doi:10.1038/280043a0.

Lockwood, G. W., and D. T. Thompson (2009), Seasonal photometric variability of Titan, 1972-2006, *Icarus*, 200, 616–626, doi:10.1016/j.icarus.2008.11.017.

Lodders, K. (2003), Solar System Abundances and Condensation Temperatures of the Elements, *ApJ*, 591, 1220–1247, doi:10.1086/375492.

Lopes, R. M. C., K. L. Mitchell, E. R. Stofan, J. I. Lunine, R. Lorenz, F. Paganelli, R. L. Kirk, C. A. Wood, S. D. Wall, L. E. Robshaw, A. D. Fortes, C. D. Neish, J. Radebaugh, E. Reffet, S. J. Ostro, C. Elachi, M. D. Allison, Y. Anderson, R. Boehmer, G. Boubin, P. Callahan, P. Encrenaz, E. Flamini, G. Francescetti, Y. Gim, G. Hamilton, S. Hensley, M. A. Janssen, W. T. K. Johnson, K. Kelleher, D. O. Muhleman, G. Ori, R. Orosei, G. Picardi, F. Posa, L. E. Roth, R. Seu, S. Shaffer, L. A. Soderblom, B. Stiles, S. Vetrella, R. D. West, L. Wye, and H. A. Zebker (2007), Cryovolcanic features on Titan's surface as revealed by the Cassini Titan Radar Mapper, *Icarus*, 186, 395–412, doi:10.1016/j.icarus.2006.09.006.

Lopes, R. M. C., E. R. Stofan, R. Peckyno, J. Radebaugh, K. L. Mitchell, G. Mitri, C. A. Wood, R. L. Kirk, S. D. Wall, J. I. Lunine, A. Hayes, R. Lorenz, T. Farr, L. Wye, J. Craig, R. J. Ollerenshaw, M. Janssen, A. Legall, F. Paganelli, R. West, B. Stiles, P. Callahan, Y. Anderson, P. Valora, L. Soderblom, and Cassini RADAR Team (2010), Distribution and interplay of geologic processes on Titan from Cassini radar data, *Icarus*, 205, 540–558, doi:10.1016/j.icarus.2009.08.010.

Lopes, R. M. C., R. L. Kirk, K. L. Mitchell, A. Legall, J. W. Barnes, A. Hayes, J. Kargel, L. Wye, J. Radebaugh, E. R. Stofan, M. A. Janssen, C. D. Neish, S. D. Wall, C. A. Wood, J. I. Lunine, and M. J. Malaska (2013), Cryovolcanism on Titan: New results from Cassini RADAR and VIMS, *Journal of Geophysical Research (Planets)*, 118, 416–435, doi:10.1002/jgre.20062.

Lopes, R. M. C., M. J. Malaska, A. Solomonidou, A. Le Gall, M. A. Janssen, C. D. Neish, E. P. Turtle, S. P. D. Birch, A. G. Hayes, J. Radebaugh, A. Coustenis, A. Schoenfeld, B. W. Stiles, R. L. Kirk, K. L. Mitchell, E. R. Stofan, and K. J. Lawrence (2016), Nature, distribution, and origin of Titan's Undifferentiated Plains, *Icarus*, 270, 162–182, doi:10.1016/j.icarus.2015.11.034.

López-Moreno, J. J., G. J. Molina-Cuberos, M. Hamelin, R. Grard, F. Simões, R. Godard, K. Schwingenschuh, C. Béghin, J. J. Berthelier, V. J. G. Brown, P. Falkner, F. Ferri, M. Fulchignoni, I. Jernej, J. M. Jerónimo, R. Rodrigo, and R. Trautner (2008), Structure of Titan's low altitude ionized layer from the Relaxation Probe onboard HUYGENS, *Geophys. Res. Lett.*, 35, L22104, doi:10.1029/2008GL035338.

López-Puertas, M., B. M. Dinelli, A. Adriani, B. Funke, M. García-Comas, M. L. Moriconi, E. D'Aversa, C. Boersma, and L. J. Allamandola (2013), Large Abundances of Polycyclic Aromatic Hydrocarbons in Titan's Upper Atmosphere, *Astrophys. J.*, 770, 132, doi:10.1088/0004-637X/770/2/132.

Lora, J. M., and J. L. Mitchell (2015), Titan's asymmetric lake distribution mediated by methane transport due to atmospheric eddies, *Geophys. Res. Lett.*, 42, 6213–6220, doi:10.1002/2015GL064912.

Lora, J. M., P. J. Goodman, J. L. Russell, and J. I. Lunine (2011), Insolation in Titan's troposphere, *Icarus*, 216, 116–119, doi:10.1016/j.icarus.2011.08.017.

Lora, J. M., J. I. Lunine, J. L. Russell, and A. G. Hayes (2014), Simulations of Titan's paleoclimate, *Icarus*, 243, 264–273, doi:10.1016/j.icarus.2014.08.042.

Lora, J. M., J. I. Lunine, and J. L. Russell (2015), GCM simulations of Titan's middle and lower atmosphere and comparison to observations, *Icarus*, 250, 516–528, doi:10.1016/j.icarus.2014.12.030.

Lorenz, R. D. (2006), Thermal interactions of the Huygens probe with the Titan environment: Constraint on near-surface wind, *Icarus*, 182, 559–566, doi:10.1016/j.icarus.2006.01.009.

Lorenz, R. D. (2014a), The flushing of Ligeia: Composition variations across Titan's seas in a simple hydrological model, *Geophys. Res. Lett.*, 41, 5764–5770, doi:10.1002/2014GL061133.

Lorenz, R. D. (2014b), Physics of saltation and sand transport on Titan: A brief review, *Icarus*, 230, 162–167, doi:10.1016/j.icarus.2013.06.023.

Lorenz, R. D., and A. G. Hayes (2012), The growth of wind-waves in Titan's hydrocarbon seas, *Icarus*, 219, 468–475, doi:10.1016/j.icarus.2012.03.002.

Lorenz, R. D., and J. Radebaugh (2009), Global pattern of Titan's dunes: Radar survey from the Cassini prime mission, *Geophys. Res. Lett.*, 36, L03,202, doi:10.1029/2008GL036850.

Lorenz, R. D., J. I. Lunine, J. A. Grier, and M. A. Fisher (1995), Prediction of aeolian features on planets: Application to Titan paleoclimatology, *J. Geophys. Res.*, 100, 26,377–26,386, doi:10.1029/95JE02708.

Lorenz, R. D., P. H. Smith, M. T. Lemmon, E. Karkoschka, G. W. Lockwood, and J. Caldwell (1997), Titan's North-South Asymmetry from HST and Voyager Imaging: Comparison with Models and Ground-Based Photometry, *Icarus*, 127, 173–189, doi:10.1006/icar.1997.5687.

Lorenz, R. D., P. H. Smith, and M. T. Lemmon (2004), Seasonal change in Titan's haze 1992–2002 from Hubble Space Telescope observations, *Geophys. Res. Lett.*, 31, L10702, doi:10.1029/2004GL019864.

Lorenz, R. D., C. A. Griffith, J. I. Lunine, C. P. McKay, and N. O. Renno (2005), Convective plumes and the scarcity of Titan's clouds, *Geophys. Res. Lett.*, 32, 1201–+, doi:10.1029/2004GL021415.

Lorenz, R. D., M. T. Lemmon, and P. H. Smith (2006a), Seasonal evolution of Titan's dark polar hood: midsummer disappearance observed by the Hubble Space Telescope, *MNRAS*, 369, 1683–1687, doi:10.1111/j.1365-2966.2006.10405.x.

Lorenz, R. D., S. Wall, J. Radebaugh, G. Boubin, E. Reffet, M. Janssen, E. Stofan, R. Lopes, R. Kirk, C. Elachi, J. Lunine, K. Mitchell, F. Paganelli, L. Soderblom, C. Wood, L. Wye, H. Zebker, Y. Anderson, S. Ostro, M. Allison, R. Boehmer, P. Callahan, P. Encrenaz, G. G. Ori, G. Francescetti, Y. Gim, G. Hamilton, S. Hensley, W. Johnson, K. Kelleher, D. Muhleman, G. Picardi, F. Posa, L. Roth, R. Seu, S. Shaffer, B. Stiles, S. Vetrella, E. Flamini, and R. West (2006b), The Sand Seas of Titan: Cassini RADAR Observations of Longitudinal Dunes, *Science*, 312, 724–727, doi:10.1126/science.1123257.

Lorenz, R. D., C. A. Wood, J. I. Lunine, S. D. Wall, R. M. Lopes, K. L. Mitchell, F. Paganelli, Y. Z. Anderson, L. Wye, C. Tsai, H. Zebker, and E. R. Stofan (2007),

Titan's young surface: Initial impact crater survey by Cassini RADAR and model comparison, *Geophys. Res. Lett.*, 34, L07,204, doi:10.1029/2006GL028971.

Lorenz, R. D., B. W. Stiles, R. L. Kirk, M. D. Allison, P. Persi del Marmo, L. Iess, J. I. Lunine, S. J. Ostro, and S. Hensley (2008a), Titan's Rotation Reveals an Internal Ocean and Changing Zonal Winds, *Science*, 319, 1649, doi:10.1126/science.1151639.

Lorenz, R. D., R. D. West, and W. T. K. Johnson (2008b), Cassini RADAR constraint on Titan's winter polar precipitation, *Icarus*, 195, 812–816, doi: 10.1016/j.icarus.2007.12.025.

Lorenz, R. D., K. L. Mitchell, R. L. Kirk, A. G. Hayes, O. Aharonson, H. A. Zebker, P. Paillou, J. Radebaugh, J. I. Lunine, M. A. Janssen, S. D. Wall, R. M. Lopes, B. Stiles, S. Ostro, G. Mitri, and E. R. Stofan (2008c), Titan's inventory of organic surface materials, *Geophys. Res. Lett.*, 35, L02206, doi:10.1029/2007GL032118.

Lorenz, R. D., R. M. Lopes, F. Paganelli, J. I. Lunine, R. L. Kirk, K. L. Mitchell, L. A. Soderblom, E. R. Stofan, G. Ori, M. Myers, H. Miyamoto, J. Radebaugh, B. Stiles, S. D. Wall, C. A. Wood, and the Cassini RADAR Team (2008d), Fluvial channels on Titan: Initial Cassini RADAR observations, *Planet. Space Sci.*, 56, 1132–1144, doi: 10.1016/j.pss.2008.02.009.

Lorenz, R. D., P. Claudin, B. Andreotti, J. Radebaugh, and T. Tokano (2010), A 3 km atmospheric boundary layer on Titan indicated by dune spacing and Huygens data, *Icarus*, 205, 719–721, doi:10.1016/j.icarus.2009.08.002.

Lorenz, R. D., L. A. Young, and F. Ferri (2014a), Gravity waves in Titan's lower stratosphere from Huygens probe in situ temperature measurements, *Icarus*, 227, 49–55, doi:10.1016/j.icarus.2013.08.025.

- Lorenz, R. D., M. R. Leese, B. Hathi, J. C. Zarnecki, A. Hagermann, P. Rosenberg, M. C. Towner, J. Garry, and H. Svedhem (2014b), Silence on Shangri-La: Attenuation of Huygens acoustic signals suggests surface volatiles, *Planet. Space Sci.*, *90*, 72–80, doi:10.1016/j.pss.2013.11.003.
- Lucas, A., O. Aharonson, C. Deledalle, A. G. Hayes, R. Kirk, and E. Howington-Kraus (2014a), Insights into Titan's geology and hydrology based on enhanced image processing of Cassini RADAR data, *Journal of Geophysical Research (Planets)*, *119*, 2149–2166, doi:10.1002/2013JE004584.
- Lucas, A., S. Rodriguez, C. Narteau, B. Charnay, S. C. Pont, T. Tokano, A. Garcia, M. Thiriet, A. G. Hayes, R. D. Lorenz, and O. Aharonson (2014b), Growth mechanisms and dune orientation on Titan, *Geophys. Res. Lett.*, *41*, 6093–6100, doi:10.1002/2014GL060971.
- Lunine, J., and S. Atreya (2008), The methane cycle on Titan, *Nature Geoscience*, *1*, 335, doi:10.1038/ngeo187.
- Lunine, J. I. (2009), Saturn's titan: A strict test for life's cosmic ubiquity, *Proceedings of the American Philosophical Society*, *153*(4), 403–418.
- Lunine, J. I. (2010), Titan and habitable planets around M-dwarfs, *Faraday Discussions*, *147*, 405, doi:10.1039/c004788k.
- Lunine, J. I., and S. M. Hörst (2011), Organic chemistry on the surface of titan, *Rendiconti Lincei*, *22*(3), 183–189, doi:10.1007/s12210-011-0130-8.
- Lunine, J. I., D. J. Stevenson, and Y. L. Yung (1983), Ethane ocean on Titan, *Science*, *222*, 1229–.

Lutz, B. L., T. Owen, and R. D. Cess (1976), Laboratory band strengths of methane and their application to the atmospheres of Jupiter, Saturn, Uranus, Neptune, and Titan, *ApJ*, 203, 541–551, doi:10.1086/154110.

Lutz, B. L., C. de Bergh, and T. Owen (1983), Titan - Discovery of carbon monoxide in its atmosphere, *Science*, 220, 1374–+.

Luz, D., T. Civeit, R. Courtin, J.-P. Lebreton, D. Gautier, P. Rannou, A. Kaufer, O. Witasse, L. Lara, and F. Ferri (2005), Characterization of zonal winds in the stratosphere of Titan with UVES, *Icarus*, 179, 497–510, doi:10.1016/j.icarus.2005.07.021.

Luz, D., T. Civeit, R. Courtin, J.-P. Lebreton, D. Gautier, O. Witasse, A. Kaufer, F. Ferri, L. Lara, T. Livengood, and T. Kostiuk (2006), Characterization of zonal winds in the stratosphere of Titan with UVES: 2. Observations coordinated with the Huygens Probe entry, *Journal of Geophysical Research (Planets)*, 111, E08S90, doi: 10.1029/2005JE002617.

MacKenzie, S. M., J. W. Barnes, C. Sotin, J. M. Soderblom, S. Le Mouélic, S. Rodriguez, K. H. Baines, B. J. Buratti, R. N. Clark, P. D. Nicholson, and T. B. McCord (2014), Evidence of Titan's climate history from evaporite distribution, *Icarus*, 243, 191–207, doi:10.1016/j.icarus.2014.08.022.

Magee, B. A., J. H. Waite, K. E. Mandt, J. Westlake, J. Bell, and D. A. Gell (2009), INMS-derived composition of Titan's upper atmosphere: Analysis methods and model comparison, *Planet. Space Sci.*, 57, 1895–1916, doi:10.1016/j.pss.2009.06.016.

Mahaffy, P. R., C. R. Webster, S. K. Atreya, H. Franz, M. Wong, P. G. Conrad, D. Harpold, J. J. Jones, L. A. Leshin, H. Manning, and et al. (2013), Abundance and Isotopic Composition of Gases in the Martian Atmosphere from the Curiosity Rover, *Science*,

341, 263–266, doi:10.1126/science.1237966.

Mahjoub, A., N. Carrasco, P.-R. Dahoo, T. Gautier, C. Szopa, and G. Cernogora (2012), Influence of methane concentration on the optical indices of Titan's aerosols analogues, *Icarus*, 221, 670–677, doi:10.1016/j.icarus.2012.08.015.

Malaska, M. J., and R. Hodyss (2014), Dissolution of benzene, naphthalene, and biphenyl in a simulated Titan lake, *Icarus*, 242, 74–81, doi:10.1016/j.icarus.2014.07.022.

Malaska, M. J., R. M. Lopes, A. G. Hayes, J. Radebaugh, R. D. Lorenz, and E. P. Turtle (2016), Material transport map of Titan: The fate of dunes, *Icarus*, 270, 183–196, doi:10.1016/j.icarus.2015.09.029.

Maltagliati, L., B. Bézard, S. Vinatier, M. M. Hedman, E. Lellouch, P. D. Nicholson, C. Sotin, R. J. de Kok, and B. Sicardy (2015), Titan's atmosphere as observed by Cassini/VIMS solar occultations: CH<sub>4</sub>, CO and evidence for C<sub>2</sub>H<sub>6</sub> absorption, *Icarus*, 248, 1–24, doi:10.1016/j.icarus.2014.10.004.

Mandt, K. E., J. H. Waite, W. Lewis, B. Magee, J. Bell, J. Lunine, O. Mousis, and D. Cordier (2009), Isotopic evolution of the major constituents of Titan's atmosphere based on Cassini data, *Planet. Space Sci.*, 57, 1917–1930, doi:10.1016/j.pss.2009.06.005.

Mandt, K. E., J. H. Waite, B. Teolis, B. A. Magee, J. Bell, J. H. Westlake, C. A. Nixon, O. Mousis, and J. I. Lunine (2012), The <sup>12</sup>C/<sup>13</sup>C Ratio on Titan from Cassini INMS Measurements and Implications for the Evolution of Methane, *ApJ*, 749, 160, doi:10.1088/0004-637X/749/2/160.

Mandt, K. E., O. Mousis, J. Lunine, and D. Gautier (2014), Protosolar Ammonia as the Unique Source of Titan's nitrogen, *ApJL*, 788, L24, doi:10.1088/2041-8205/788/2/L24.

Marley, M. S., A. S. Ackerman, J. N. Cuzzi, and D. Kitzmann (2013), *Clouds and Hazes in Exoplanet Atmospheres*, pp. 367–391.

Marounina, N., G. Tobie, S. Carpy, J. Monteux, B. Charnay, and O. Grasset (2015), Evolution of Titan's atmosphere during the Late Heavy Bombardment, *Icarus*, 257, 324–335, doi:10.1016/j.icarus.2015.05.011.

Marten, A., T. Hidayat, Y. Biraud, and R. Moreno (2002), New Millimeter Heterodyne Observations of Titan: Vertical Distributions of Nitriles HCN, HC<sub>3</sub>N, CH<sub>3</sub>CN, and the Isotopic Ratio <sup>15</sup>N/<sup>14</sup>N in Its Atmosphere, *Icarus*, 158, 532–544, doi:10.1006/icar.2002.6897.

Marty, B., M. Chaussidon, R. C. Wiens, A. J. G. Jurewicz, and D. S. Burnett (2011), A <sup>15</sup>N-Poor Isotopic Composition for the Solar System As Shown by Genesis Solar Wind Samples, *Science*, 332, 1533, doi:10.1126/science.1204656.

Mastrogiuseppe, M., V. Poggiali, A. Hayes, R. Lorenz, J. Lunine, G. Picardi, R. Seu, E. Flamini, G. Mitri, C. Notarnicola, P. Paillou, and H. Zebker (2014), The bathymetry of a Titan sea, *Geophys. Res. Lett.*, 41, 1432–1437, doi:10.1002/2013GL058618.

Mayo, L. A., and R. E. Samuelson (2005), Condensate clouds in Titan's north polar stratosphere, *Icarus*, 176, 316–330, doi:10.1016/j.icarus.2005.01.020.

McCord, T. B., G. B. Hansen, B. J. Buratti, R. N. Clark, D. P. Cruikshank, E. D'Aversa, C. A. Griffith, E. K. H. Baines, R. H. Brown, C. M. Dalle Ore, G. Filacchione, V. Formisano, C. A. Hibbitts, R. Jaumann, J. I. Lunine, R. M. Nelson, C. Sotin, and the Cassini VIMS Team (2006), Composition of Titan's surface from Cassini VIMS, *Planet. Space Sci.*, 54, 1524–1539, doi:10.1016/j.pss.2006.06.007.

McCord, T. B., P. Hayne, J.-P. Combe, G. B. Hanse, J. W. Barnes, J. Rodriguez, S. Le Mouélic, K. H. Baines, R. H. Brown, B. J. Buratti, C. Sotin, P. Nicholson, R. Jaumann, R. Nelson, and The Cassini VIMS Team (2008), Titan's Surface: Search for spectral diversity and composition using the Cassini VIMS investigation, *Icarus*, 194, 212–242, doi:10.1016/j.icarus.2007.08.039.

McDonald, G. D., A. G. Hayes, R. C. Ewing, J. M. Lora, C. E. Newman, T. Tokano, A. Lucas, A. Soto, and G. Chen (2016), Variations in Titan's dune orientations as a result of orbital forcing, *Icarus*, 270, 197–210, doi:10.1016/j.icarus.2015.11.036.

McKay, C. P., T. W. Scattergood, J. B. Pollack, W. J. Borucki, and H. T. van Ghyseghem (1988), High-temperature shock formation of N<sub>2</sub> and organics on primordial Titan, *Nature*, 332, 520–522, doi:10.1038/332520a0.

McKay, C. P., J. B. Pollack, and R. Courtin (1989), The thermal structure of Titan's atmosphere, *Icarus*, 80, 23–53, doi:10.1016/0019-1035(89)90160-7.

McKay, C. P., J. B. Pollack, and R. Courtin (1991), The greenhouse and antigreenhouse effects on Titan, *Science*, 253, 1118–1121, doi:10.1126/science.253.5024.1118.

McKay, C. P., A. Coustenis, R. E. Samuelson, M. T. Lemmon, R. D. Lorenz, M. Cabane, P. Rannou, and P. Drossart (2001), Physical properties of the organic aerosols and clouds on Titan, *Planet. Space Sci.*, 49, 79–99, doi:10.1016/S0032-0633(00)00051-9.

McKeegan, K. D., A. P. A. Kallio, V. S. Heber, G. Jarzebinski, P. H. Mao, C. D. Coath, T. Kunihiro, R. C. Wiens, J. E. Nordholt, R. W. Moses, D. B. Reisenfeld, A. J. G. Jurewicz, and D. S. Burnett (2011), The Oxygen Isotopic Composition of the Sun Inferred from Captured Solar Wind, *Science*, 332, 1528, doi:10.1126/science.1204636.

Meibom, A., A. N. Krot, F. Robert, S. Mostefaoui, S. S. Russell, M. I. Petaev, and M. Gounelle (2007), Nitrogen and Carbon Isotopic Composition of the Sun Inferred from a High-Temperature Solar Nebular Condensate, *ApJL*, 656, L33–L36, doi: 10.1086/512052.

Mitchell, J. L. (2008), The drying of Titan's dunes: Titan's methane hydrology and its impact on atmospheric circulation, *Journal of Geophysical Research (Planets)*, 113, E08015, doi:10.1029/2007JE003017.

Mitchell, J. L. (2009), Coupling Convectively Driven Atmospheric Circulation to Surface Rotation: Evidence for Active Methane Weather in the Observed Spin Rate Drift of Titan, *ApJ*, 692, 168–173, doi:10.1088/0004-637X/692/1/168.

Mitchell, J. L. (2012), Titan's Transport-driven Methane Cycle, *ApJL*, 756, L26, doi: 10.1088/2041-8205/756/2/L26.

Mitchell, J. L., and J. M. Lora (2016), The Climate of Titan, *Annual Review of Earth and Planetary Sciences*, 44, 353–380, doi:10.1146/annurev-earth-060115-012428.

Mitchell, J. L., R. T. Pierrehumbert, D. M. W. Frierson, and R. Caballero (2006), The dynamics behind Titan's methane clouds, *Proceedings of the National Academy of Science*, 103, 18,421–18,426, doi:10.1073/pnas.0605074103.

Mitchell, J. L., R. T. Pierrehumbert, D. M. W. Frierson, and R. Caballero (2009), The impact of methane thermodynamics on seasonal convection and circulation in a model Titan atmosphere, *Icarus*, 203, 250–264, doi:10.1016/j.icarus.2009.03.043.

Mitchell, J. L., M. Ádámkovics, R. Caballero, and E. P. Turtle (2011), Locally enhanced precipitation organized by planetary-scale waves on Titan, *Nature Geoscience*, 4, 589–592, doi:10.1038/ngeo1219.

- Mitchell, J. L., G. K. Vallis, and S. F. Potter (2014), Effects of the Seasonal Cycle on Subsolar Rotation in Planetary Atmospheres, *ApJ*, 787, 23, doi:10.1088/0004-637X/787/1/23.
- Mitchell, K. L., R. L. Kirk, R. M. C. Lopes, J. Radabaugh, R. D. Lorenz, and Cassini RADAR Team (2010), Cryovolcanism on Titan: Latest Evidence from Cassini RADAR Imagery and Topography, in *AAS/Division for Planetary Sciences Meeting Abstracts #42, Bulletin of the American Astronomical Society*, vol. 42, pp. 1075–+.
- Mitri, G., A. P. Showman, J. I. Lunine, and R. D. Lorenz (2007), Hydrocarbon lakes on Titan, *Icarus*, 186, 385–394, doi:10.1016/j.icarus.2006.09.004.
- Mitri, G., A. Coustenis, G. Fanchini, A. G. Hayes, L. Iess, K. Khurana, J.-P. Lebreton, R. M. Lopes, R. D. Lorenz, R. Merigliola, M. L. Moriconi, R. Orosei, C. Sotin, E. Stofan, G. Tobie, T. Tokano, and F. Tosi (2014), The exploration of Titan with an orbiter and a lake probe, *Planet. Space Sci.*, 104, 78–92, doi:10.1016/j.pss.2014.07.009.
- Molina-Cuberos, G. J., J. J. López-Moreno, R. Rodrigo, L. M. Lara, and K. O'Brien (1999a), Ionization by cosmic rays of the atmosphere of Titan, *Planet. Space Sci.*, 47, 1347–1354, doi:10.1016/S0032-0633(99)00056-2.
- Molina-Cuberos, G. J., J. J. López-Moreno, R. Rodrigo, and L. M. Lara (1999b), Chemistry of the galactic cosmic ray induced ionosphere of Titan, *J. Geophys. Res.*, 104, 21,997–22,024, doi:10.1029/1998JE001001.
- Molina-Cuberos, G. J., J. J. López-Moreno, and R. Rodrigo (2000), Influence of electrophilic species on the lower ionosphere of Titan, *GRL*, 27, 1351–1354, doi:10.1029/1999GL010771.
- Molina-Cuberos, G. J., H. Lammer, W. Stumptner, K. Schwingenschuh, H. O. Rucker, J. J. López-Moreno, R. Rodrigo, and T. Tokano (2001), Ionospheric layer induced

by meteoric ionization in Titan's atmosphere, *Planet. Space Sci.*, *49*, 143–153, doi: 10.1016/S0032-0633(00)00133-1.

Moore, J. M., and A. D. Howard (2010), Are the basins of Titan's Hotei Regio and Tui Regio sites of former low latitude seas?, *Geophys. Res. Lett.*, *37*, L22,205, doi: 10.1029/2010GL045234.

Moore, J. M., and R. T. Pappalardo (2011), Titan: An exogenic world?, *Icarus*, *212*, 790–806, doi:10.1016/j.icarus.2011.01.019.

Moreno, R., A. Marten, and T. Hidayat (2005), Interferometric measurements of zonal winds on Titan, *Astronomy and Astrophysics*, *437*, 319–328, doi:10.1051/0004-6361:20042117.

Moreno, R., E. Lellouch, L. M. Lara, R. Courtin, D. Bockelée-Morvan, P. Hartogh, M. Rengel, N. Biver, M. Banaszkiewicz, and A. González (2011), First detection of hydrogen isocyanide (HNC) in Titan's atmosphere, *Astronomy and Astrophysics*, *536*, L12, doi:10.1051/0004-6361/201118189.

Moreno, R., E. Lellouch, L. M. Lara, H. Feuchtgruber, M. Rengel, P. Hartogh, and R. Courtin (2012), The abundance, vertical distribution and origin of H<sub>2</sub>O in Titan's atmosphere: Herschel observations and photochemical modelling, *Icarus*, *221*, 753–767, doi:10.1016/j.icarus.2012.09.006.

Moriconi, M. L., J. I. Lunine, A. Adriani, E. D'Aversa, A. Negrão, G. Filacchione, and A. Coradini (2010), Characterization of Titan's Ontario Lacus region from Cassini/VIMS observations, *Icarus*, *210*, 823–831, doi:10.1016/j.icarus.2010.07.023.

Morrison, D., D. P. Cruikshank, and R. E. Murphy (1972), Temperatures of Titan and the Galilean Satellites at 20 Microns, *ApJL*, *173*, L143+, doi:10.1086/180934.

Mousis, O., J. I. Lunine, S. Picaud, D. Cordier, J. H. Waite, Jr., and K. E. Mandt (2011), Removal of Titan's Atmospheric Noble Gases by Their Sequestration in Surface Clathrates, *ApJL*, 740, L9, doi:10.1088/2041-8205/740/1/L9.

Mousis, O., J. I. Lunine, A. G. Hayes, and J. D. Hofgartner (2016), The fate of ethane in Titan's hydrocarbon lakes and seas, *Icarus*, 270, 37–40, doi: 10.1016/j.icarus.2015.06.024.

Muhleman, D. O., A. W. Grossman, B. J. Butler, and M. A. Slade (1990), Radar reflectivity of Titan, *Science*, 248, 975–980, doi:10.1126/science.248.4958.975.

Müller-Wodarg, I. C. F., R. V. Yelle, N. Borggren, and J. H. Waite (2006), Waves and horizontal structures in Titan's thermosphere, *Journal of Geophysical Research (Space Physics)*, 111(A10), A12315, doi:10.1029/2006JA011961.

Müller-Wodarg, I. C. F., R. V. Yelle, J. Cui, and J. H. Waite (2008), Horizontal structures and dynamics of Titan's thermosphere, *J. Geophys. Res.*, 113(E12), 10,005–+, doi: 10.1029/2007JE003033.

Neish, C. D., and R. D. Lorenz (2012), Titan's global crater population: A new assessment, *Planet. Space Sci.*, 60, 26–33, doi:10.1016/j.pss.2011.02.016.

Neish, C. D., and R. D. Lorenz (2014), Elevation distribution of Titan's craters suggests extensive wetlands, *Icarus*, 228, 27–34, doi:10.1016/j.icarus.2013.09.024.

Neish, C. D., R. D. Lorenz, and D. P. O'Brien (2006), The potential for prebiotic chemistry in the possible cryovolcanic dome Ganesa Macula on Titan, *International Journal of Astrobiology*, 5, 57–65, doi:10.1017/S1473550406002898.

Neish, C. D., Á. Somogyi, and M. A. Smith (2010a), Titan's Primordial Soup: Formation of Amino Acids via Low-Temperature Hydrolysis of Tholins, *Astrobiology*, 10, 337–347,

doi:10.1089/ast.2009.0402.

Neish, C. D., R. D. Lorenz, R. L. Kirk, and L. C. Wye (2010b), Radarclinometry of the sand seas of Africa's Namibia and Saturn's moon Titan, *Icarus*, 208, 385–394, doi:10.1016/j.icarus.2010.01.023.

Neish, C. D., R. L. Kirk, R. D. Lorenz, V. J. Bray, P. Schenk, B. W. Stiles, E. Turtle, K. Mitchell, A. Hayes, and Cassini Radar Team (2013), Crater topography on Titan: Implications for landscape evolution, *Icarus*, 223, 82–90, doi:10.1016/j.icarus.2012.11.030.

Neish, C. D., J. W. Barnes, C. Sotin, S. MacKenzie, J. M. Soderblom, S. Le Mouélic, R. L. Kirk, B. W. Stiles, M. J. Malaska, A. Le Gall, R. H. Brown, K. H. Baines, B. Buratti, R. N. Clark, and P. D. Nicholson (2015), Spectral properties of Titan's impact craters imply chemical weathering of its surface, *Geophys. Res. Lett.*, 42, 3746–3754, doi:10.1002/2015GL063824.

Nelson, R. M., L. W. Kamp, R. M. C. Lopes, D. L. Matson, R. L. Kirk, B. W. Hapke, S. D. Wall, M. D. Boryta, F. E. Leader, W. D. Smythe, K. L. Mitchell, K. H. Baines, R. Jaumann, C. Sotin, R. N. Clark, D. P. Cruikshank, P. Drossart, J. I. Lunine, M. Combes, G. Bellucci, J. Bibring, F. Capaccioni, P. Cerroni, A. Coradini, V. Formisano, G. Filacchione, Y. Langevin, T. B. McCord, V. Mennella, P. D. Nicholson, B. Sicardy, P. G. J. Irwin, and J. C. Pearl (2009), Photometric changes on Saturn's Titan: Evidence for active cryovolcanism, *Geophys. Res. Lett.*, 36, L04,202, doi:10.1029/2008GL036206.

Newman, C. E., C. Lee, Y. Lian, M. I. Richardson, and A. D. Toigo (2011), Stratospheric superrotation in the TitanWRF model, *Icarus*, 213, 636–654, doi:10.1016/j.icarus.2011.03.025.

Newman, C. E., M. I. Richardson, Y. Lian, and C. Lee (2016), Simulating Titan's methane cycle with the TitanWRF General Circulation Model, *Icarus*, 267, 106–134, doi:10.1016/j.icarus.2015.11.028.

Niemann, H. B., S. K. Atreya, G. R. Carignan, T. M. Donahue, J. A. Haberman, D. N. Harpold, R. E. Hartle, D. M. Hunten, W. T. Kasprzak, P. R. Mahaffy, T. C. Owen, and S. H. Way (1998), The composition of the Jovian atmosphere as determined by the Galileo probe mass spectrometer, *J. Geophys. Res.*, 103, 22,831–22,846, doi:10.1029/98JE01050.

Niemann, H. B., S. K. Atreya, S. J. Bauer, G. R. Carignan, J. E. Demick, R. L. Frost, D. Gautier, J. A. Haberman, D. N. Harpold, D. M. Hunten, G. Israel, J. I. Lunine, W. T. Kasprzak, T. C. Owen, M. Paulkovich, F. Raulin, E. Raaen, and S. H. Way (2005), The abundances of constituents of Titan's atmosphere from the GCMS instrument on the Huygens probe, *Nature*, 438, 779–784, doi:10.1038/nature04122.

Niemann, H. B., S. K. Atreya, J. E. Demick, D. Gautier, J. A. Haberman, D. N. Harpold, W. T. Kasprzak, J. I. Lunine, T. C. Owen, and F. Raulin (2010), Composition of Titan's lower atmosphere and simple surface volatiles as measured by the Cassini-Huygens probe gas chromatograph mass spectrometer experiment, *J. Geophys. Res.*, 115, E12,006, doi: 10.1029/2010JE003659.

Nixon, C. A., R. K. Achterberg, N. A. Teanby, P. G. J. Irwin, J.-M. Flaud, I. Kleiner, A. Dehayem-Kamadjieu, L. R. Brown, R. L. Sams, B. Bézard, A. Coustenis, T. M. Ansty, A. Mamoutkine, S. Vinatier, G. L. Bjoraker, D. E. Jennings, P. N. Romani, and F. M. Flasar (2010), Upper limits for undetected trace species in the stratosphere of titan, *Faraday Discuss.*, 147, 65–81, doi:10.1039/C003771K.

- Nixon, C. A., B. Temelso, S. Vinatier, N. A. Teanby, B. Bézard, R. K. Achterberg, K. E. Mandt, C. D. Sherrill, P. G. J. Irwin, D. E. Jennings, P. N. Romani, A. Coustenis, and F. M. Flasar (2012), Isotopic Ratios in Titan's Methane: Measurements and Modeling, *ApJ*, 749, 159, doi:10.1088/0004-637X/749/2/159.
- Nixon, C. A., D. E. Jennings, B. Bézard, S. Vinatier, N. A. Teanby, K. Sung, T. M. Ansty, P. G. J. Irwin, N. Gorius, V. Cottini, A. Coustenis, and F. M. Flasar (2013a), Detection of Propene in Titan's Stratosphere, *ApJL*, 776, L14, doi:10.1088/2041-8205/776/1/L14.
- Nixon, C. A., N. A. Teanby, P. G. J. Irwin, and S. M. Hörst (2013b), Upper limits for PH<sub>3</sub> and H<sub>2</sub>S in Titan's atmosphere from Cassini CIRS, *Icarus*, 224, 253–256, doi:10.1016/j.icarus.2013.02.024.
- Noll, K. S., T. R. Geballe, and R. F. Knacke (1995), Detection of H 2 18O in Jupiter, *ApJL*, 453, L49, doi:10.1086/513302.
- Owen, T., and H. B. Niemann (2009), The origin of Titan's atmosphere: some recent advances, *Philosophical Transactions of the Royal Society of London Series A*, 367, 607–615, doi:10.1098/rsta.2008.0247.
- Owen, T., P. R. Mahaffy, H. B. Niemann, S. Atreya, and M. Wong (2001), Protosolar Nitrogen, *ApJL*, 553, L77–L79, doi:10.1086/320501.
- Pauzat, F., Y. Ellinger, O. Mousis, M. Ali-Dib, and O. Ozgurel (2013), Gas-phase Sequestration of Noble Gases in the Protosolar Nebula: Possible Consequences on the Outer Solar System Composition, *ApJ*, 777, 29, doi:10.1088/0004-637X/777/1/29.
- Penteado, P. F., C. A. Griffith, M. G. Tomasko, S. Engel, C. See, L. Doose, K. H. Baines, R. H. Brown, B. J. Buratti, R. Clark, P. Nicholson, and C. Sotin (2010), Latitudinal variations in Titan's methane and haze from Cassini VIMS observations, *Icarus*, 206,

352–365, doi:10.1016/j.icarus.2009.11.003.

Perron, J. T., M. P. Lamb, C. D. Koven, I. Y. Fung, E. Yager, and M. Ádámkovics (2006), Valley formation and methane precipitation rates on Titan, *J. Geophys. Res.*, *111*, 11,001–+, doi:10.1029/2005JE002602.

Poch, O., P. Coll, A. Buch, S. I. Ramírez, and F. Raulin (2012), Production yields of organics of astrobiological interest from H<sub>2</sub>O-NH<sub>3</sub> hydrolysis of Titan's tholins, *Planet. Space Sci.*, *61*, 114–123, doi:10.1016/j.pss.2011.04.009.

Podolak, M., and A. Bar-Nun (1979), A constraint on the distribution of Titan's atmospheric aerosol, *Icarus*, *39*, 272–276, doi:10.1016/0019-1035(79)90169-6.

Podolak, M., N. Noy, and A. Bar-Nun (1979), Photochemical aerosols in Titan's atmosphere, *Icarus*, *40*, 193–198, doi:10.1016/0019-1035(79)90065-4.

Porco, C. C., E. Baker, J. Barbara, K. Beurle, A. Brahic, J. A. Burns, S. Charnoz, N. Cooper, D. D. Dawson, A. D. Del Genio, T. Denk, L. Dones, U. Dyudina, M. W. Evans, S. Fussner, B. Giese, K. Grazier, P. Helfenstein, A. P. Ingersoll, R. A. Jacobson, T. V. Johnson, A. McEwen, C. D. Murray, G. Neukum, W. M. Owen, J. Perry, T. Roatsch, J. Spitale, S. Squyres, P. Thomas, M. Tiscareno, E. P. Turtle, A. R. Vasavada, J. Veverka, R. Wagner, and R. West (2005), Imaging of Titan from the Cassini spacecraft, *Nature*, *434*, 159–168, doi:10.1038/nature03436.

Quirico, E., G. Montagnac, V. Lees, P. F. McMillan, C. Szopa, G. Cernogora, J. Rouzaud, P. Simon, J. Bernard, P. Coll, N. Fray, R. D. Minard, F. Raulin, B. Reynard, and B. Schmitt (2008), New experimental constraints on the composition and structure of tholins, *Icarus*, *198*, 218–231, doi:10.1016/j.icarus.2008.07.012.

Radebaugh, J., R. D. Lorenz, R. L. Kirk, J. I. Lunine, E. R. Stofan, R. M. C. Lopes, S. D. Wall, and the Cassini Radar Team (2007), Mountains on Titan observed by Cassini Radar, *Icarus*, 192, 77–91, doi:10.1016/j.icarus.2007.06.020.

Radebaugh, J., R. D. Lorenz, J. I. Lunine, S. D. Wall, G. Boubin, E. Reffet, R. L. Kirk, R. M. Lopes, E. R. Stofan, L. Soderblom, M. Allison, M. Janssen, P. Paillou, P. Callahan, C. Spencer, and The Cassini Radar Team (2008), Dunes on Titan observed by Cassini Radar, *Icarus*, 194, 690–703, doi:10.1016/j.icarus.2007.10.015.

Radebaugh, J., R. D. Lorenz, S. D. Wall, R. L. Kirk, C. A. Wood, J. I. Lunine, E. R. Stofan, R. M. C. Lopes, P. Valora, T. G. Farr, A. Hayes, B. Stiles, G. Mitri, H. Zebker, M. Janssen, L. Wye, A. Legall, K. L. Mitchell, F. Paganelli, R. D. West, E. L. Schaller, and Cassini Radar Team (2011), Regional geomorphology and history of Titan's Xanadu province, *Icarus*, 211, 672–685, doi:10.1016/j.icarus.2010.07.022.

Rafkin, S. C. R., and E. L. Barth (2015), Environmental control of deep convective clouds on Titan: The combined effect of CAPE and wind shear on storm dynamics, morphology, and lifetime, *Journal of Geophysical Research (Planets)*, 120, 739–759, doi: 10.1002/2014JE004749.

Rages, K., and J. B. Pollack (1980), Titan aerosols - Optical properties and vertical distribution, *Icarus*, 41, 119–130, doi:10.1016/0019-1035(80)90164-5.

Rages, K., and J. B. Pollack (1983), Vertical distribution of scattering hazes in Titan's upper atmosphere, *Icarus*, 55, 50–62, doi:10.1016/0019-1035(83)90049-0.

Rages, K., J. B. Pollack, and P. H. Smith (1983), Size estimates of Titan's aerosols based on Voyager high-phase-angle images, *J. Geophys. Res.*, 88, 8721–8728, doi: 10.1029/JA088iA11p08721.

Ramírez, S. I., P. Coll, A. da Silva, R. Navarro-González, J. Lafait, and F. Raulin (2002), Complex Refractive Index of Titan's Aerosol Analogues in the 200-900 nm Domain, *Icarus*, 156, 515–529, doi:10.1006/icar.2001.6783.

Rannou, P., M. Cabane, R. Botet, and E. Chassefière (1997), A new interpretation of scattered light measurements at Titan's limb, *JGR*, 102, 10,997–11,014, doi: 10.1029/97JE00719.

Rannou, P., C. Ferrari, K. Rages, M. Roos-Serote, and M. Cabane (2000), Characterization of Aerosols in the Detached Haze Layer of Titan, *Icarus*, 147, 267–281, doi: 10.1006/icar.2000.6416.

Rannou, P., F. Hourdin, and C. P. McKay (2002), A wind origin for Titan's haze structure, *Nature*, 418, 853–856.

Rannou, P., C. P. McKay, and R. D. Lorenz (2003), A model of Titan's haze of fractal aerosols constrained by multiple observations, *Planet. Space Sci.*, 51, 963–976, doi: 10.1016/j.pss.2003.05.008.

Rannou, P., F. Hourdin, C. P. McKay, and D. Luz (2004), A coupled dynamics-microphysics model of Titan's atmosphere, *Icarus*, 170, 443–462, doi: 10.1016/j.icarus.2004.03.007.

Rannou, P., S. Lebonnois, F. Hourdin, and D. Luz (2005), Titan atmosphere database, *Advances in Space Research*, 36, 2194–2198, doi:10.1016/j.asr.2005.09.041.

Rannou, P., F. Montmessin, F. Hourdin, and S. Lebonnois (2006), The Latitudinal Distribution of Clouds on Titan, *Science*, 311, 201–205, doi:10.1126/science.1118424.

Rannou, P., T. Cours, S. Le Mouélic, S. Rodriguez, C. Sotin, P. Drossart, and R. Brown (2010), Titan haze distribution and optical properties retrieved from recent observa-

tions, *Icarus*, 208, 850–867, doi:10.1016/j.icarus.2010.03.016.

Rannou, P., S. Le Mouélic, C. Sotin, and R. H. Brown (2012), Cloud and Haze in the Winter Polar Region of Titan Observed with Visual and Infrared Mapping Spectrometer on Board Cassini, *ApJ*, 748, 4, doi:10.1088/0004-637X/748/1/4.

Rannou, P., D. Toledo, P. Lavvas, E. D'Aversa, M. L. Moriconi, A. Adriani, S. Le Mouélic, C. Sotin, and R. Brown (2016), Titan's surface spectra at the Huygens landing site and Shangri-La, *Icarus*, 270, 291–306, doi:10.1016/j.icarus.2015.09.016.

Read, P., J. Barstow, B. Charnay, S. Chelvaniththilan, P. Irwin, S. Knight, S. Lebonnois, S. Lewis, J. Mendonça, and L. Montabone (2015), Global energy budgets and trenberth diagrams for the climates of terrestrial and gas giant planets, *Quarterly Journal of the Royal Meteorological Society*.

Rengel, M., H. Sagawa, P. Hartogh, E. Lellouch, H. Feuchtgruber, R. Moreno, C. Jarchow, R. Courtin, J. Cernicharo, and L. M. Lara (2014), Herschel/PACS spectroscopy of trace gases of the stratosphere of Titan, *Astronomy and Astrophysics*, 561, A4, doi: 10.1051/0004-6361/201321945.

Richard, A., N. Rambaux, and B. Charnay (2014), Librational response of a deformed 3-layer Titan perturbed by non-Keplerian orbit and atmospheric couplings, *Planet. Space Sci.*, 93, 22–34, doi:10.1016/j.pss.2014.02.006.

Richardson, M. I., A. D. Toigo, and C. E. Newman (2007), PlanetWRF: A general purpose, local to global numerical model for planetary atmospheric and climate dynamics, *Journal of Geophysical Research (Planets)*, 112, E09,001, doi:10.1029/2006JE002825.

Robinson, T. D., L. Maltagliati, M. S. Marley, and J. J. Fortney (2014), Titan solar occultation observations reveal transit spectra of a hazy world, *PNAS*, 111, 9042–9047,

doi:10.1073/pnas.1403473111.

Rodriguez, S., S. Le Mouélic, P. Rannou, G. Tobie, K. H. Baines, J. W. Barnes, C. A. Griffith, M. Hirtzig, K. M. Pitman, C. Sotin, R. H. Brown, B. J. Buratti, R. N. Clark, and P. D. Nicholson (2009), Global circulation as the main source of cloud activity on Titan, *Nature*, *459*, 678–682, doi:10.1038/nature08014.

Rodriguez, S., S. Le Mouélic, P. Rannou, C. Sotin, R. H. Brown, J. W. Barnes, C. A. Griffith, J. Burgalat, K. H. Baines, B. J. Buratti, R. N. Clark, and P. D. Nicholson (2011), Titan's cloud seasonal activity from winter to spring with Cassini/VIMS, *Icarus*, *216*, 89–110, doi:10.1016/j.icarus.2011.07.031.

Rodriguez, S., A. Garcia, A. Lucas, T. Appéré, A. Le Gall, E. Reffet, L. Le Corre, S. Le Mouélic, T. Cornet, S. Courrech du Pont, C. Narteau, O. Bourgeois, J. Radebaugh, K. Arnold, J. W. Barnes, K. Stephan, R. Jaumann, C. Sotin, R. H. Brown, R. D. Lorenz, and E. P. Turtle (2014), Global mapping and characterization of Titan's dune fields with Cassini: Correlation between RADAR and VIMS observations, *Icarus*, *230*, 168–179, doi:10.1016/j.icarus.2013.11.017.

Roe, H. G. (2012), Titan's Methane Weather, *Annual Review of Earth and Planetary Sciences*, *40*, 355–382, doi:10.1146/annurev-earth-040809-152548.

Roe, H. G., and W. M. Grundy (2012), Buoyancy of ice in the CH<sub>4</sub>-N<sub>2</sub> system, *Icarus*, *219*, 733–736, doi:10.1016/j.icarus.2012.04.007.

Roe, H. G., I. de Pater, B. A. Macintosh, and C. P. McKay (2002), Titan's Clouds from Gemini and Keck Adaptive Optics Imaging, *ApJ*, *581*, 1399–1406, doi:10.1086/344403.

Roe, H. G., T. K. Greathouse, M. J. Richter, and J. H. Lacy (2003), Propane on Titan, *ApJL*, *597*, L65–L68, doi:10.1086/379816.

- Roe, H. G., A. H. Bouchez, C. A. Trujillo, E. L. Schaller, and M. E. Brown (2005), Discovery of Temperate Latitude Clouds on Titan, *ApJL*, 618, L49–L52, doi:10.1086/427499.
- Roman, M. T., R. A. West, D. J. Banfield, P. J. Gierasch, R. K. Achterberg, C. A. Nixon, and P. C. Thomas (2009), Determining a tilt in Titan's north-south albedo asymmetry from Cassini images, *Icarus*, 203, 242–249, doi:10.1016/j.icarus.2009.04.021.
- Rossow, W. B., and G. P. Williams (1979), Large-scale motion in the Venus stratosphere, *Journal of Atmospheric Sciences*, 36, 377–389, doi:10.1175/1520-0469(1979)036j0377:LSMITV;2.0.CO;2.
- Rousselot, P., O. Pirali, E. Jehin, M. Vervloet, D. Hutsemékers, J. Manfroid, D. Cordier, M.-A. Martin-Drumel, S. Gruet, C. Arpigny, A. Decock, and O. Mousis (2014), Toward a Unique Nitrogen Isotopic Ratio in Cometary Ices, *ApJL*, 780, L17, doi:10.1088/2041-8205/780/2/L17.
- Sagan, C., and B. N. Khare (1979), Tholins - Organic chemistry of interstellar grains and gas, *Nature*, 277, 102–107, doi:10.1038/277102a0.
- Sagan, C., and W. R. Thompson (1984), Production and condensation of organic gases in the atmosphere of Titan, *Icarus*, 59, 133–161, doi:10.1016/0019-1035(84)90018-6.
- Samuelson, R. E., R. A. Hanel, V. G. Kunde, and W. C. Maguire (1981), Mean molecular weight and hydrogen abundance of Titan's atmosphere, *Nature*, 292, 688–693, doi:10.1038/292688a0.
- Samuelson, R. E., W. C. Maguire, R. A. Hanel, V. G. Kunde, D. E. Jennings, Y. L. Yung, and A. C. Aikin (1983), CO<sub>2</sub> on Titan, *J. Geophys. Res.*, 88, 8709–8715.
- Samuelson, R. E., L. A. Mayo, M. A. Knuckles, and R. J. Khanna (1997), C<sub>4</sub>N<sub>2</sub> ice in Titan's north polar stratosphere, *Planet. Space Sci.*, 45, 941–948, doi:10.1016/S0032-

0633(97)00088-3.

Samuelson, R. E., M. D. Smith, R. K. Achterberg, and J. C. Pearl (2007), Cassini

CIRS update on stratospheric ices at Titan's winter pole, *Icarus*, 189, 63–71, doi: 10.1016/j.icarus.2007.02.005.

Sarker, N., A. Somogyi, J. I. Lunine, and M. A. Smith (2003), Titan Aerosol Analogues: Analysis of the Nonvolatile Tholins, *Astrobiology*, 3, 719–726, doi: 10.1089/153110703322736042.

Savage, C. J., J. Radabaugh, E. H. Christiansen, and R. D. Lorenz (2014), Implications of dune pattern analysis for Titan's surface history, *Icarus*, 230, 180–190, doi: 10.1016/j.icarus.2013.08.009.

Schaller, E. L., M. E. Brown, H. G. Roe, and A. H. Bouchez (2006a), A large cloud outburst at Titan's south pole, *Icarus*, 182, 224–229, doi:10.1016/j.icarus.2005.12.021.

Schaller, E. L., M. E. Brown, H. G. Roe, A. H. Bouchez, and C. A. Trujillo (2006b), Dissipation of Titan's south polar clouds, *Icarus*, 184, 517–523, doi: 10.1016/j.icarus.2006.05.025.

Schaller, E. L., H. G. Roe, T. Schneider, and M. E. Brown (2009), Storms in the tropics of Titan, *Nature*, 460, 873–875, doi:10.1038/nature08193.

Schinder, P. J., F. M. Flasar, E. A. Marouf, R. G. French, C. A. McGhee, A. J. Kliore, N. J. Rappaport, E. Barbinis, D. Fleischman, and A. Anabtawi (2011), The structure of Titan's atmosphere from Cassini radio occultations, *Icarus*, 215, 460–474, doi: 10.1016/j.icarus.2011.07.030.

Schinder, P. J., F. M. Flasar, E. A. Marouf, R. G. French, C. A. McGhee, A. J. Kliore, N. J. Rappaport, E. Barbinis, D. Fleischman, and A. Anabtawi (2012), The structure of

Titan's atmosphere from Cassini radio occultations: Occultations from the Prime and Equinox missions, *Icarus*, 221, 1020–1031, doi:10.1016/j.icarus.2012.10.021.

Schneider, T., S. D. B. Graves, E. L. Schaller, and M. E. Brown (2012), Polar methane accumulation and rainstorms on Titan from simulations of the methane cycle, *Nature*, 481, 58–61, doi:10.1038/nature10666.

Schröder, S. E., and H. U. Keller (2008), The reflectance spectrum of Titan's surface at the Huygens landing site determined by the descent imager/spectral radiometer, *Planet. Space Sci.*, 56, 753–769, doi:10.1016/j.pss.2007.10.011.

Schröder, S. E., E. Karkoschka, and R. D. Lorenz (2012), Bouncing on Titan: Motion of the Huygens probe in the seconds after landing, *Planet. Space Sci.*, 73, 327–340, doi:10.1016/j.pss.2012.08.007.

Sciamma-O'Brien, E., N. Carrasco, C. Szopa, A. Buch, and G. Cernogora (2010), Titan's atmosphere: An optimal gas mixture for aerosol production?, *Icarus*, 209, 704–714, doi:10.1016/j.icarus.2010.04.009.

Sciamma-O'Brien, E., P.-R. Dahoo, E. Hadamcik, N. Carrasco, E. Quirico, C. Szopa, and G. Cernogora (2012), Optical constants from 370 nm to 900 nm of Titan tholins produced in a low pressure RF plasma discharge, *Icarus*, 218, 356–363, doi:10.1016/j.icarus.2011.12.014.

Sciamma-O'Brien, E., C. L. Ricketts, and F. Salama (2014), The Titan Haze Simulation experiment on COSMIC: Probing Titan's atmospheric chemistry at low temperature, *Icarus*, 243, 325–336, doi:10.1016/j.icarus.2014.08.004.

Sebree, J. A., M. G. Trainer, M. J. Loeffler, and C. M. Anderson (2014), Titan aerosol analog absorption features produced from aromatics in the far infrared, *Icarus*, 236,

146–152, doi:10.1016/j.icarus.2014.03.039.

Sekine, Y., H. Imanaka, T. Matsui, B. N. Khare, E. L. O. Bakes, C. P. McKay, and S. Sugita (2008a), The role of organic haze in Titan's atmospheric chemistry. I. Laboratory investigation on heterogeneous reaction of atomic hydrogen with Titan tholin, *Icarus*, 194, 186–200, doi:10.1016/j.icarus.2007.08.031.

Sekine, Y., S. Lebonnois, H. Imanaka, T. Matsui, E. L. O. Bakes, C. P. McKay, B. N. Khare, and S. Sugita (2008b), The role of organic haze in Titan's atmospheric chemistry. II. Effect of heterogeneous reaction to the hydrogen budget and chemical composition of the atmosphere, *Icarus*, 194, 201–211, doi:10.1016/j.icarus.2007.08.030.

Sekine, Y., H. Genda, S. Sugita, T. Kadono, and T. Matsui (2011), Replacement and late formation of atmospheric N<sub>2</sub> on undifferentiated Titan by impacts, *Nature Geoscience*, 4, 359–362, doi:10.1038/ngeo1147.

Serigano, J., C. A. Nixon, M. A. Cordiner, P. G. J. Irwin, N. A. Teanby, S. B. Charnley, and J. E. Lindberg (2016), Isotopic Ratios of Carbon and Oxygen in Titan's CO using ALMA, *ApJL*, 821, L8, doi:10.3847/2041-8205/821/1/L8.

Shemansky, D. E., A. I. F. Stewart, R. A. West, L. W. Esposito, J. T. Hallett, and X. Liu (2005), The Cassini UVIS Stellar Probe of the Titan Atmosphere, *Science*, 308, 978–982, doi:10.1126/science.1111790.

Shinnaka, Y., H. Kawakita, H. Kobayashi, M. Nagashima, and D. C. Boice (2014), <sup>14</sup>NH<sub>2</sub>/<sup>15</sup>NH<sub>2</sub> Ratio in Comet C/2012 S1 (ISON) Observed during its Outburst in 2013 November, *ApJL*, 782, L16, doi:10.1088/2041-8205/782/2/L16.

Sicardy, B., A. Brahic, C. Ferrari, D. Gautier, J. Lecacheux, E. Lellouch, F. Roques, J. E. Arlot, F. Colas, W. Thuillot, F. Sevre, J. L. Vidal, C. Blanco, S. Cristaldi, C. Buil,

- A. Klotz, and E. Thouvenot (1990), Probing Titan's atmosphere by stellar occultation, *Nature*, 343, 350–353, doi:10.1038/343350a0.
- Sicardy, B., F. Ferri, F. Roques, J. Lecacheux, S. Pau, N. Brosch, Y. Nevo, W. B. Hubbard, H. J. Reitsema, C. Blanco, E. Carreira, W. Beisker, C. Bittner, H.-J. Bode, M. Bruns, H. Denzau, M. Nezel, E. Riedel, H. Struckmann, G. Appleby, R. W. Forrest, I. K. M. Nicolson, A. J. Hollis, and R. Miles (1999), The Structure of Titan's Stratosphere from the 28 Sgr Occultation, *Icarus*, 142, 357–390, doi:10.1006/icar.1999.6219.
- Sicardy, B., F. Colas, T. Widemann, A. Bellucci, W. Beisker, M. Kretlow, F. Ferri, S. Lacour, J. Lecacheux, E. Lellouch, S. Pau, S. Renner, F. Roques, A. Fienga, C. Etienne, C. Martinez, I. S. Glass, D. Baba, T. Nagayama, T. Nagata, S. Itting-Enke, K. Bath, H. Bode, F. Bode, H. Lüdemann, J. Lüdemann, D. Neubauer, A. Tegtmeier, C. Tegtmeier, B. Thomé, F. Hund, C. deWitt, B. Fraser, A. Jansen, T. Jones, P. Schoenau, C. Turk, P. Meintjies, M. Hernandez, D. Fiel, E. Frappa, A. Peyrot, J. P. Teng, M. Viginand, G. Hesler, T. Payet, R. R. Howell, M. Kidger, J. L. Ortiz, O. Naranjo, P. Rosenzweig, and M. Rapaport (2006), The two Titan stellar occultations of 14 November 2003, *J. Geophys. Res.*, 111(E10), 11–+, doi:10.1029/2005JE002624.
- Sim, C. K., S. J. Kim, R. Courtin, M. Sohn, and D.-H. Lee (2013), The two-micron spectral characteristics of the Titanian haze derived from Cassini/VIMS solar occultation spectra, *Planet. Space Sci.*, 88, 93–99, doi:10.1016/j.pss.2013.10.003.
- Sittler, E. C., A. Ali, J. F. Cooper, R. E. Hartle, R. E. Johnson, A. J. Coates, and D. T. Young (2009), Heavy ion formation in Titan's ionosphere: Magnetospheric introduction of free oxygen and a source of Titan's aerosols?, *Planet. Space Sci.*, 57, 1547–1557, doi:10.1016/j.pss.2009.07.017.

- Smith, B. A., L. Soderblom, R. F. Beebe, J. M. Boyce, G. Briggs, A. Bunker, S. A. Collins, C. Hansen, T. V. Johnson, J. L. Mitchell, R. J. Terrile, M. H. Carr, A. F. Cook, J. N. Cuzzi, J. B. Pollack, G. E. Danielson, A. P. Ingersoll, M. E. Davies, G. E. Hunt, H. Masursky, E. M. Shoemaker, D. Morrison, T. Owen, C. Sagan, J. Veverka, R. Strom, and V. E. Suomi (1981), Encounter with Saturn - Voyager 1 imaging science results, *Science*, *212*, 163–191, doi:10.1126/science.212.4491.163.
- Smith, B. A., L. Soderblom, R. Batson, P. Bridges, J. Inge, H. Masursky, E. Shoemaker, R. Beebe, J. Boyce, G. Briggs, A. Bunker, S. A. Collins, C. J. Hansen, T. V. Johnson, J. L. Mitchell, R. J. Terrile, A. F. Cook, J. Cuzzi, J. B. Pollack, G. E. Danielson, A. Ingersoll, M. E. Davies, G. E. Hunt, D. Morrison, T. Owen, C. Sagan, J. Veverka, R. Strom, and V. E. Suomi (1982a), A new look at the Saturn system: The Voyager 2 images, *Science*, *215*, 505–537.
- Smith, G. R., D. F. Strobel, A. L. Broadfoot, B. R. Sandel, D. E. Shemansky, and J. B. Holberg (1982b), Titan's upper atmosphere - Composition and temperature from the EUV solar occultation results, *JGR*, *87*, 1351–1359, doi:10.1029/JA087iA03p01351.
- Smith, P. H. (1980), The radius of Titan from Pioneer Saturn data, *J. Geophys. Res.*, *85*, 5943–5947, doi:10.1029/JA085iA11p05943.
- Smith, P. H., M. T. Lemmon, R. D. Lorenz, L. A. Sromovsky, J. J. Caldwell, and M. D. Allison (1996), Titan's Surface, Revealed by HST Imaging, *Icarus*, *119*, 336–349, doi:10.1006/icar.1996.0023.
- Snowden, D., R. V. Yelle, J. Cui, J.-E. Wahlund, N. J. T. Edberg, and K. Ågren (2013), The thermal structure of Titan's upper atmosphere, I: Temperature profiles from Cassini INMS observations, *Icarus*, *226*, 552–582, doi:10.1016/j.icarus.2013.06.006.

- Soderblom, J. M., R. H. Brown, L. A. Soderblom, J. W. Barnes, R. Jaumann, S. L. Mouélic, C. Sotin, K. Stephan, K. H. Baines, B. J. Buratti, R. N. Clark, and P. D. Nicholson (2010), Geology of the Selk crater region on Titan from Cassini VIMS observations, *Icarus*, 208, 905–912, doi:10.1016/j.icarus.2010.03.001.
- Soderblom, L. A., M. G. Tomasko, B. A. Archinal, T. L. Becker, M. W. Bushroe, D. A. Cook, L. R. Doose, D. M. Galuszka, T. M. Hare, E. Howington-Kraus, E. Karkoschka, R. L. Kirk, J. I. Lunine, E. A. McFarlane, B. L. Redding, B. Rizk, M. R. Rosiek, C. See, and P. H. Smith (2007a), Topography and geomorphology of the Huygens landing site on Titan, *Planet. Space Sci.*, 55, 2015–2024, doi:10.1016/j.pss.2007.04.015.
- Soderblom, L. A., R. L. Kirk, J. I. Lunine, J. A. Anderson, K. H. Baines, J. W. Barnes, J. M. Barrett, R. H. Brown, B. J. Buratti, R. N. Clark, D. P. Cruikshank, C. Elachi, M. A. Janssen, R. Jaumann, E. Karkoschka, S. L. Mouélic, R. M. Lopes, R. D. Lorenz, T. B. McCord, P. D. Nicholson, J. Radabaugh, B. Rizk, C. Sotin, E. R. Stofan, T. L. Sucharski, M. G. Tomasko, and S. D. Wall (2007b), Correlations between Cassini VIMS spectra and RADAR SAR images: Implications for Titan's surface composition and the character of the Huygens Probe Landing Site, *Planet. Space Sci.*, 55, 2025–2036, doi:10.1016/j.pss.2007.04.014.
- Soderblom, L. A., R. H. Brown, J. M. Soderblom, J. W. Barnes, R. L. Kirk, C. Sotin, R. Jaumann, D. J. MacKinnon, D. W. Mackowski, K. H. Baines, B. J. Buratti, R. N. Clark, and P. D. Nicholson (2009), The geology of Hotei Regio, Titan: Correlation of Cassini VIMS and RADAR, *Icarus*, 204, 610–618, doi:10.1016/j.icarus.2009.07.033.
- Sotin, C., R. Jaumann, B. J. Buratti, R. H. Brown, R. N. Clark, L. A. Soderblom, K. H. Baines, G. Bellucci, J. Bibring, F. Capaccioni, P. Cerroni, M. Combes, A. Coradini,

- D. P. Cruikshank, P. Drossart, V. Formisano, Y. Langevin, D. L. Matson, T. B. McCord, R. M. Nelson, P. D. Nicholson, B. Sicardy, S. Le Mouelic, S. Rodriguez, K. Stephan, and C. K. Scholz (2005), Release of volatiles from a possible cryovolcano from near-infrared imaging of Titan, *Nature*, 435, 786–789, doi:10.1038/nature03596.
- Sotin, C., K. J. Lawrence, B. Reinhardt, J. W. Barnes, R. H. Brown, A. G. Hayes, S. Le Mouélic, S. Rodriguez, J. M. Soderblom, L. A. Soderblom, K. H. Baines, B. J. Buratti, R. N. Clark, R. Jaumann, P. D. Nicholson, and K. Stephan (2012), Observations of Titan's Northern lakes at 5  $\mu\text{m}$ : Implications for the organic cycle and geology, *Icarus*, 221, 768–786, doi:10.1016/j.icarus.2012.08.017.
- Sromovsky, L. A., V. E. Suomi, J. B. Pollack, R. J. Krauss, S. S. Limaye, T. Owen, H. E. Revercomb, and C. Sagan (1981), Implications of Titan's north-south brightness asymmetry, *Nature*, 292, 698–702, doi:10.1038/292698a0.
- Stephan, K., R. Jaumann, R. H. Brown, J. M. Soderblom, L. A. Soderblom, J. W. Barnes, C. Sotin, C. A. Griffith, R. L. Kirk, K. H. Baines, B. J. Buratti, R. N. Clark, D. M. Lytle, R. M. Nelson, and P. D. Nicholson (2010), Specular reflection on Titan: Liquids in Kraken Mare, *Geophys. Res. Lett.*, 37, L07,104, doi:10.1029/2009GL042312.
- Stevens, M. H., J. S. Evans, J. Lumpe, J. H. Westlake, J. M. Ajello, E. T. Bradley, and L. W. Esposito (2015), Molecular nitrogen and methane density retrievals from Cassini UVIS dayglow observations of Titan's upper atmosphere, *Icarus*, 247, 301–312, doi:10.1016/j.icarus.2014.10.008.
- Stevenson, J., J. Lunine, and P. Clancy (2015), Membrane alternatives in worlds without oxygen: Creation of an azotosome, *Science Advances*, 1, 1400067, doi:10.1126/sciadv.1400067.

- Stiles, B. W., R. L. Kirk, R. D. Lorenz, S. Hensley, E. Lee, S. J. Ostro, M. D. Allison, P. S. Callahan, Y. Gim, L. Iess, P. Perci del Marmo, G. Hamilton, W. T. K. Johnson, R. D. West, and Cassini RADAR Team (2008), Determining Titan's Spin State from Cassini RADAR Images, *AJ*, 135, 1669–1680, doi:10.1088/0004-6256/135/5/1669.
- Stiles, B. W., S. Hensley, Y. Gim, D. M. Bates, R. L. Kirk, A. Hayes, J. Radebaugh, R. D. Lorenz, K. L. Mitchell, P. S. Callahan, et al. (2009), Determining titan surface topography from cassini sar data, *Icarus*, 202(2), 584–598.
- Stiles, B. W., R. L. Kirk, R. D. Lorenz, S. Hensley, E. Lee, S. J. Ostro, M. D. Allison, P. S. Callahan, Y. Gim, L. Iess, P. Perci del Marmo, G. Hamilton, W. T. K. Johnson, R. D. West, and Cassini RADAR Team (2010), Erratum: “Determining Titan's Spin State from Cassini Radar Images”, *AJ*, 139, 311, doi:10.1088/0004-6256/139/1/311.
- Stofan, E. R., C. Elachi, J. I. Lunine, R. D. Lorenz, B. Stiles, K. L. Mitchell, S. Ostro, L. Soderblom, C. Wood, H. Zebker, S. Wall, M. Janssen, R. Kirk, R. Lopes, F. Pa-ganelli, J. Radebaugh, L. Wye, Y. Anderson, M. Allison, R. Boehmer, P. Callahan, P. Encrenaz, E. Flamini, G. Francescetti, Y. Gim, G. Hamilton, S. Hensley, W. T. K. Johnson, K. Kelleher, D. Muhleman, P. Paillou, G. Picardi, F. Posa, L. Roth, R. Seu, S. Shaffer, S. Vetrella, and R. West (2007), The lakes of Titan, *Nature*, 445, 61–64, doi:10.1038/nature05438.
- Strobel, D. F. (1974), The Photochemistry of Hydrocarbons in the Atmosphere of Titan, *Icarus*, 21, 466–+, doi:10.1016/0019-1035(74)90149-3.
- Strobel, D. F. (1982), Chemistry and evolution of Titan's atmosphere, *Planet. Space Sci.*, 30, 839–848, doi:10.1016/0032-0633(82)90116-7.

Strobel, D. F. (2006), Gravitational tidal waves in Titan's upper atmosphere, *Icarus*, 182, 251–258, doi:10.1016/j.icarus.2005.12.015.

Strobel, D. F. (2010), Molecular hydrogen in Titan's atmosphere: Implications of the measured tropospheric and thermospheric mole fractions, *Icarus*, 208, 878–886, doi:10.1016/j.icarus.2010.03.003.

Strobel, D. F. (2012), Hydrogen and methane in Titan's atmosphere: chemistry, diffusion, escape, and the Hunten limiting flux principle (This article is part of a Special Issue that honours the work of Dr. Donald M. Hunten FRSC who passed away in December 2010 after a very illustrious career), *Canadian Journal of Physics*, 90, 795–805, doi:10.1139/p11-131.

Strobel, D. F., and J. Cui (2014), *Titan's upper atmosphere/exosphere, escape processes, and rates*, pp. 355–375.

Strobel, D. F., S. K. Atreya, B. Bézard, F. Ferri, F. M. Flasar, M. Fulchignoni, E. Lellouch, and I. Müller-Wodarg (2009), Atmospheric structure and composition, in *Titan from Cassini-Huygens*, pp. 235–257, Springer.

Tan, S. P., J. S. Kargel, and G. M. Marion (2013), Titan's atmosphere and surface liquid: New calculation using Statistical Associating Fluid Theory, *Icarus*, 222, 53–72, doi:10.1016/j.icarus.2012.10.032.

Tan, S. P., J. S. Kargel, D. E. Jennings, M. Mastrogiovanni, H. Adidharma, and G. M. Marion (2015), Titan's liquids: Exotic behavior and its implications on global fluid circulation, *Icarus*, 250, 64–75, doi:10.1016/j.icarus.2014.11.029.

Teanby, N. A., P. G. J. Irwin, R. de Kok, C. A. Nixon, A. Coustenis, B. Bézard, S. B. Calcutt, N. E. Bowles, F. M. Flasar, L. Fletcher, C. Howett, and F. W. Taylor (2006),

Latitudinal variations of HCN, HC<sub>3</sub>N, and C<sub>2</sub>N<sub>2</sub> in Titan's stratosphere derived from Cassini CIRS data, *Icarus*, 181, 243–255, doi:10.1016/j.icarus.2005.11.008.

Teanby, N. A., R. de Kok, P. G. J. Irwin, S. Osprey, S. Vinatier, P. J. Gierasch, P. L. Read, F. M. Flasar, B. J. Conrath, R. K. Achterberg, B. Bézard, C. A. Nixon, and S. B. Calcutt (2008a), Titan's winter polar vortex structure revealed by chemical tracers, *J. Geophys. Res.*, 113(E12), E12,003, doi:10.1029/2008JE003218.

Teanby, N. A., P. G. J. Irwin, R. de Kok, C. A. Nixon, A. Coustenis, E. Royer, S. B. Calcutt, N. E. Bowles, L. Fletcher, C. Howett, and F. W. Taylor (2008b), Global and temporal variations in hydrocarbons and nitriles in Titan's stratosphere for northern winter observed by Cassini/CIRS, *Icarus*, 193, 595–611, doi:10.1016/j.icarus.2007.08.017.

Teanby, N. A., P. G. J. Irwin, and R. de Kok (2010a), Compositional evidence for Titan's stratospheric tilt, *Planet. Space Sci.*, 58, 792–800, doi:10.1016/j.pss.2009.12.005.

Teanby, N. A., P. G. J. Irwin, R. de Kok, and C. A. Nixon (2010b), Seasonal Changes in Titan's Polar Trace Gas Abundance Observed by Cassini, *ApJL*, 724, L84–L89, doi: 10.1088/2041-8205/724/1/L84.

Teanby, N. A., P. G. J. Irwin, C. A. Nixon, R. de Kok, S. Vinatier, A. Coustenis, E. Sefton-Nash, S. B. Calcutt, and F. M. Flasar (2012), Active upper-atmosphere chemistry and dynamics from polar circulation reversal on Titan, *Nature*, 491, 732–735, doi:10.1038/nature11611.

Teanby, N. A., P. G. J. Irwin, C. A. Nixon, R. Courtin, B. M. Swinyard, R. Moreno, E. Lellouch, M. Rengel, and P. Hartogh (2013), Constraints on Titan's middle atmosphere ammonia abundance from Herschel/SPIRE sub-millimetre spectra, *Planet. Space Sci.*, 75, 136–147, doi:10.1016/j.pss.2012.11.008.

- Thissen, R., V. Vuitton, P. Lavvas, J. Lemaire, C. Dehon, O. Dutuit, M. A. Smith, S. Turchini, D. Catone, R. V. Yelle, P. Pernot, A. Somogyi, and M. Coreno (2009), Laboratory studies of molecular growth in the titan ionosphere, *J. Phys. Chem. A*, *113*(42), 11,211–11,220, doi:10.1021/jp9050353, pMID: 19769328.
- Tobie, G., O. Grasset, J. I. Lunine, A. Mocquet, and C. Sotin (2005), Titan's internal structure inferred from a coupled thermal-orbital model, *Icarus*, *175*, 496–502, doi:10.1016/j.icarus.2004.12.007.
- Tobie, G., J. I. Lunine, and C. Sotin (2006), Episodic outgassing as the origin of atmospheric methane on Titan, *Nature*, *440*, 61–64, doi:10.1038/nature04497.
- Tobie, G., D. Gautier, and F. Hersant (2012), Titan's Bulk Composition Constrained by Cassini-Huygens: Implication for Internal Outgassing, *ApJ*, *752*, 125, doi:10.1088/0004-637X/752/2/125.
- Tobie, G., N. A. Teanby, A. Coustenis, R. Jaumann, F. Raulin, J. Schmidt, N. Carrasco, A. J. Coates, D. Cordier, R. De Kok, W. D. Geppert, J.-P. Lebreton, A. Lefevre, T. A. Livengood, K. E. Mandt, G. Mitri, F. Nimmo, C. A. Nixon, L. Norman, R. T. Pappalardo, F. Postberg, S. Rodriguez, D. Schulze-Makuch, J. M. Soderblom, A. Solomonidou, K. Stephan, E. R. Stofan, E. P. Turtle, R. J. Wagner, R. A. West, and J. H. Westlake (2014), Science goals and mission concept for the future exploration of Titan and Enceladus, *Planet. Space Sci.*, *104*, 59–77, doi:10.1016/j.pss.2014.10.002.
- Tokano, T. (2007), Near-surface winds at the Huygens site on Titan: Interpretation by means of a general circulation model, *Planet. Space Sci.*, *55*, 1990–2009, doi:10.1016/j.pss.2007.04.011.

Tokano, T. (2008), Dune-forming winds on Titan and the influence of topography, *Icarus*, 194, 243–262, doi:10.1016/j.icarus.2007.10.007.

Tokano, T. (2009), Limnological Structure of Titan's Hydrocarbon Lakes and Its Astrobiological Implication, *Astrobiology*, 9, 147–164, doi:10.1089/ast.2007.0220.

Tokano, T. (2010a), Westward rotation of the atmospheric angular momentum vector of Titan by thermal tides, *Planet. Space Sci.*, 58, 814–829, doi:10.1016/j.pss.2010.01.001.

Tokano, T. (2010b), Relevance of fast westerlies at equinox for the eastward elongation of Titan's dunes, *Aeolian Research*, 2, 113–127.

Tokano, T. (2014), Non-uniform global methane distribution in Titan's troposphere evidenced by Cassini radio occultations, *Icarus*, 231, 1–12, doi:10.1016/j.icarus.2013.11.030.

Tokano, T., and R. D. Lorenz (2016), Sun-stirred Kraken Mare: Circulation in Titan's seas induced by solar heating and methane precipitation, *Icarus*, 270, 67–84, doi:10.1016/j.icarus.2015.08.033.

Tokano, T., and F. M. Neubauer (2005), Wind-induced seasonal angular momentum exchange at Titan's surface and its influence on Titan's length-of-day, *Geophys. Res. Lett.*, 32, L24203, doi:10.1029/2005GL024456.

Tokano, T., F. M. Neubauer, M. Laube, and C. P. McKay (1999), Seasonal variation of Titan's atmospheric structuresimulated by a general circulation model, *Planet. Space Sci.*, 47, 493–520, doi:10.1016/S0032-0633(99)00011-2.

Tokano, T., F. Ferri, G. Colombatti, T. Mäkinen, and M. Fulchignoni (2006a), Titan's planetary boundary layer structure at the Huygens landing site, *Journal of Geophysical Research (Planets)*, 111, E08007, doi:10.1029/2006JE002704.

Tokano, T., C. P. McKay, F. M. Neubauer, S. K. Atreya, F. Ferri, M. Fulchignoni, and H. B. Niemann (2006b), Methane drizzle on Titan, *Nature*, *442*, 432–435, doi: 10.1038/nature04948.

Tokano, T., T. Van Hoolst, and Ö. Karatekin (2011), Polar motion of Titan forced by the atmosphere, *Journal of Geophysical Research (Planets)*, *116*, E05002, doi: 10.1029/2010JE003758.

Tokano, T., R. D. Lorenz, and T. Van Hoolst (2014), Numerical simulation of tides and oceanic angular momentum of Titan's hydrocarbon seas, *Icarus*, *242*, 188–201, doi: 10.1016/j.icarus.2014.08.021.

Tomasko, M. G. (1980), Preliminary results of polarimetry and photometry of Titan at large phase angles from Pioneer 11, *J. Geophys. Res.*, *85*, 5937–5942, doi: 10.1029/JA085iA11p05937.

Tomasko, M. G., and P. H. Smith (1982), Photometry and polarimetry of Titan - Pioneer 11 observations and their implications for aerosol properties, *Icarus*, *51*, 65–95, doi: 10.1016/0019-1035(82)90030-6.

Tomasko, M. G., B. Archinal, T. Becker, B. Bézard, M. Bushroe, M. Combes, D. Cook, A. Coustenis, C. de Bergh, L. E. Dafoe, L. Doose, S. Douté, A. Eibl, S. Engel, F. Gliem, B. Grieger, K. Holso, E. Howington-Kraus, E. Karkoschka, H. U. Keller, R. Kirk, R. Kramm, M. Küppers, P. Lanagan, E. Lellouch, M. Lemmon, J. Lunine, E. McFarlane, J. Moores, G. M. Prout, B. Rizk, M. Rosiek, P. Rueffer, S. E. Schröder, B. Schmitt, C. See, P. Smith, L. Soderblom, N. Thomas, and R. West (2005), Rain, winds and haze during the Huygens probe's descent to Titan's surface, *Nature*, *438*, 765–778, doi: 10.1038/nature04126.

Tomasko, M. G., L. Doose, S. Engel, L. E. Dafoe, R. West, M. Lemmon, E. Karkoschka, and C. See (2008), A model of Titan's aerosols based on measurements made inside the atmosphere, *Planet. Space Sci.*, 56, 669–707, doi:10.1016/j.pss.2007.11.019.

Tomasko, M. G., L. R. Doose, L. E. Dafoe, and C. See (2009), Limits on the size of aerosols from measurements of linear polarization in Titan's atmosphere, *Icarus*, 204, 271–283, doi:10.1016/j.icarus.2009.05.034.

Toon, O. B., C. P. McKay, C. A. Griffith, and R. P. Turco (1992), A physical model of Titan's aerosols, *Icarus*, 95, 24–53, doi:10.1016/0019-1035(92)90188-D.

Toublanc, D., J. P. Parisot, J. Brillet, D. Gautier, F. Raulin, and C. P. McKay (1995), Photochemical modeling of Titan's atmosphere, *Icarus*, 113, 2–26, doi:10.1006/icar.1995.1002.

Trafton, L. (1972a), On the Possible Detection of H<sub>2</sub> in Titan's Atmosphere, *ApJ*, 175, 285–+, doi:10.1086/151556.

Trafton, L. (1972b), The Bulk Composition of Titan's Atmosphere, *ApJ*, 175, 295–+, doi:10.1086/151557.

Trafton, L. (1975), The morphology of Titan's methane bands. I - Comparison with a reflecting layer model, *ApJ*, 195, 805–814, doi:10.1086/153385.

Trainer, M. G., J. L. Jimenez, Y. L. Yung, O. B. Toon, and M. A. Tolbert (2012), Nitrogen Incorporation in CH<sub>4</sub>-N<sub>2</sub> Photochemical Aerosol Produced by Far Ultraviolet Irradiation, *Astrobiology*, 12, 315–326, doi:10.1089/ast.2011.0754.

Trainer, M. G., J. A. Sebree, Y. H. Yoon, and M. A. Tolbert (2013), The Influence of Benzene as a Trace Reactant in Titan Aerosol Analogs, *ApJL*, 766, L4, doi:10.1088/2041-8205/766/1/L4.

Tran, B. N., J. P. Ferris, and J. J. Chera (2003), The photochemical formation of a titan haze analog. Structural analysis by x-ray photoelectron and infrared spectroscopy, *Icarus*, 162, 114–124, doi:10.1016/S0019-1035(02)00069-6.

Tsai, I.-C., M.-C. Liang, and J.-P. Chen (2012), Methane-Nitrogen Binary Nucleation: A New Microphysical Mechanism for Cloud Formation in Titan's Atmosphere, *ApJ*, 747, 36, doi:10.1088/0004-637X/747/1/36.

Turtle, E. P. (2016), Personal Communication.

Turtle, E. P., J. E. Perry, A. S. McEwen, A. D. Del Genio, J. Barbara, R. A. West, D. D. Dawson, and C. C. Porco (2009), Cassini imaging of Titan's high-latitude lakes, clouds, and south-polar surface changes, *Geophys. Res. Lett.*, 36, L02,204, doi: 10.1029/2008GL036186.

Turtle, E. P., A. D. Del Genio, J. M. Barbara, J. E. Perry, E. L. Schaller, A. S. McEwen, R. A. West, and T. L. Ray (2011a), Seasonal changes in Titan's meteorology, *Geophys. Res. Lett.*, 38, L03,203, doi:10.1029/2010GL046266.

Turtle, E. P., J. E. Perry, A. G. Hayes, R. D. Lorenz, J. W. Barnes, A. S. McEwen, R. A. West, A. D. Del Genio, J. M. Barbara, J. I. Lunine, E. L. Schaller, T. L. Ray, R. M. C. Lopes, and E. R. Stofan (2011b), Rapid and Extensive Surface Changes Near Titan's Equator: Evidence of April Showers, *Science*, 331, 1414–1417, doi: 10.1126/science.1201063.

Van Hoolst, T., N. Rambaux, Ö. Karatekin, and R.-M. Baland (2009), The effect of gravitational and pressure torques on Titan's length-of-day variations, *Icarus*, 200, 256–264, doi:10.1016/j.icarus.2008.11.009.

- Vasavada, A. R., S. M. Hörst, M. R. Kennedy, A. P. Ingersoll, C. C. Porco, A. D. Del Genio, and R. A. West (2006), Cassini imaging of Saturn: Southern hemisphere winds and vortices, *Journal of Geophysical Research (Planets)*, 111, E05004, doi: 10.1029/2005JE002563.
- Vervack, R. J., B. R. Sandel, and D. F. Strobel (2004), New perspectives on Titan's upper atmosphere from a reanalysis of the Voyager 1 UVS solar occultations, *Icarus*, 170, 91–112, doi:10.1016/j.icarus.2004.03.005.
- Veretka, J. (1973), Titan: Polarimetric Evidence for an Optically Thick Atmosphere, *Icarus*, 18, 657–+, doi:10.1016/0019-1035(73)90069-9.
- Vinatier, S., B. Bézard, T. Fouchet, N. A. Teanby, R. de Kok, P. G. J. Irwin, B. J. Conrath, C. A. Nixon, P. N. Romani, F. M. Flasar, and A. Coustenis (2007), Vertical abundance profiles of hydrocarbons in Titan's atmosphere at 15° S and 80° N retrieved from Cassini/CIRS spectra, *Icarus*, 188, 120–138, doi:10.1016/j.icarus.2006.10.031.
- Vinatier, S., B. Bézard, C. A. Nixon, A. Mamoutkine, R. C. Carlson, D. E. Jennings, E. A. Guandique, N. A. Teanby, G. L. Bjoraker, F. M. Flasar, and V. G. Kunde (2010a), Analysis of Cassini/CIRS limb spectra of Titan acquired during the nominal mission. I. Hydrocarbons, nitriles and CO<sub>2</sub> vertical mixing ratio profiles, *Icarus*, 205, 559–570, doi:10.1016/j.icarus.2009.08.013.
- Vinatier, S., B. Bézard, R. de Kok, C. M. Anderson, R. E. Samuelson, C. A. Nixon, A. Mamoutkine, R. C. Carlson, D. E. Jennings, E. A. Guandique, G. L. Bjoraker, F. Michael Flasar, and V. G. Kunde (2010b), Analysis of Cassini/CIRS limb spectra of Titan acquired during the nominal mission II: Aerosol extinction profiles in the 600-1420 cm<sup>-1</sup> spectral range, *Icarus*, 210, 852–866, doi:10.1016/j.icarus.2010.06.024.

Vinatier, S., P. Rannou, C. M. Anderson, B. Bézard, R. de Kok, and R. E. Samuelson (2012), Optical constants of Titan's stratospheric aerosols in the 70-1500 cm<sup>-1</sup> spectral range constrained by Cassini/CIRS observations, *Icarus*, 219, 5–12, doi: 10.1016/j.icarus.2012.02.009.

Vinatier, S., B. Bézard, S. Lebonnois, N. A. Teanby, R. K. Achterberg, N. Gorius, A. Mamoutkine, E. Guandique, A. Jolly, D. E. Jennings, and F. M. Flasar (2015), Seasonal variations in Titan's middle atmosphere during the northern spring derived from Cassini/CIRS observations, *Icarus*, 250, 95–115, doi:10.1016/j.icarus.2014.11.019.

Vixie, G., J. W. Barnes, B. Jackson, S. Rodriguez, S. Le Mouélic, C. Sotin, S. MacKenzie, and P. Wilson (2015), Possible temperate lakes on Titan, *Icarus*, 257, 313–323, doi: 10.1016/j.icarus.2015.05.009.

Vuitton, V., R. V. Yelle, and M. J. McEwan (2007), Ion chemistry and N-containing molecules in Titan's upper atmosphere, *Icarus*, 191, 722–742, doi: 10.1016/j.icarus.2007.06.023.

Vuitton, V., R. V. Yelle, and J. Cui (2008), Formation and distribution of benzene on Titan, *J. Geophys. Res.*, 113(E12), 5007–+, doi:10.1029/2007JE002997.

Vuitton, V., P. Lavvas, R. V. Yelle, M. Galand, A. Wellbrock, G. R. Lewis, A. J. Coates, and J. Wahlund (2009a), Negative ion chemistry in Titan's upper atmosphere, *Planet. Space Sci.*, 57, 1558–1572, doi:10.1016/j.pss.2009.04.004.

Vuitton, V., B. N. Tran, P. D. Persans, and J. P. Ferris (2009b), Determination of the complex refractive indices of Titan haze analogs using photothermal deflection spectroscopy, *Icarus*, 203, 663–671, doi:10.1016/j.icarus.2009.04.016.

Vuitton, V., R. V. Yelle, P. Lavvas, and S. J. Klippenstein (2012), Rapid Association Reactions at Low Pressure: Impact on the Formation of Hydrocarbons on Titan, *ApJ*, 744, 11, doi:10.1088/0004-637X/744/1/11.

Vuitton, V., O. Dutuit, M. A. Smith, and N. Balucani (2014), *Chemistry of Titan's Atmosphere*, pp. 224–271.

Wahlund, J.-E., R. Boström, G. Gustafsson, D. A. Gurnett, W. S. Kurth, A. Pedersen, T. F. Averkamp, G. B. Hospodarsky, A. M. Persoon, P. Canu, F. M. Neubauer, M. K. Dougherty, A. I. Eriksson, M. W. Morooka, R. Gill, M. André, L. Eliasson, and I. Müller-Wodarg (2005), Cassini Measurements of Cold Plasma in the Ionosphere of Titan, *Science*, 308, 986–989, doi:10.1126/science.1109807.

Wahlund, J.-E., M. Galand, I. Müller-Wodarg, J. Cui, R. V. Yelle, F. J. Crary, K. Mandt, B. Magee, J. H. Waite, D. T. Young, A. J. Coates, P. Garnier, K. Ågren, M. André, A. I. Eriksson, T. E. Cravens, V. Vuitton, D. A. Gurnett, and W. S. Kurth (2009), On the amount of heavy molecular ions in Titan's ionosphere, *Planet. Space Sci.*, 57, 1857–1865, doi:10.1016/j.pss.2009.07.014.

Waite, J. H., D. T. Young, T. E. Cravens, A. J. Coates, F. J. Crary, B. Magee, and J. Westlake (2007), The Process of Tholin Formation in Titan's Upper Atmosphere, *Science*, 316, 870–, doi:10.1126/science.1139727.

Waite, J. H., Jr., W. S. Lewis, B. A. Magee, J. I. Lunine, W. B. McKinnon, C. R. Glein, O. Mousis, D. T. Young, T. Brockwell, J. Westlake, M.-J. Nguyen, B. D. Teolis, H. B. Niemann, R. L. McNutt, M. Perry, and W.-H. Ip (2009), Liquid water on Enceladus from observations of ammonia and  $^{40}\text{Ar}$  in the plume, *Nature*, 460, 487–490, doi:10.1038/nature08153.

- Wall, S. D., R. M. Lopes, E. R. Stofan, C. A. Wood, J. L. Radebaugh, S. M. Hörst, B. W. Stiles, R. M. Nelson, L. W. Kamp, M. A. Janssen, R. D. Lorenz, J. I. Lunine, T. G. Farr, G. Mitri, P. Paillou, F. Paganelli, and K. L. Mitchell (2009), Cassini RADAR images at Hotei Arcus and western Xanadu, Titan: Evidence for geologically recent cryovolcanic activity, *Geophys. Res. Lett.*, 36, L04,203, doi:10.1029/2008GL036415.
- Wang, C. C., S. K. Atreya, and R. Signorell (2010), Evidence for layered methane clouds in Titan's troposphere, *Icarus*, 206, 787–790, doi:10.1016/j.icarus.2009.11.022.
- Wang, P., and J. L. Mitchell (2014), Planetary ageostrophic instability leads to superrotation, *Geophys. Res. Lett.*, 41, 4118–4126, doi:10.1002/2014GL060345.
- Webster, C. R., P. R. Mahaffy, G. J. Flesch, P. B. Niles, J. H. Jones, L. A. Leshin, S. K. Atreya, J. C. Stern, L. E. Christensen, T. Owen, H. Franz, R. O. Pepin, A. Steele, and aff9 (2013), Isotope Ratios of H, C, and O in CO<sub>2</sub> and H<sub>2</sub>O of the Martian Atmosphere, *Science*, 341, 260–263, doi:10.1126/science.1237961.
- West, R., P. Rannou, P. Lavvas, B. Seignovert, E. P. Turtle, J. Perry, A. Ovanessian, and M. Roy (2016a), The disappearance and reappearance of Titan's detached haze layer, in *AAS/Division for Planetary Sciences Meeting Abstracts*, *AAS/Division for Planetary Sciences Meeting Abstracts*, vol. 48, p. 515.06.
- West, R. A. (1991), Optical properties of aggregate particles whose outer diameter is comparable to the wavelength, *App. Optics*, 30, 5316–5324, doi:10.1364/AO.30.005316.
- West, R. A., and P. H. Smith (1991), Evidence for aggregate particles in the atmospheres of Titan and Jupiter, *Icarus*, 90, 330–333, doi:10.1016/0019-1035(91)90113-8.
- West, R. A., H. Hart, K. E. Simmons, C. W. Hord, L. W. Esposito, A. L. Lane, R. B. Pomphrey, D. L. Coffeen, and M. Sato (1983), Voyager 2 photopolarimeter observations

- of Titan, *J. Geophys. Res.*, 88, 8699–8708, doi:10.1029/JA088iA11p08699.
- West, R. A., J. Balloch, P. Dumont, P. Lavvas, R. Lorenz, P. Rannou, T. Ray, and E. P. Turtle (2011), The evolution of Titan's detached haze layer near equinox in 2009, *Geophys. Res. Lett.*, 38, L06,204, doi:10.1029/2011GL046843.
- West, R. A., P. Lavvas, C. Anderson, and K. Imanaka (2014), *Titan's haze*, pp. 285–321.
- West, R. A., A. D. Del Genio, J. M. Barbara, D. Toledo, P. Lavvas, P. Rannou, E. P. Turtle, and J. Perry (2016b), Cassini Imaging Science Subsystem observations of Titan's south polar cloud, *Icarus*, 270, 399–408, doi:10.1016/j.icarus.2014.11.038.
- Westlake, J. H., J. M. Bell, J. H. Waite, Jr., R. E. Johnson, J. G. Luhmann, K. E. Mandt, B. A. Magee, and A. M. Rymer (2011), Titan's thermospheric response to various plasma environments, *Journal of Geophysical Research (Space Physics)*, 116, A03318, doi:10.1029/2010JA016251.
- Westlake, J. H., J. H. Waite, Jr., K. E. Mandt, N. Carrasco, J. M. Bell, B. A. Magee, and J.-E. Wahlund (2012), Titan's ionospheric composition and structure: Photochemical modeling of Cassini INMS data, *Journal of Geophysical Research (Planets)*, 117, E01003, doi:10.1029/2011JE003883.
- Williams, K. E., C. P. McKay, and F. Persson (2012), The surface energy balance at the Huygens landing site and the moist surface conditions on Titan, *Planet. Space Sci.*, 60, 376–385, doi:10.1016/j.pss.2011.11.005.
- Wilson, E. H., and S. K. Atreya (2003), Chemical sources of haze formation in Titan's atmosphere, *Planet. Space Sci.*, 51, 1017–1033, doi:10.1016/j.pss.2003.06.003.
- Wilson, E. H., and S. K. Atreya (2004), Current state of modeling the photochemistry of Titan's mutually dependent atmosphere and ionosphere, *J. Geophys. Res.*, 109, 6002–+, doi:10.1029/2003JE002622.

doi:10.1029/2003JE002181.

Wong, A.-S., C. G. Morgan, Y. L. Yung, and T. Owen (2002), Evolution of CO on Titan,

*Icarus*, 155, 382–392, doi:10.1006/icar.2001.6720.

Wong, M. H., S. K. Atreya, P. N. Mahaffy, H. B. Franz, C. Malespin, M. G. Trainer, J. C.

Stern, P. G. Conrad, H. L. K. Manning, R. O. Pepin, R. H. Becker, C. P. McKay, T. C.

Owen, R. Navarro-González, J. H. Jones, B. M. Jakosky, and A. Steele (2013), Isotopes

of nitrogen on Mars: Atmospheric measurements by Curiosity's mass spectrometer,

*Geophys. Res. Lett.*, 40, 6033–6037, doi:10.1002/2013GL057840.

Wood, C. A., R. Lorenz, R. Kirk, R. Lopes, K. Mitchell, E. Stofan, and Cassini

RADAR Team (2010), Impact craters on Titan, *Icarus*, 206, 334–344, doi:

10.1016/j.icarus.2009.08.021.

Wye, L. C., H. A. Zebker, and R. D. Lorenz (2009), Smoothness of Titan's Ontario

Lacus: Constraints from Cassini RADAR specular reflection data, *Geophys. Res. Lett.*,

36, L16201, doi:10.1029/2009GL039588.

Yelle, R. V. (1991), Non-LTE models of Titan's upper atmosphere, *ApJ*, 383, 380–400,

doi:10.1086/170796.

Yelle, R. V., J. Cui, and I. C. F. Müller-Wodarg (2008), Methane escape from Titan's

atmosphere, *J. Geophys. Res.*, 113(E12), 10,003–+, doi:10.1029/2007JE003031.

Yelle, R. V., V. Vuitton, P. Lavvas, S. J. Klippenstein, M. A. Smith, S. M. Hörlst, and

J. Cui (2010), Formation of NH<sub>3</sub> and CH<sub>2</sub>NH in Titan's upper atmosphere, *Faraday*

*Discuss.*, 147, 31–49, doi:10.1039/C004787M.

Yelle, R. V., D. S. Snowden, and I. C. F. Müller-Wodarg (2014), *Titan's upper atmosphere:*

*thermal structure, dynamics, and energetics*, pp. 322–354.

- Yoon, Y. H., S. M. Hörst, R. K. Hicks, R. Li, J. A. de Gouw, and M. A. Tolbert (2014), The role of benzene photolysis in Titan haze formation, *Icarus*, 233, 233–241, doi: 10.1016/j.icarus.2014.02.006.
- Yung, Y. L. (1987), An update of nitrile photochemistry on Titan, *Icarus*, 72, 468–472, doi:10.1016/0019-1035(87)90186-2.
- Yung, Y. L., M. Allen, and J. P. Pinto (1984), Photochemistry of the atmosphere of Titan - Comparison between model and observations, *ApJ*, 55, 465–506, doi:10.1086/190963.
- Zalucha, A., A. Fitzsimmons, J. L. Elliot, J. Thomas-Osip, H. B. Hammel, V. S. Dhillon, T. R. Marsh, F. W. Taylor, and P. G. J. Irwin (2007), The 2003 November 14 occultation by Titan of TYC 1343-1865-1. II. Analysis of light curves, *Icarus*, 192, 503–518, doi: 10.1016/j.icarus.2007.08.008.
- Zarnecki, J. C., M. R. Leese, B. Hathi, A. J. Ball, A. Hagermann, M. C. Towner, R. D. Lorenz, J. A. M. McDonnell, S. F. Green, M. R. Patel, T. J. Ringrose, P. D. Rosenberg, K. R. Atkinson, M. D. Paton, M. Banaszkiewicz, B. C. Clark, F. Ferri, M. Fulchignoni, N. A. L. Ghafoor, G. Kargl, H. Svedhem, J. Delderfield, M. Grande, D. J. Parker, P. G. Challenor, and J. E. Geake (2005), A soft solid surface on Titan as revealed by the Huygens Surface Science Package, *Nature*, 438, 792–795, doi:10.1038/nature04211.
- Zebker, H., A. Hayes, M. Janssen, A. Le Gall, R. Lorenz, and L. Wye (2014), Surface of Ligeia Mare, Titan, from Cassini altimeter and radiometer analysis, *Geophys. Res. Lett.*, 41, 308–313, doi:10.1002/2013GL058877.
- Zellner, B. (1973), The Polarization of Titan, *Icarus*, 18, 661–+, doi:10.1016/0019-1035(73)90070-5.

Zhou, L., W. Zheng, R. I. Kaiser, A. Landera, A. M. Mebel, M.-C. Liang, and Y. L. Yung  
(2010), Cosmic-ray-mediated Formation of Benzene on the Surface of Saturn's Moon  
Titan, *ApJ*, 718, 1243–1251, doi:10.1088/0004-637X/718/2/1243.

Zhu, X. (2006), Maintenance of equatorial superrotation in the atmospheres of Venus and  
Titan, *Planet. Space Sci.*, 54, 761–773, doi:10.1016/j.pss.2006.05.004.

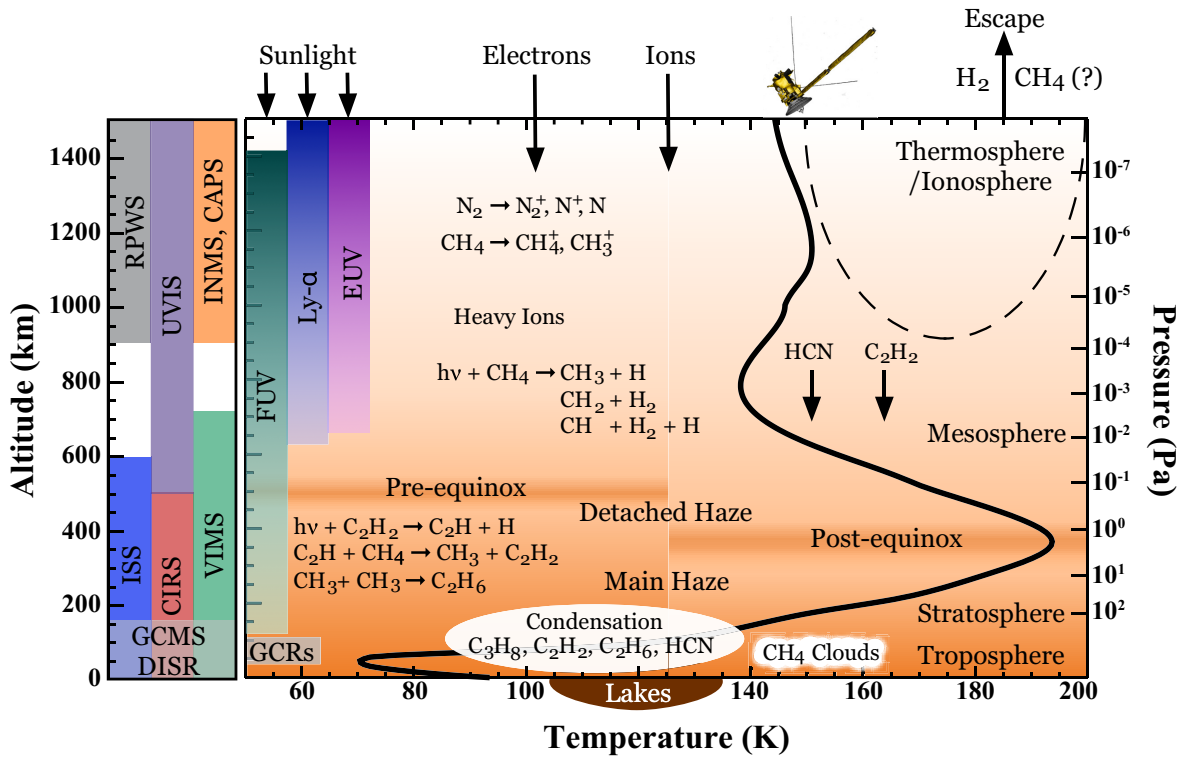


**Figure 1.** Shown here is a representative temperature profile for Titan's atmosphere, some of the major chemical processes, and the approximate altitude coverage of the instruments carried by Cassini-Huygens.

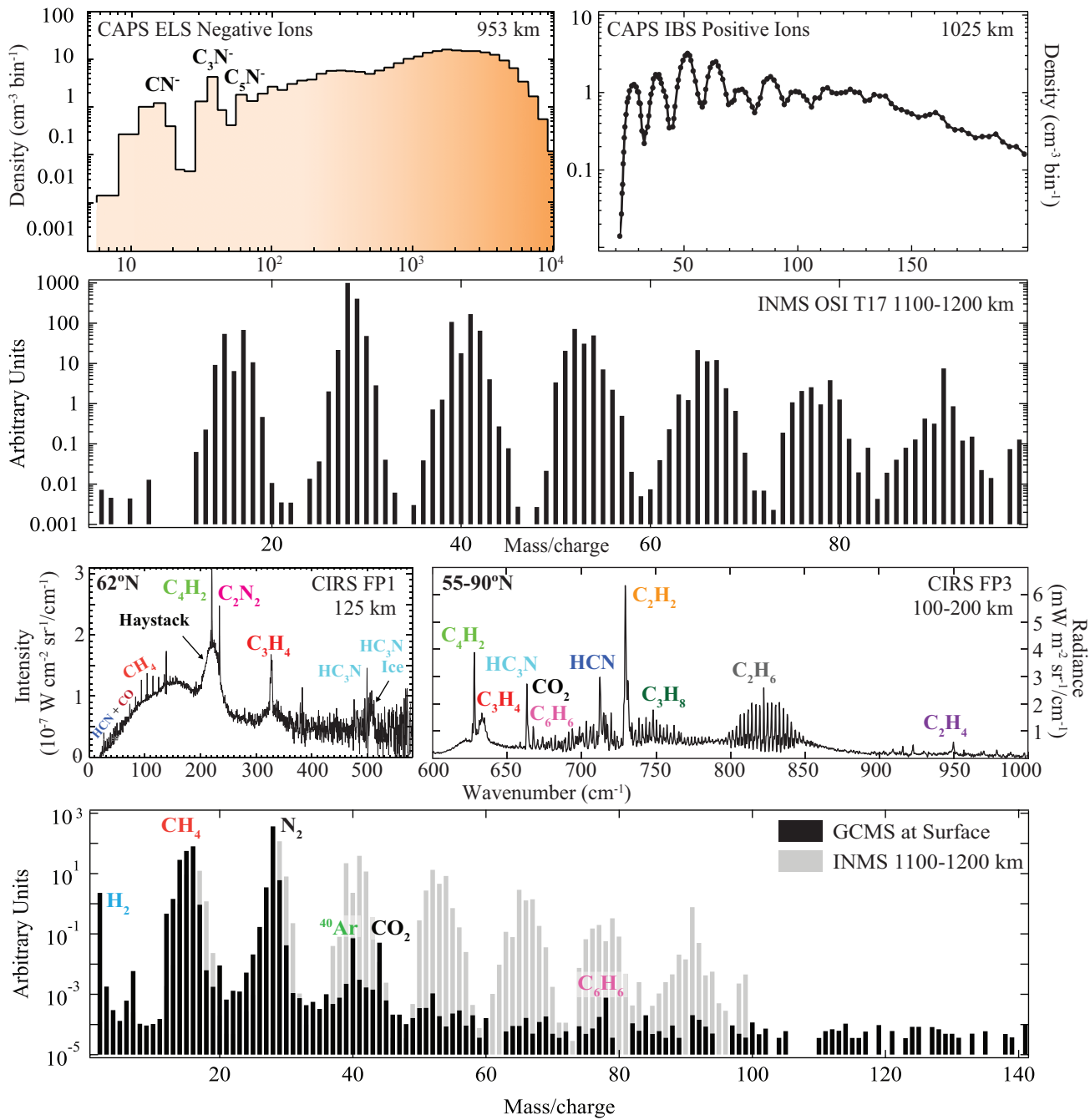


**Figure 2.** The wealth of *in situ* and remote sensing measurements of the composition of Titan's atmosphere from Cassini-Huygens allow us to understand the atmosphere as a system. Shown here are measurements of the thermosphere/ionosphere from CAPS ELS (top left, adapted from *Coates et al.* [2007]; *Vuitton et al.* [2009a]) and IBS (top right, adapted from *Crary et al.* [2009]) and INMS. CIRS measurements of the stratosphere reveal the composition of ices and gases (FP1 data adapted from *Anderson et al.* [2014], FP3 data adapted from *Bézard* [2009]). Measurements from the GCMS in Titan's troposphere (bottom, adapted from *Niemann et al.* [2010]) reveal that many of the trace gases produced in the thermosphere are lost to subsequent chemistry and condensation before reaching the surface.

	Production	Loss
	<b>Hydrogen (<math>H_2</math>)</b> $CH_4$ photolysis	Escape
	<b>Carbon Monoxide (<math>CO</math>)</b> $O(^3P) + CH_3 \rightarrow H_2CO + H$ $H_2CO + h\nu \rightarrow CO + H_2/2H$	$CO + OH \rightarrow CO_2 + H$
	<b>Ethane (<math>C_2H_6</math>)</b> $CH_3 + CH_3 + M \rightarrow C_2H_6 + M$	Condensation
	<b>Acetylene (<math>C_2H_2</math>)</b> $C_2H + CH_4 \rightarrow C_2H_2 + H_2$	$C_2H_2 + h\nu \rightarrow C_2H + H$ Condensation
	<b>Propane (<math>C_3H_8</math>)</b> $CH_3 + C_2H_5 + M \rightarrow C_3H_8 + M$	Condensation
	<b>Ethylene (<math>C_2H_4</math>)</b> $CH + CH_4 \rightarrow C_2H_4 + H$ $^3CH_2 + CH_3 \rightarrow C_2H_4 + H$	$C_2H_4 + h\nu \rightarrow C_2H_2 + H_2/2H$
	<b>Hydrogen Cyanide (<math>HCN</math>)</b> $N(^4S) + CH_3 \rightarrow H_2CN + H$ $H_2CN + H \rightarrow HCN + H_2$	Condensation
	<b>Carbon Dioxide (<math>CO_2</math>)</b> $CO + OH \rightarrow CO_2 + H$	Condensation
	<b>Methylacetylene (<math>CH_3CCH</math>)</b> $CH + C_2H_4 \rightarrow C_3H_4 + H$	$C_3H_4 + h\nu \rightarrow C_3H_3 + H$ $H + CH_3CCH \rightarrow C_3H_5$
	<b>Diacetylene (<math>C_4H_2</math>)</b> $C_2H + C_2H_2 \rightarrow C_4H_2 + H$	$C_4H_2 + h\nu \rightarrow C_4H + H$

**Figure 3.** Shown here are the 10 most abundant photochemically generated molecules in Titan's equatorial stratosphere in approximately decreasing order of abundance with their major atmospheric production and loss pathways listed (see e.g., *Vuitton et al. [2014]*).

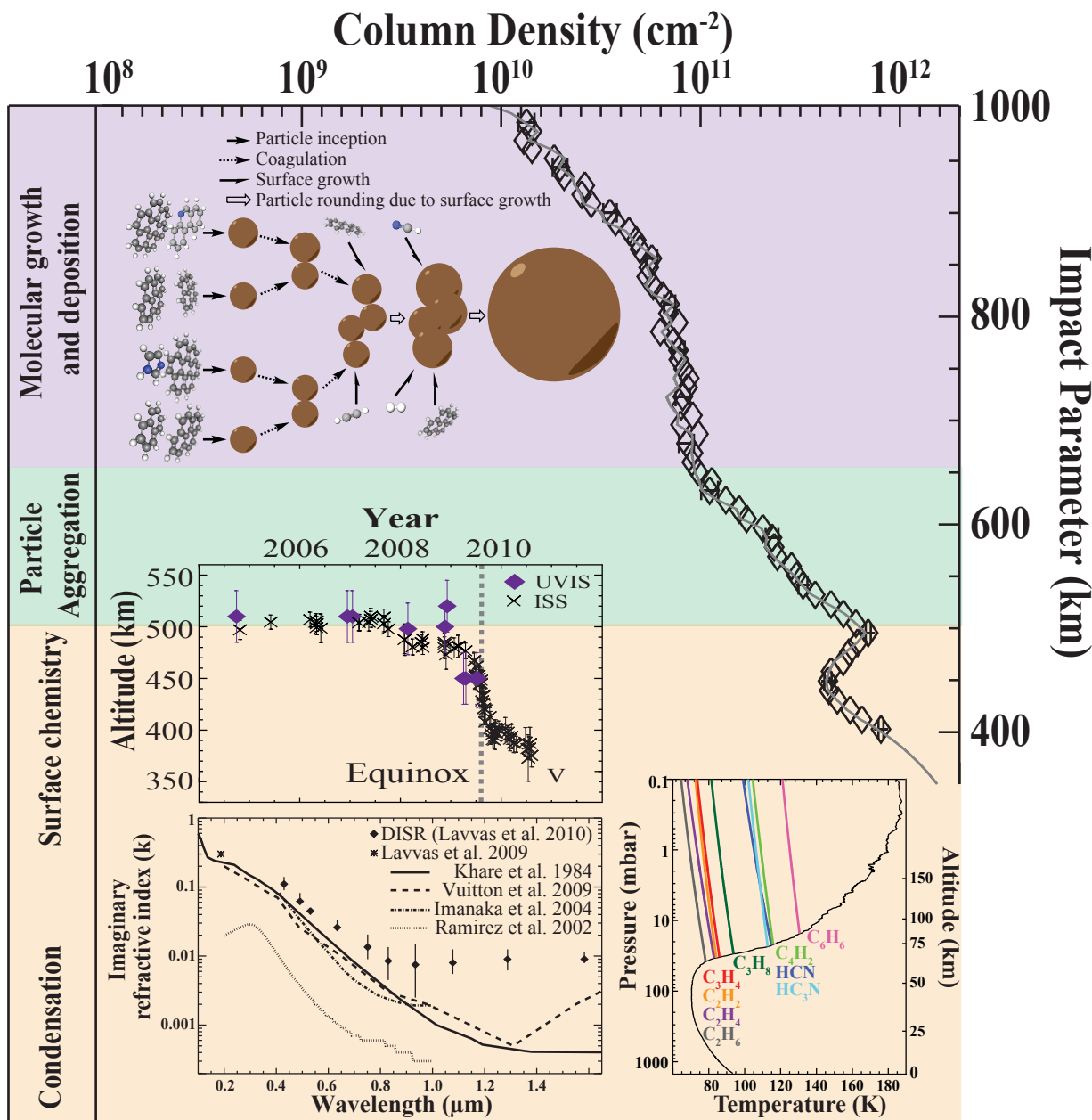


**Figure 4.** Cassini revealed the presence of particles in Titan's atmosphere from the surface to the ionosphere. The column density from 400 to 1000 km is shown here (assuming a constant particle size, radius=12.5 nm, with altitude; particle size changes with altitude in Titan's atmosphere) and the detached haze layer is a prominent feature (adapted from *Koskinen et al.* [2011]). Shown at the top is a model of particle inception and growth from *Lavvas et al.* [2011b]. The model divides Titan's atmosphere into 3 broad regions to explain how particles evolve as they descend through Titan's atmosphere; note that these regions refer to the dominant process in each region but the processes happen over a larger altitude range. Deep in the atmosphere, they may serve as nucleation sites for condensation and the plot at the bottom right shows where vapor pressure curves for a number of species cross the temperature profile at the Huygens landing site (adapted from *Lavvas et al.* [2011c]). A comparison of DISR measurements of Titan's aerosol particles to laboratory analogues is shown bottom left (adapted from *Lavvas et al.* [2010]). The detached haze layer changes altitude as a function of season as shown in the middle plot (adapted from *West et al.* [2011]; *Koskinen et al.* [2011]).

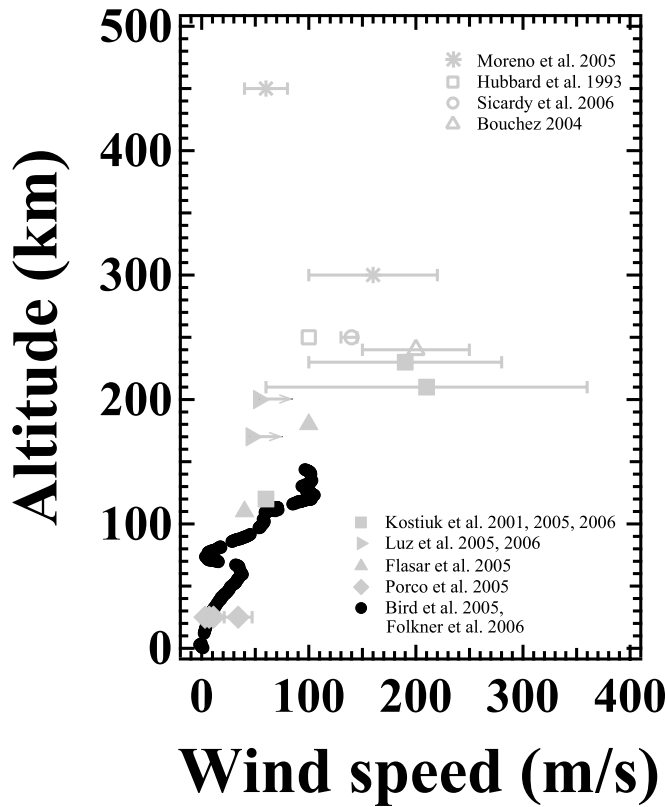


**Figure 5.** Measurements from various techniques reveal that wind speeds are relatively low in the troposphere but in the stratosphere there are superrotating winds. Black circles are the measurements from the Doppler Wind Experiment (DWE) [Bird *et al.*, 2005; Folkner *et al.*, 2006]. Cloud tracking measurements from [Porco *et al.*, 2005] are shown as filled diamonds; the altitude for these clouds is not well constrained and shown here is a presumed upper limit. The measurements made from doppler shifts in the emission lines of atmospheric constituents are shown as filled squares [Kostiuk *et al.*, 2001, 2005, 2006], filled right pointing triangles (arrows indicate these measurements are lower limits) [Luz *et al.*, 2005, 2006], and asterisks [Moreno *et al.*, 2005]. Hubbard *et al.* [1993] (open square), Sicardy *et al.* [2006] (open circle), and Bouchez [2004] (open triangle) used stellar occultations to estimate the stratospheric wind speeds. Wind speeds calculated from the thermal wind equation using Cassini CIRS temperature measurements near the Huygens' landing site are shown as triangles [Flasar *et al.*, 2005]. Note that although there is some spatial and temporal overlap, this plot does not necessarily represent a snapshot of Titan's atmosphere at one place and time.

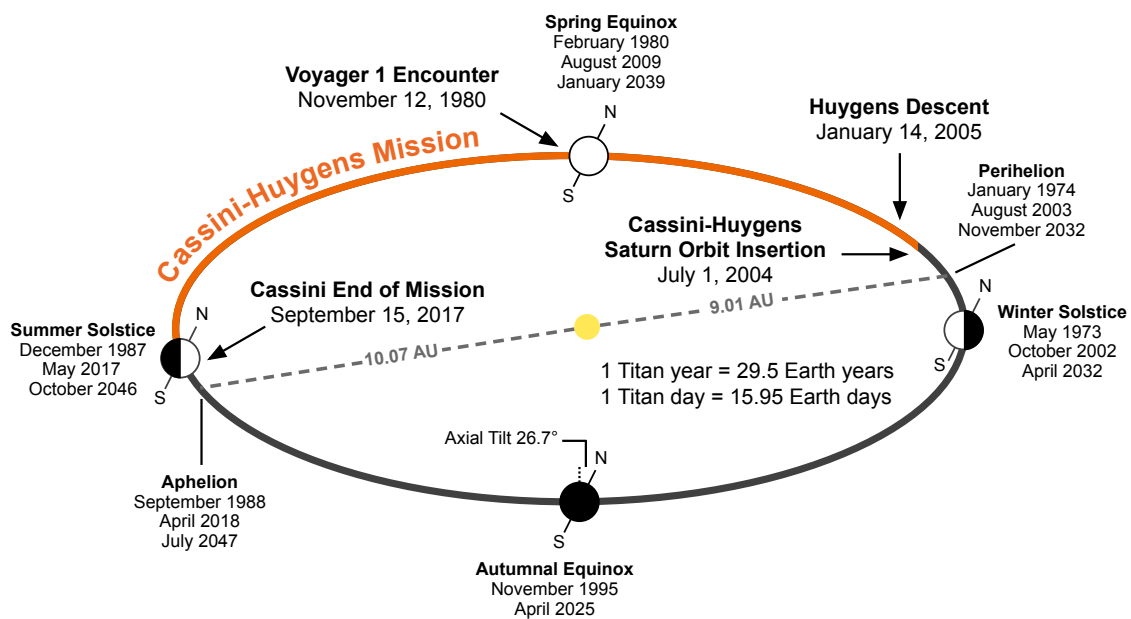


**Figure 6.** Shown here is schematic of Titan's orbit, which notes the length and timing of the Cassini-Huygens mission.

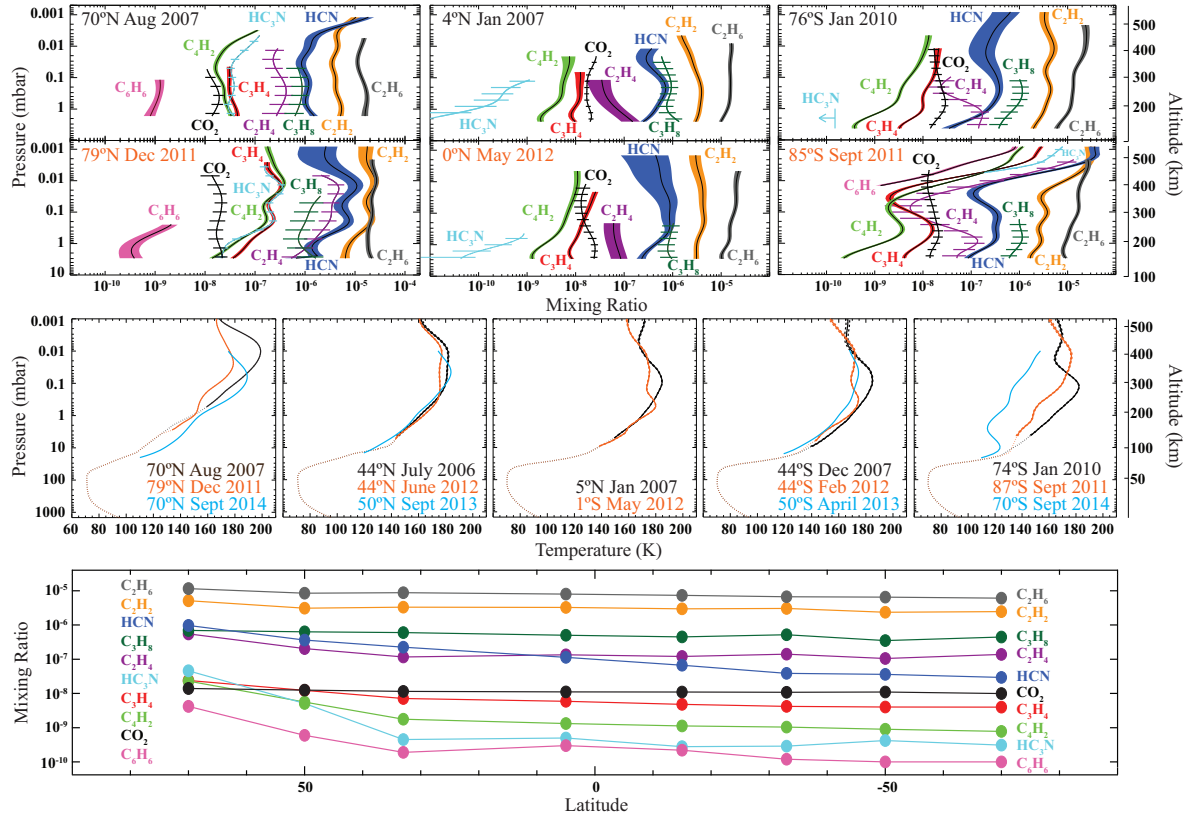


**Figure 7.** This compilation of Cassini CIRS measurements adapted from *Coustenis et al.* [2010], *Vinatier et al.* [2015], and *Coustenis et al.* [2016] shows variations in stratospheric composition and temperature with latitude and season. The top panels compare limb composition measurements at northern, equatorial, and southern latitudes before and after the August 2009 equinox (with the exception of the south pole which shows that the significant changes on composition happen post-equinox) [*Vinatier et al.*, 2015]. The middle panel shows the evolution of temperature with season and compares temperature profiles near 70°N, 44°N, the equator, 44°S, and the south pole [*Vinatier et al.*, 2015; *Coustenis et al.*, 2016]. The bottom panel shows the CIRS nadir measurements (with contribution function peaks near ~5-10 mbar) from 2004 to 2008 demonstrating the significant north (winter) polar enrichment of short lived species [*Coustenis et al.*, 2010]. For the top and middle panels, the altitude scale is from the equatorial measurements; pressure is the relevant coordinate and applies to all panels. For the temperature profiles, the dashed line indicates regions of the atmosphere where CIRS limb measurements do not constrain the temperature (see *Vinatier et al.* [2015]).

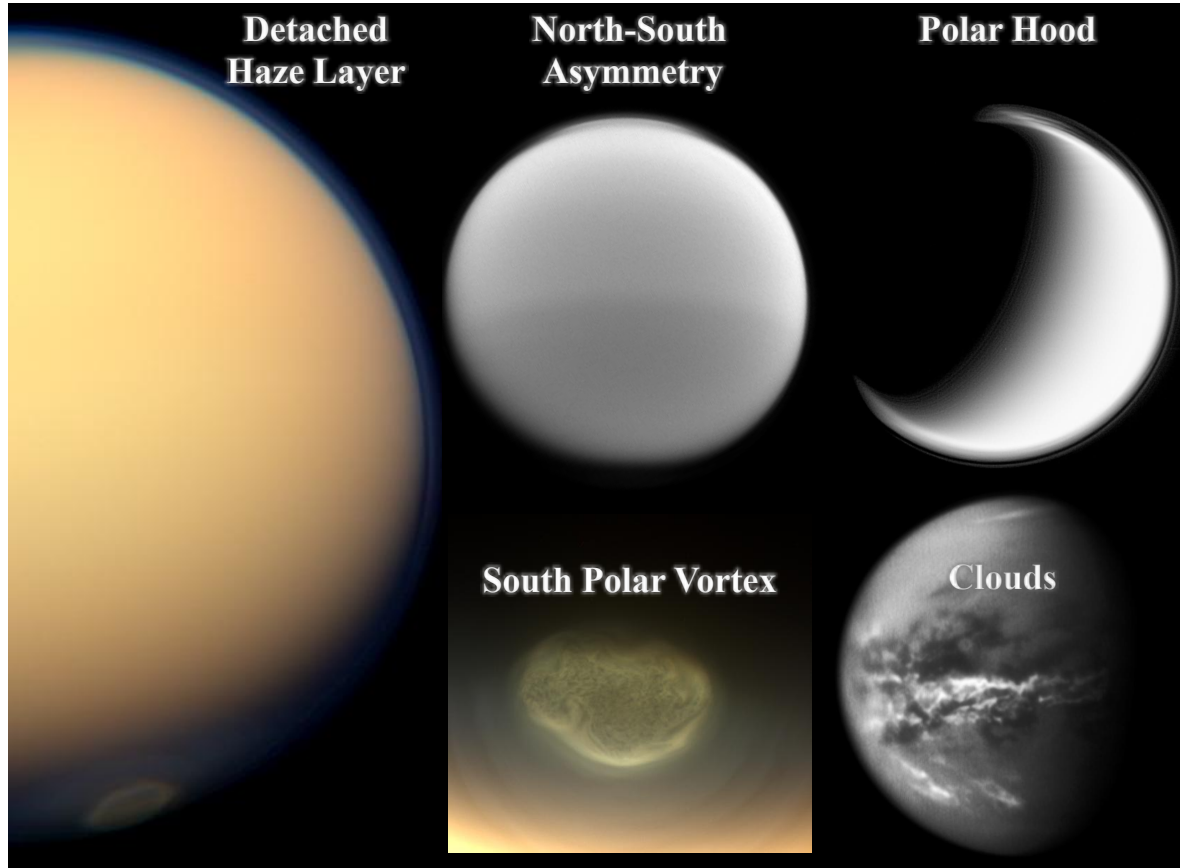


**Figure 8.** Shown here are examples of some of Titan's distinctive atmospheric features. At the left, a natural color view of Titan from 2012 (PIA14925; July 25, 2012) showing the detached haze layer and the newly formed vortex at the south pole (shown also bottom middle, PIA14919; June 27, 2012). The north-south asymmetry in the haze is shown top middle (PIA14610; January 31, 2012). Titan's north polar hood stands out in the image shown top right (PIA08137; January 27, 2006). At the bottom right, extensive methane clouds at a number of different latitudes, including the equator, show the post-equinox shift in cloud location (PIA12810; October 18, 2010). All image credits are NASA/JPL/Space Science Institute.

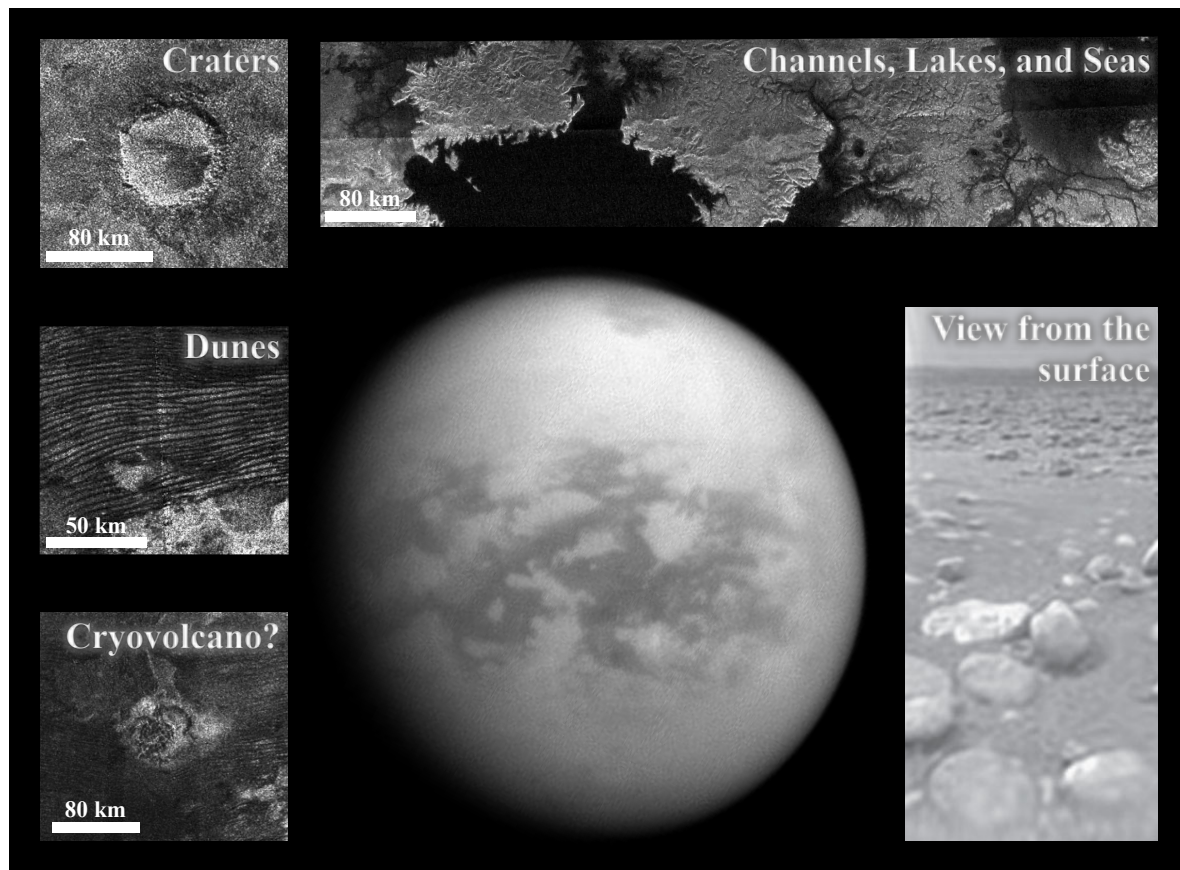


**Figure 9.** Shown here are examples of some of the surface features discussed in the text.

The crater shown (top left) is Sinlap, which has a diameter of 79 km (PIA16638, NASA/JPL-Caltech/ASI/GSFC). An example of Titan's equatorial dunes from the Shangri-la dunes is shown middle left (PIA12037, NASA/JPL-Caltech/ASI). Doom Mons and Sotra Patera, a putative cryovolcanic region, are shown bottom left (PIA09182, NASA/JPL-Caltech/ASI). At the top is Kraken Mare (left) and Ligeia Mare (right) and associated channel systems (PIA09217, NASA/JPL-Caltech/ASI). Shown bottom right is the view from the surface taken by the Descent Imager Spectral Radiometer carried by Huygens. The cobbles in the foreground are 10 to 15 cm (PIA06440, ESA/NASA/JPL/University of Arizona). The middle image was taken at 938 nm (CB3 filter), which sees down to the surface. The dark equatorial regions are Titan's expansive dune fields, while the dark regions at the north pole are lakes and seas (PIA14584, NASA/JPL-Caltech/Space Science Institute).

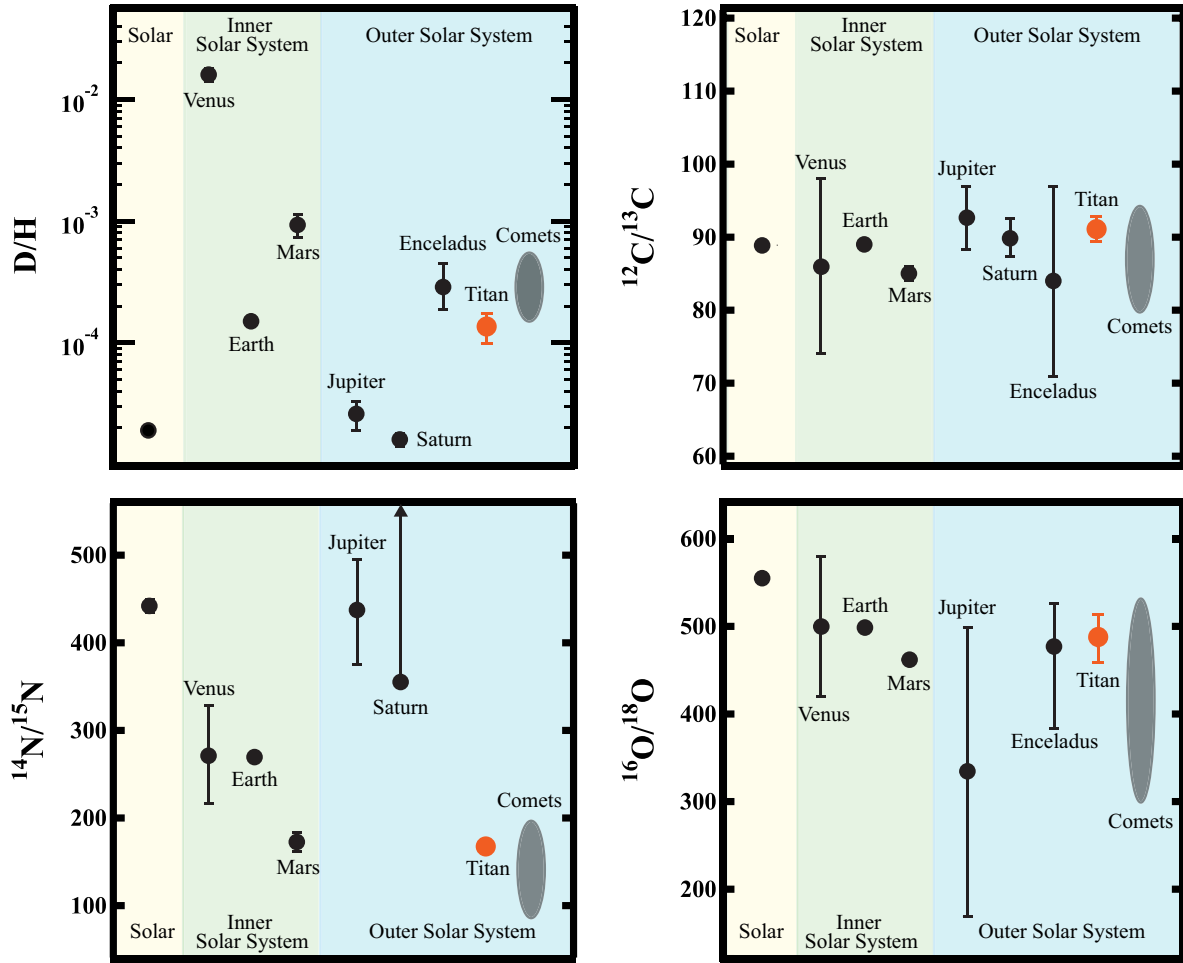


**Figure 10.** Titan's isotope ratios for H, C, N, and O compared with other solar system measurements. Solar- H [Lodders, 2003], C [Meibom et al., 2007], N [Marty et al., 2011], O [McKeegan et al., 2011], Venus- H<sub>2</sub>O [Donahue et al., 1982], CO<sub>2</sub> [Bezard et al., 1987], N<sub>2</sub> [Hoffman et al., 1979], CO<sub>2</sub> [Hoffman et al., 1980], Earth- VSMOW (H, O), VPDB (C), N<sub>2</sub>, Mars- H<sub>2</sub>O [Webster et al., 2013], CO<sub>2</sub> [Mahaffy et al., 2013], N<sub>2</sub> [Wong et al., 2013], CO<sub>2</sub> [Mahaffy et al., 2013], Jupiter- H<sub>2</sub> [Niemann et al., 1998], CH<sub>4</sub> [Niemann et al., 1998], NH<sub>3</sub> [Owen et al., 2001], H<sub>2</sub>O [Noll et al., 1995], Saturn- H<sub>2</sub> [Fletcher et al., 2009], CH<sub>4</sub> [Fletcher et al., 2009], NH<sub>3</sub> [Fletcher et al., 2014], Enceladus- H<sub>2</sub>O, CO<sub>2</sub>, H<sub>2</sub>O [Waite et al., 2009], Titan- CH<sub>4</sub> [Niemann et al., 2010], N<sub>2</sub>, [Niemann et al., 2010], CO [Serigano et al., 2016], Comets- H<sub>2</sub>O [Bockelée-Morvan et al., 2015], CO<sub>2</sub> [Bockelée-Morvan et al., 2015], NH<sub>2</sub> [Rousselot et al., 2014], H<sub>2</sub>O [Bockelée-Morvan et al., 2015].

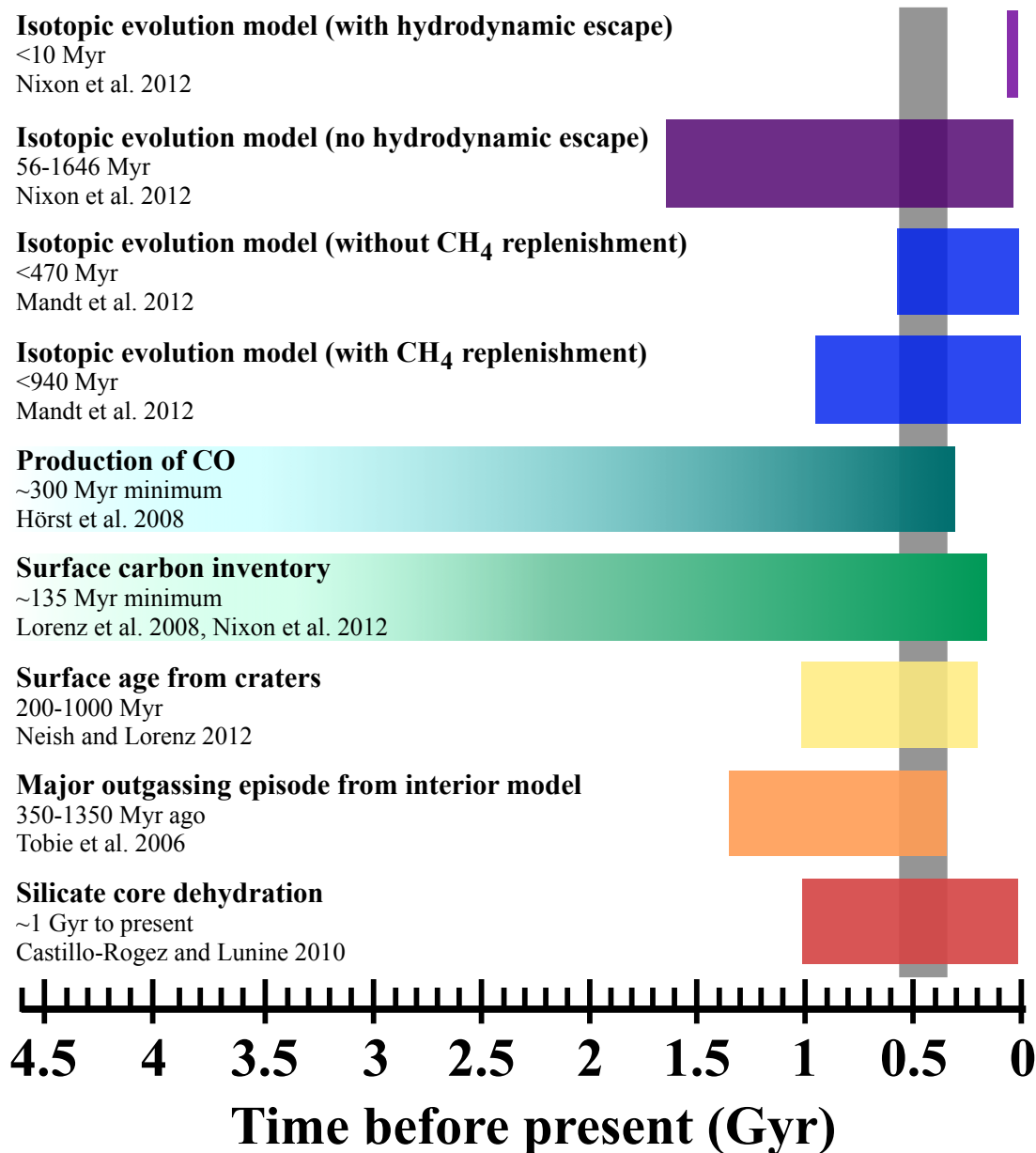


**Figure 11.** Constraints on the age of Titan's atmosphere from various measurements and models [Tobie et al., 2006; Hörst et al., 2008; Lorenz et al., 2008d; Castillo-Rogez and Lunine, 2010; Neish and Lorenz, 2012; Nixon et al., 2012; Mandt et al., 2012].

Table 1: Composition of Titan's Neutral Atmosphere

Formula	Ground Based <sup>(a)</sup>	ISO(f)/Herschel	Stratosphere		UVIS <sup>(r)</sup>	Mesosphere	Thermosphere INMS (CSN) <sup>(s)</sup>
			CIRS <sup>(l)</sup>	9.6±2.4×10 <sup>-4(m)</sup>			
H <sub>2</sub>							3.9±0.01×10 <sup>-3</sup>
<sup>40</sup> Ar							1.1±0.03×10 <sup>-5</sup>
C <sub>2</sub> H <sub>2</sub>	5.5±0.5×10 <sup>-6</sup>	2.97×10 <sup>-6</sup>		5.9±0.6×10 <sup>-5</sup>		3.1±1.1×10 <sup>-4</sup>	
C <sub>2</sub> H <sub>4</sub>	1.2±0.3×10 <sup>-7</sup>	1.2×10 <sup>-7</sup>		1.6±0.7×10 <sup>-6</sup>		3.1±1.1×10 <sup>-4</sup>	
C <sub>2</sub> H <sub>6</sub>	2.0±0.8×10 <sup>-5</sup>	7.3×10 <sup>-6</sup>				7.3±2.6×10 <sup>-5</sup>	
CH <sub>3</sub> C <sub>2</sub> H	1.2±0.4×10 <sup>-8</sup>	4.8×10 <sup>-9</sup>				1.4±0.9×10 <sup>-4</sup>	
C <sub>3</sub> H <sub>6</sub>	6.2±1.2×10 <sup>-7</sup> <sup>(b)</sup>	2.0±1.0×10 <sup>-7</sup>		2.6±1.6×10 <sup>-9</sup> <sup>(n)</sup>		2.3±0.2×10 <sup>-6(t)</sup>	
C <sub>3</sub> H <sub>8</sub>		2.0±0.5×10 <sup>-9</sup>		4.5×10 <sup>-7</sup>		<4.8×10 <sup>-5</sup>	
C <sub>4</sub> H <sub>2</sub>		4.0±3.0×10 <sup>-10</sup>		1.12×10 <sup>-9</sup>		6.4±2.7×10 <sup>-5</sup>	
C <sub>6</sub> H <sub>6</sub>	5×10 <sup>-7</sup>	3.0±0.5×10 <sup>-7</sup>		2.2×10 <sup>-10</sup>		2.3±0.3×10 <sup>-7</sup>	
HCN		4.9±0.3×10 <sup>-9(g)</sup>		6.7×10 <sup>-8</sup>		1.6±0.7×10 <sup>-5</sup>	
HNC	3×10 <sup>-11</sup>	5.0±3.5×10 <sup>-10</sup>		2.8×10 <sup>-10</sup>		2.4±0.3×10 <sup>-6</sup>	3.2±0.7×10 <sup>-5</sup>
HC <sub>3</sub> N	8×10 <sup>-9</sup>			<1.1×10 <sup>-7</sup> <sup>(o)</sup>			3.1±0.7×10 <sup>-5</sup>
C <sub>2</sub> H <sub>5</sub> CN	2.8×10 <sup>-10(d)</sup>						
C <sub>2</sub> N <sub>2</sub>				9×10 <sup>-10(p)</sup>		4.8±0.8×10 <sup>-5</sup>	
NH <sub>3</sub>				<1.9×10 <sup>-10(h)</sup>		2.99±0.22×10 <sup>-5</sup>	
CO	5.1±0.4×10 <sup>-5(e)</sup>	4.0 ± 5 × 10 <sup>-5(i)</sup>		4.7±0.8×10 <sup>-5(q)</sup>			
H <sub>2</sub> O		8×10 <sup>-9(j)/7×10<sup>-10(k)</sup></sup>		4.5±1.5×10 <sup>-10(q)</sup>		<3.42×10 <sup>-6</sup>	
CO <sub>2</sub>		2.0±0.2×10 <sup>-8</sup>		1.1×10 <sup>-8</sup>		<8.49×10 <sup>-7</sup>	

All values come from the source and work referenced in the table header unless otherwise noted in the table.

<sup>(a)</sup> Marten et al. [2002] (at 200 km) <sup>(b)</sup> Roe et al. [2003] <sup>(c)</sup> Cordiner et al. [2014] (constant profile at 400 km)

<sup>(d)</sup> Cordiner et al. [2015] (gradient profile at 200 km) <sup>(e)</sup> Gurwell [2004] <sup>(f)</sup> Coustenis et al. [2003]

<sup>(g)</sup> Moreno et al. [2011] (constant profile at 400 km) <sup>(h)</sup> Teanby et al. [2013] (3- $\sigma$  upper limit, peak sensitivity at 75 km) <sup>(i)</sup> Courtin et al. [2011] <sup>(j)</sup> Coustenis et al. [1998] (at 5°S) <sup>(k)</sup> Moreno et al. [2012] (from the S<sub>a</sub> profile at 400 km) <sup>(l)</sup> Coustenis et al. [2010] (at 5°S; HCN, C<sub>6</sub>H<sub>6</sub>, C<sub>3</sub>H<sub>8</sub>, C<sub>4</sub>H<sub>2</sub>, and HC<sub>3</sub>N exhibit latitudinal variations [Coustenis et al., 2007]), values averaged over TB-T44 assuming constant vertical profiles, for vertical variations see Vinatier et al. [2010a]) <sup>(m)</sup> Courtin et al. [2007]

<sup>(o)</sup> Nixon et al. [2010] (3- $\sigma$  upper limits at 25°S) <sup>(p)</sup> Teanby et al. [2006] (3- $\sigma$  upper limit at 50°N)

<sup>(n)</sup> Nixon et al. [2013a] (at 225 km) <sup>(q)</sup> Cottini et al. [2012] (using constant VMR at 230 km)

<sup>(r)</sup> Koskinen et al. [2011] (at ~600 km) <sup>(s)</sup> Cui et al. [2009] (at 1077 km from T5, 16, 18, 19, 21, 23, 25-30, 32, 36, 37 using INMS CSN mode, *italics* indicates corrected values, signals from C<sub>2</sub>H<sub>2</sub> and C<sub>2</sub>H<sub>4</sub> are difficult to separate so the reported value is for both species combined) <sup>(t)</sup> Magee et al. [2009] (global average at 1050 km)